SEASONAL AND INTERANNUAL DIFFERENCES IN SURFACE CHLOROPHYLL AND INTEGRATED WATER COLUMN CHLOROPHYLL STOCKS IN THE NORTHEASTERN GULF OF MEXICO

A Thesis

by

WILLIAM W. FLETCHER

Submitted to the Office of Graduate Studies of
Texas A&M University
in partial fulfillment of the requirements for the degree of

MASTER OF SCIENCE

August 2004

Major Subject: Oceanography

SEASONAL AND INTERANNUAL DIFFERENCES IN SURFACE CHLOROPHYLL AND INTEGRATED WATER COLUMN CHLOROPHYLL STOCKS IN THE NORTHEASTERN GULF OF MEXICO

A Thesis

by

WILLIAM W. FLETCHER

Submitted to Texas A&M University
in partial fulfillment of the requirements
for the degree of

MASTER OF SCIENCE

Approved as to style and content by:

Douglas C. Biggs (Co-Chair of committee)	Norman L. Guinasso, Jr. (Co-Chair of committee)
James L. Pinckney (Member)	Daniel L. Roelke (Member)
Wilford D. Gardner (Head of Department)	

August 2004

Major Subject: Oceanography

ABSTRACT

Seasonal and Interannual Differences in Surface Chlorophyll and Integrated Water Column Chlorophyll Stocks in the Northeastern Gulf of Mexico. (August 2004)

William W. Fletcher, B.A., Kenyon College

Co-Chairs of Advisory Committee: Dr. Douglas Biggs
Dr. Norman Guinasso Jr.

During the Northeastern Gulf of Mexico Chemical and Hydrography study (NEGOM-COH), nine oceanographic cruises were fielded during the spring, summer and fall seasons from November 1997 to August 2000. Surface chlorophyll-α fluorescence, salinity, and temperature data were logged once a minute from the R/V *Gyre* and subsurface chlorophyll-α fluorescence, salinity, temperature, and nutrients were profiled when the ship stopped to make stations. Each cruise occupied 94-98 stations, partitioned among 11 cross-margin transects of water depths between 10 m to 1000 m.

Overall chlorophyll-α abundance within the study area is forced by the amount of freshwater discharge. Seasonal and interannual differences are largely determined by the monthly mean streamflow for the major rivers within the NEGOM area, particularly the Mississippi River. However, an important forcing function for transport of river water to the outer continental shelf and slope is the periodic presence of anticyclonic slope eddies. Especially when these slope eddies were centered south and east of the Mississippi River delta, they entrained and so redistributed low salinity green water to a wider area within the NEGOM region than could be predicted by mean monthly streamflow alone. The mean surface chlorophyll-α concentrations, and in particular the distribution of relatively high surface chlorophyll-α concentrations off-shelf, were strongly dependent upon entrainment of freshwater by these slope eddies, especially during the three summer cruises. Interannual variability in the summertime entrainment of low salinity green water was driven by summer-to-summer differences in sea surface height (SSH) of the slope eddy(s), and in how far they extended on margin.

Satellite observations of ocean color showed that freshwater entrainment by anticyclonic eddies persisted for a temporal scale of several weeks each summer. Satellite-derived surface chlorophyll-α concentrations were positively correlated with in situ measurements of surface chlorophyll-α, with greatest agreement between satellite and ship measurements of surface chlorophyll-α at concentrations <1.5 mg/m^3. Because subsurface chlorophyll-α concentrations were often elevated at depths greater than the first optical depth, satellite measurements of chlorophyll-α concentration generally underestimated integrated chlorophyll-α standing stocks within the euphotic zone.

DEDICATION

This thesis is dedicated to my parents, Stephen and Judith Fletcher, and to my sister, Kathryn Fletcher.

ACKNOWLEDGEMENTS

I would like to thank my committee members, Dr. Doug Biggs for his willing support, guidance and infinite patience; Dr. Norman Guinasso, Jr. for his generous help with data processing and comments; Dr. Jay Pinckney for the thoroughness of his editorial comments; and Dr. Dan Roelke for his genuinely useful and much appreciated comments and advice.

I would also like to thank Dr. Chuanmin Hu and his graduate student, Bisman Nababan of the University of South Florida, for providing me with the SeaWiFS data used and for processing this data into a form that would be coherent to me. Thanks must also go to the students, faculty, and staff of the Department of Oceanography at Texas A&M University for their friendly support during my time here at Texas A&M.

Finally, I must give thanks to my parents and family for their support and love during my time at Texas A&M. I would like to thank my dad for first teaching me how to fish, and thus bringing about my love for all aquatic environments. I would like to thank my mom for never neglecting to give me a call every now and then, despite the adoption of my two younger "sisters", Phoebe and Deme. Thanks go to my sister for keeping me in good humor during my times of frustration. Lastly, thanks are given to my friends here at A&M and elsewhere, particularly Lark, Michael, Mike, Will, Erin, Jen, and Laurie.

Data collection was supported by MMS contract 1435-01-97-CT-30851 for The NEGOM Chemical Oceanography and Hydrography project. Data analysis was supported by a subcontract to TAMU from USF from USF NASA grant NAG5-10738 to study "Impacts of Large River Plumes on Carbon and Salt Fluxes in the Surface Ocean."

TABLE OF CONTENTS

LIST OF FIGURES

FIGURE Page

FIGURE Page

LIST OF TABLES

CHAPTER I
GENERAL INTRODUCTION

Hydrographic data analyzed for this MS thesis were collected during the Northeastern Gulf of Mexico Physical Oceanography Program (NEGOM): Chemical Oceanography and Hydrography Study (NEGOM-COH). This program was funded through the Minerals Management Service (MMS) of the U.S. Department of the Interior as research contract 1435-01-97-CT-30851 to Dr. W.D. Nowlin and co-investigators from the Department of Oceanography at Texas A&M University (TAMU).

The NEGOM-COH project design was to make a series of oceanographic cruises that would be able to characterize chemical oceanography and hydrographic parameters with fine scale spatial resolution, and with temporal resolution sufficient to observe seasonal variations in these parameters. While the primary emphasis of the NEGOM-COH program was on chemical oceanography and hydrography, additional measurements of opportunity taken during each of the 9 cruises allow the fine scale analyses of chlorophyll-α (chl-α) standing stocks in x, y, z space, within the study region. Analyses of these chl-α standing stocks are the basis for this thesis, using ship measurements of chl-α fluorescence collected during the NEGOM program which have been supplemented with measurements from satellites in earth orbit.

The NEGOM fieldwork consisted of nine oceanographic cruises aboard R/V *Gyre* from November 1997 to August 2000. Cruises were fielded every 3-6 months, so that one fall/winter cruise, one spring cruise and one summer cruise were done in each of the study years. Each cruise took measurements at 94-98 stations spaced along 11 cross-shelf transects from the Mississippi River outflow to Tampa Bay. Figure 1 shows the location of CTD stations for the NEGOM cruise tracks. Each of these transects begins in a water depth of 10 meters and continues to the 1000 meter isobath. Vertical profiles

---

This thesis follows the style and format of the *Journal of Geophysical Research.*

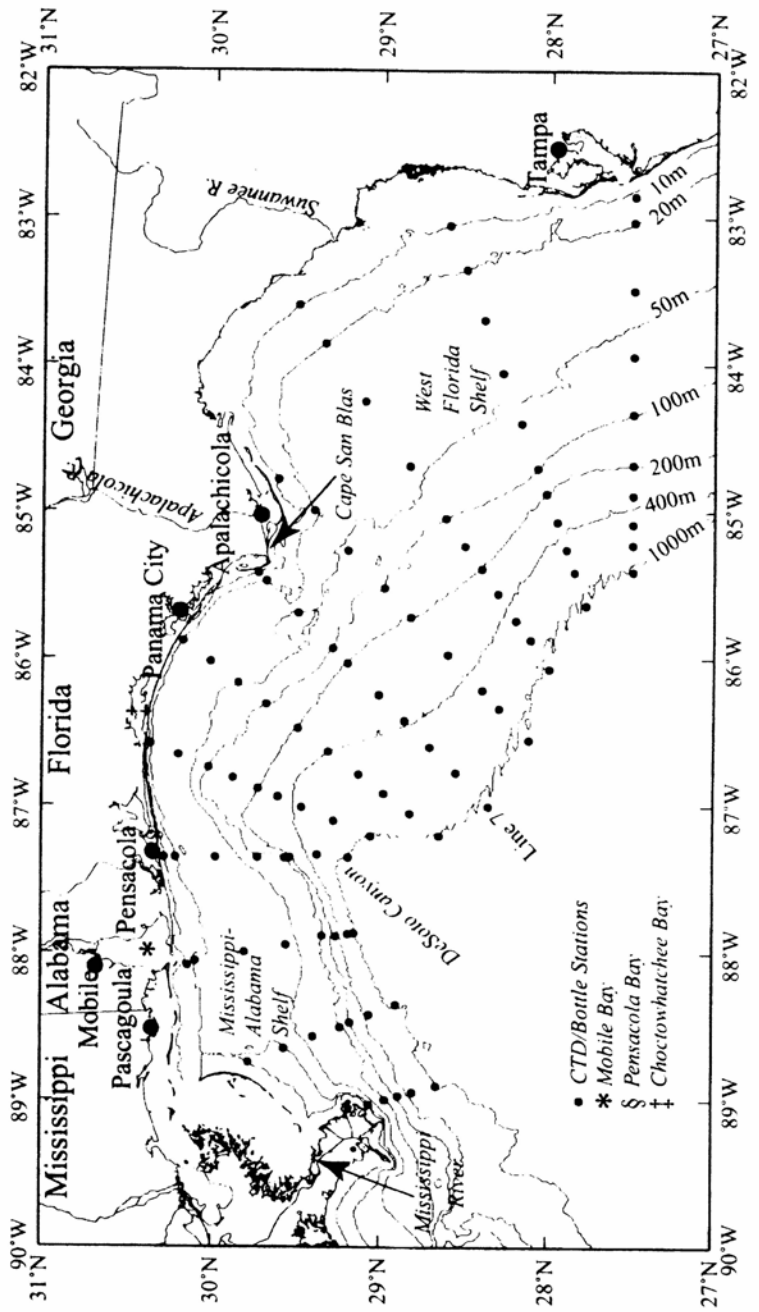

Figure 1. Locations of CTD sampling stations within the NEGOM study region. Figure from Qian et al., 2003.

were taken with a CTD rosette multi-sampler outfitted with a Chelsea Designs Aquatrakka submersible fluorometer, from just below surface to the ocean bottom.

The NEGOM project involved a wide variety of data collection techniques. Comprehensive descriptions of all NEGOM-COH data parameters and techniques can be found in Jochens et al. [2002]. The primary field measurements used for this thesis are vertical salinity profiles, surface chl-α extractions, vertical fluorometry profiles, and vertical photosynthetically available radiance (PAR) profiles. The vertical salinity profiles were used to calculate the volume of freshwater (<35psu) at each station. Surface chl-α extractions were used to calibrate surface fluorescence that was logged every 1 minute while underway and every 0.5 meters vertically at each CTD station so that fluorescence could be used as a proxy for chl-α concentrations. Vertical fluorometry profiles were used in turn to calculate total integrated water column chl-α. The vertical PAR profiles were used to calculate the integration depths based upon the percentage of surface light penetration to depth.

The secondary data source for this thesis is that of the remotely sensed data for surface chl-α concentration, collected by the SeaWiFS satellite. These data are broken into week-long averages for each of the CTD stations throughout the period of the NEGOM study. These data include both periods during research cruises and all periods in between research cruises. The SeaWiFS data were collated and provided by Chuanmin Hu and Bisman Nababan of the University of South Florida.

The principal objective of this thesis is to describe the spatial, seasonal and interannual variation in freshwater abundance and chl-α abundance within the northeastern region of the Gulf of Mexico. The first step was to calculate the amount of freshwater at each sampling station for each of the nine of the NEGOM cruises. Freshwater inflow into the NEGOM region is important because it carries elevated phytoplankton biomass seaward on to the coastal margin during inflows of river water. This freshwater can also stimulate in situ primary productivity in the surface waters when and where the river water retains measurable dissolved inorganic nitrate and phosphate concentrations [Gonzalez-Rodas, 1999; Belabbassi, 2001]. Thus, the relative

abundance of freshwater can create high chl-α concentrations in what would otherwise be considered the oligotrophic waters of the outer shelf and continental slope [Lohrenz et al., 1999]. Freshwater abundance is the subject of the second chapter of this thesis due to this ability to contribute to chl-α abundance. This adds particular relevance to the high variability in the abundance of freshwater within the NEGOM region and the factors that determine freshwater abundance.

The third chapter of the thesis is a comparison of chl-α abundance based upon season, year and hydrographic regime. This comparison of chl-α abundance uses two separate methods; 1) the measurements of surface chl-α and 2) calculation of total integrated chl-α through the water column to differing depths based upon salinity and light penetration. These integration depths are the 35 psu halocline (where applicable), the 36.8% surface light penetration depth (1st optical depth), the 18% surface light penetration depth (secchi disc depth), and the 1% surface light penetration depth (herein assumed to be the net photosynthesis compensation depth).

The purpose of the depth integrated chl-α calculations is to determine how representative the surface chl-α concentrations are of the overall chl-α abundance through the water column. Due to the varying hydrographic regimes found within the study area, there are several different vertical profiles of chl-α concentrations [Wawrik et al., 2003]. For example, surface chl-α concentrations at some stations may be more or less representative of the overall chl-α abundance integrated to differing depths, while at others where a deep chl-α maximum (DCM) is prominent the surface concentrations alone will underestimate total integrated chl-α mass. This variability in how well surface chl-α measurements predict overall chl-α abundance will of course influence how well satellite measurements of surface chl-α predict overall chl-α abundance through the water column.

The fourth chapter of this thesis analyzes the correlation between surface chl-α concentration and integrated chl-α abundance according to separate hydrographic regimes. This is done with the expectation that surface chl-α measurements will be more representative of total chl-α abundance under some hydrographic regimes compared to

others. This, in turn, permits the determination at which conditions satellite measurements of surface chl-α concentrations are most applicable and appropriate.

Chapter IVof this thesis has two separate components, both of which are based upon satellite measurements of surface chl-α. The initial portion of the satellite analysis (part one: ship and satellite comparisons) presents the comparison of ship-based data with satellite measurements taken during the same study periods. The purpose of this aspect of the study is to verify that satellite measurements accurately reflect ship-based measurements for the differing hydrographic regimes that are found throughout the study area. This stage of the analysis also permits the matching of river water to high chl-α concentrations within the study area. The area of these high chl-α freshwater intrusions have been outlined in the false color images of surface chl-α concentration. This allowed the tracking of the freshwater through the study area as well as the determination of the frequency and relative intensity of freshwater intrusions into the NEGOM region.

The other portion of the satellite analysis (chapter IV, part two: correlations and climatology) involves the observation of surface chl-α distribution both during the cruise periods and during the periods when cruises were not conducted. The advantages of satellite observation are that it can provide relatively high resolution data over a large study area and these data can be collected frequently. The satellite advantage of near continual coverage through time allows us to determine whether our cruise snapshot is representative of the entire season or whether the conditions encountered during a cruise are atypical compared the majority of the season or year of study. It is this advantage of satellites that is the primary basis for the integration of satellite methods with the NEGOM cruise data. The satellite surface chl-α data are being used to gauge how representative the data from each cruise are of the overall seasonal conditions of surface chl-α concentration.

Chapter V presents an overall synthesis of the previous chapters, and chapter VI summarizes the principal conclusions. Appendix A presents correlation analyses derived

from the statistical package SAS, and appendix B archives some additional methodological, cruise-by-cruise presentations of metadata files.

CHAPTER II
FRESHWATER INPUTS AND FRESHWATER REDISTRIBUTION

2.1. Introduction

2.1.1. Overall Circulation Patterns

The circulation patterns within the NEGOM region are very complicated and it is difficult to fully describe them on a seasonal basis. The complicated pattern for this circulation is based upon a number of different factors. The first of these factors is the presence of eddies over the continental slope. Furthermore, the presence of these eddies is not constant in time nor does it necessarily coincide with any particular season. Second, while there is an overall seasonal pattern in wind direction within the NEGOM region, there is a great deal of interannual variability with these winds. There are also high frequency shifts in wind directions within the same season, which leads to rapid shifts in current speeds and directions [Jochens et al., 2002].

The overall patterns of circulation are highly variable at interannual as well as at relatively short time spans. However, when eddies are present over the continental slope they have a significant effect on the overall circulation within the NEGOM area and are frequently the dominant force in defining the circulation patterns.

2.1.2. River Influences

A total of seventeen rivers discharge into the NEGOM study area. The mean daily discharge rates are summarized in Table 1. Maximum mean discharge rates for the rivers typically occur during the spring. The minimum mean discharge rates occur during the early winter period. There is significant river discharge through the summer period as well. There is also a great deal of variability in river discharge on an interannual and seasonal basis. It is also important to acknowledge that maximum river discharges are generally in short term pulses of high flow rates based upon flooding events. The dominant river outflow into the NEGOM region is from the Mississippi

River. The other significant rivers eastward of this primarily only influence nearshore and inner shelf areas [Jochens et al., 2002]. A comparison of the daily mean streamflows of the Mississippi River and the combined streamflow of the other regional rivers is given in Figure 2.

Table 1. Summary list of rivers draining into the NEGOM region with mean daily discharge rates from USGS records. Data provided by the U.S Geological Survey.

River	Mean Daily Discharge (km^3/day)
Mississippi River at Tarbert's Landing, LA	1.18
Suwannee River at Branford, FL	0.017
Steinhatchee River near Cross City, FL	<0.001
Fenholloway River near Foley, FL	<0.001
Econfina River near Perry, FL	<0.001
Aucilla River near Scanlon, FL	.001
Ochlockonee River near Bloxham, FL	.004
Apalachicola River near Sumatra, FL	.063
Choctawhatchee River near Bruce, FL	.017
Yellow River at Milligan, FL	.003
Blackwater River near Baker, Fl	<0.001
Escambia River near Molino, Fl	.018
Perdido River at Barrineau Park, FL	.002
Alabama River at Millers Ferry, AL	.079
Tombigbee River at Demopolis,AL	.073
Pascagoula River at Graham Ferry,MS	.026
Pearl River near Monticello, MS	.017

In addition to analyzing the discharge of freshwater into the study area, it is also important to note spatial variations in the freshwater content. The amount of freshwater within the study area is strongly influenced by entrainment of surface waters by slope eddies, which are highly variable in their location, duration and strength [Sturges and Leben, 2000]. As a result, the distribution of freshwater may be highly variable while the overall freshwater content in the study area is the same.

River discharges into the area introduce low salinity, high nutrient waters into the ocean surface region. This introduction of high nutrient water into the surface waters can significantly increase phytoplankton production. There are also effects on the circulation of water within the NEGOM region based upon the added buoyancy from the river water [Jochens et al., 2002].

2.1.3. Loop Current Eddies

When the Loop Current moves northward towards the NEGOM study area, mesoscale anticyclonic eddies are often shed from the Loop Current. The presence of these slope eddies adjacent to the Mississippi River plume can entrain freshwater and redistribute this into the NEGOM region in a periodic fashion on a relatively small time scale [Muller-Karger et al., 1991]. These slope eddies are shed at an average rate of one every 11 months, but the process is stochastic and does not follow a specific seasonal pattern [Sturges, 1994]. Due to the significance of Loop Current eddies in determining how much river water enters the NEGOM region, the overall pattern of freshwater abundance may not follow the seasonal pattern of freshwater flow from the Mississippi River.

2.1.4. Purpose of Research

As freshwater flow into the NEGOM region is an important source of nutrients to the surface waters of the outer shelf and slope, it is important to determine the factors that determine freshwater abundance and distribution. It is expected that river flow into the NEGOM region is the major factor determining the abundance of freshwater within the NEGOM region. However, the presence of Loop Current eddies interacting with the Mississippi River outflow can potentially have a strong influence on the distribution of freshwater into the region. I have hypothesized that the interaction of Loop Current eddies with the Mississippi River outflow is a major factor in determining the abundance and distribution of freshwater in the NEGOM region.

This question is tested by comparing estimates of the relative volume of freshwater in the NEGOM region with the total streamflow into the NEGOM region during the cruise period. The relative volume of freshwater within the study area is estimated by integrating the freshwater volume through the water column. This should give a more accurate gauge of the total volume of freshwater compared to analysis based solely on the subsurface depth for a particular halopleth (e.g. depth of 35 psu as per Belabbassi [2001]), or based upon surface salinity alone. This section also addresses the

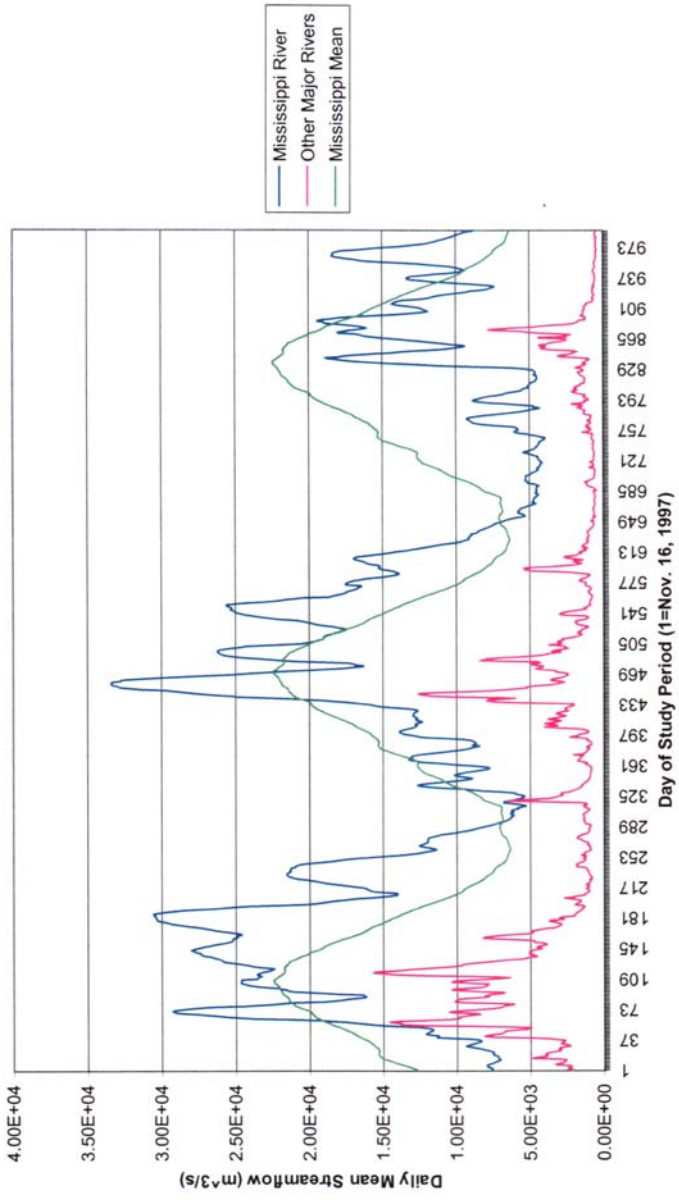

Figure 2. Streamflow data for the major rivers in the NEGOM region during the NEGOM study period. The dark blue line represents the daily mean streamflow for the Mississippi River at Tarbert's Landing, LA. Pink line represents the sum of other major rivers within the study area. Yellow line is the 64 year average for the daily mean streamflow of the Mississippi River at Tarbert's Landing.

question of how well surface salinity predicts the associated integrated freshwater volume beneath the ocean surface. This potentially allows for estimates of integrated freshwater volume based upon surface salinity measurements that were logged once per minute along the track of each NEGOM cruise and so are much more readily available than full water column data.

2.2. Methods

2.2.1. Instruments

The primary source of data for this section was from continuous vertical profiling using a Sea-Bird 911+ pumped CTD system that was attached horizontally to the lower part of the frame of a General Oceanics 12-place rosette with 10 liter Niskin bottles. Continuous vertical profiles of salinity were taken for all CTD stations of each cruise, with data being logged at 0.5 meter intervals. Because the CTD was mounted at the base of the rosette frame and because the surface bottle was generally tripped when the top of the rosette was submerged to a depth of about 1 meter, the CTD data generally begin at a depth between 2-4 meters deep for each station. In addition, a thermosalinograph logged measurements once a minute from a depth of 3.5 meters while underway.

2.2.2. Data Sources Used

For this section of the study, sea surface salinity was estimated from the shallowest CTD measurement of salinity. In the majority of stations this depth was shallower than the 3.5 meter deep intake of the continuous thermosalinograph. The salinity at the shallowest CTD measurement (3.0 meter average depth) was used as a proxy for the actual sea surface salinity for the sake of freshwater integration calculations. The depth of the 35 psu halocline was determined from the CTD data for each station. The first depth at which the salinity was 35 psu or greater was used as the depth of the 35 psu halocline.

River discharge rates were based upon data provided by the U.S. Geological Survey and the U.S Army Corps of Engineers. The calculations for the Mississippi River discharge rates for each cruise were taken from the Tarbert's Landing gauging station. River discharge rates were also used for six other regional rivers eastward of the Mississippi River outflow. These rivers and their mean flow rates are summarized in Table 2.

Table 2. Select rivers used to calculate freshwater flow into the NEGOM study area. Data provided by the U.S. Geological Survey.

River	Discharge Rate (m^3/sec)	Length of Record (years)
Mississippi	13,549	64
Alabama	952	22
Tombigbee	856	37
Pascagoula	340	5
Pearl	194	60
Apalachicola	771	21
Suwanee	201	67

2.2.3. Freshwater Calculations

To estimate the amount of freshwater being discharged into the NEGOM study area during the individual cruises, calculations were made based upon the data from the U.S. Geological Survey and the U.S Army Corps of Engineers. Daily mean stream flow data was averaged for a time period encompassing one week previous to and during the first week of each cruise. The mean stream flow for this two week period is used as a relative estimate for comparing the freshwater discharge entering the NEGOM area based upon the different cruise periods.

The calculation of total integrated water column freshwater content was made using the CTD salinity measurements at discrete 0.5 meter intervals. The volume of

zero psu freshwater for each 0.5 meter depth bin was calculated according to the simple equation below:

$$V_0 = ((35\text{-}S)V_i)/35$$

Where V_0 = Volume of zero psu water (m^3)
And V_i = Volume of integration layer = 0.5 m^3

This equation was applied to each 0.5 meter depth bin which had salinity less than 35 psu. Next, all depth bins for that CTD station were summed according to the following equation:

$$V_{(X)} \quad \sum_{i=1}^{n} (35\text{-}S_i)V_i$$

Where $V_{(X)}$ = Total volume of zero psu water for that station (m^3) per surface area of ocean (m^2)
and S_i = salinity in bin i at depth X
and V_i = volume in integration bin i (0.5 m^3)
and n = the number of integrations for depth X

As noted above, actual sea surface salinity was estimated from the shallowest CTD measurement taken for any given CTD station. For the depth bins shallower than this measurement (3.0 meter average depth) the salinity for the shallowest CTD measurement was extended to the surface. While this may underestimate the total volume of zero psu water for each station, the consistency of this technique allows for relative comparisons between stations and cruises.

2.2.4. Regional Designation Criteria

The separation of stations according to hydrographic region is an important component in the analyses within this chapter and the following chapters. As a result, it

is necessary to define the designated hydrographic regions used in this study and to explain the criteria used to assign them within each category. The three designations are "freshwater" stations, "bluewater" stations and "coastal" stations.

Freshwater stations are categorized according to the amount of freshwater found in the water column, and to a lesser extent the surface chl-α concentrations. The primary criteria used is the total integrated freshwater abundance for these stations. Any station with more than 0.33 m^3/m^2 of freshwater within the water column was categorized as being a freshwater station. This set amount (0.33 m^3/m^2) was decided upon by observing the behavior of the surface waters in conjunction with freshwater abundance. It was decided that the stations that had this threshold amount of integrated freshwater were strongly influenced by the amount of freshwater in terms of surface chl-α and light extinction. The freshwater designation is made without any consideration made to the overall depth of the station or location.

Bluewater stations are those characterized by having relatively low surface chl-α concentrations, relatively low light extinction coefficients and the presence of deep chl-α maximums. In this study, the bluewater stations were effectively the default category for all stations. If the stations were not dominated by freshwater influences and were not categorized as coastal stations, they were designated as bluewater stations.

Coastal stations were those located in water depths of 50 meters or less, were not dominated by freshwater influences and had a euphotic zone that extended to within 10 meters of the ocean bottom. These stations typically had relatively high surface chl concentrations, relatively high chl-α concentrations through the water column and frequently had high chl-α concentrations near the bottom.

All correlation calculations are done using the Pearson correlation test through SAS or Minitab, and comparisons of mean values are done using ANOVA with the same software.

2.3. Results

2.3.1. Seasonal Trends in Freshwater Distribution and Abundance

This section describes the seasonal patterns of distribution and abundance of freshwater, as defined by water of salinity < 35 psu, within the NEGOM survey area. The focus of this section is on the nearshore distribution of freshwater within the study area as well as on the total vertically integrated water column freshwater content. Freshwater data for the nine separate cruises are summarized in Table 3.

Table 3. Summary of freshwater parameters for NEGOM cruises. Mean 35 psu depth is calculated using only stations with surface salinity <35 psu.

Cruise	# of Stations	# of Freshwater Stations	River Flow (m^3/sec)	Integrated Freshwater (m^3/m^2)	Max. Surface Salinity	Min. Surface Salinity	Mean Surface Salinity	Mean 35 psu Depth
NEGOM1	94	10	7705	10.06	36.18	30.85	35.31	17.87
NEGOM2	98	42	29,408	52.01	36.43	20.40	33.51	12.84
NEGOM3	98	76	12,967	105.28	35.78	24.72	31.52	14.43
NEGOM4	98	10	12,339	10.72	36.27	15.24	35.17	14.09
NEGOM5	98	32	23,681	36.55	36.38	16.19	33.71	14.02
NEGOM6	98	72	7447	86.82	36.38	21.75	31.86	14.56
NEGOM7	98	3	4856	3.02	36.44	31.33	35.70	11.50
NEGOM8	98	7	17,779	7.97	36.50	27.38	35.83	12.46
NEGOM9	98	39	8752	38.20	36.84	25.62	33.70	11.98

River discharge rates averaged from the week previous to and the first week of each cruise are given for comparison. Individual river discharge data for the cruise periods are summarized in Table 2. The primary sources of data are shipboard measurements of underway salinity at z=3.5 m combined with CTD stations at which salinity was measured through the water column. River discharge rates are provided by the U.S. Geological Survey and the U.S Army Corps of Engineers.

2.3.1.1. Spatial Freshwater Distribution for Winter Cruises (NEGOM1, NEGOM4 and NEGOM7)

For all three of the winter cruises, freshwater distribution within the NEGOM region was spatially limited. There were only 10, 10, and 3 stations, respectively, at which the upper water column had >0.33 m^3/m^2 of integrated zero psu freshwater. Most of these stations were relatively nearshore stations near river outflows, but they also included the 200, 500 and 1000m stations in line 2 of NEGOM cruise 1. In 1997 these line 2 stations show a tongue of freshwater extending eastward and offshore from the Birdsfoot Delta. Surface salinity contour plots for the winter cruises are given in Figure 3.

During the winter cruises, the distribution of freshwater was associated with the proximity to individual river outflow areas. Each of these freshwater pockets was separated from the others based upon river location. The stations that have freshwater present during these cruises are isolated to specific near river outflow areas. This isolation of freshwater areas indicates little or no mixing of freshwater between different river sources within the study area for these three cruises. Lateral transport of freshwater during these three cruise periods was apparently low, based upon weak wind measurements and current measurements taken during the cruise period (Jochens et al. 2002).

At stations which had >0.33 m^3 of integrated freshwater, the depth of the 35 psu halocline varied between 7 meters and 35 meters, following the general trend of increasing depth with increasing distance from freshwater source due to vertical mixing and dilution.

2.3.1.2. Spatial Freshwater Distribution for Spring Cruises (NEGOM2, NEGOM5 and NEGOM8)

Freshwater distribution within the NEGOM region was generally more extensive among the spring cruises than for the winter cruises. There were 42, 32, and 7 stations, respectively, at which the upper water column had >0.33 m^3/m^2 of integrated zero psu freshwater. Most of these stations were relatively nearshore stations, with some exceptions. For both the spring, 1998 (N2) and spring, 1999 (N5) cruises, freshwater was found extending far offshore for lines 2 and 3. There was an area encompassing the nearshore stations of lines 1 through 3 that had surface freshwater present for all three of the spring cruises. Surface salinity contour plots for the spring cruises are given in Figure 4.

For the time periods during these cruises, the overall spatial distribution of freshwater near the separate river outflow areas appears to mirror the relative outflow of the associated river. The freshwater distribution for spring, 1998 (N2) includes all of the nearshore stations extending westward to include all lines of the cruise track. This pattern was most likely caused by river discharge rates that were significantly higher in 1998 than mean discharge rates for that time of year, particularly for the Mississippi, Apalachicola and Suwannee rivers. Similarly, the limited distribution of freshwater for the spring, 2000 (N8) cruise period is a reflection of significantly low mean discharge rates in 2000 for that time of year for all of the major rivers flowing into the NEGOM study area. At stations which had >0.33 m^3 of integrated freshwater, the depth of the 35 psu halocline varied between 4 meters and 30 meters. There is no discernable trend between the 35 psu halocline depth and any other parameters of freshwater distribution for the spring cruises.

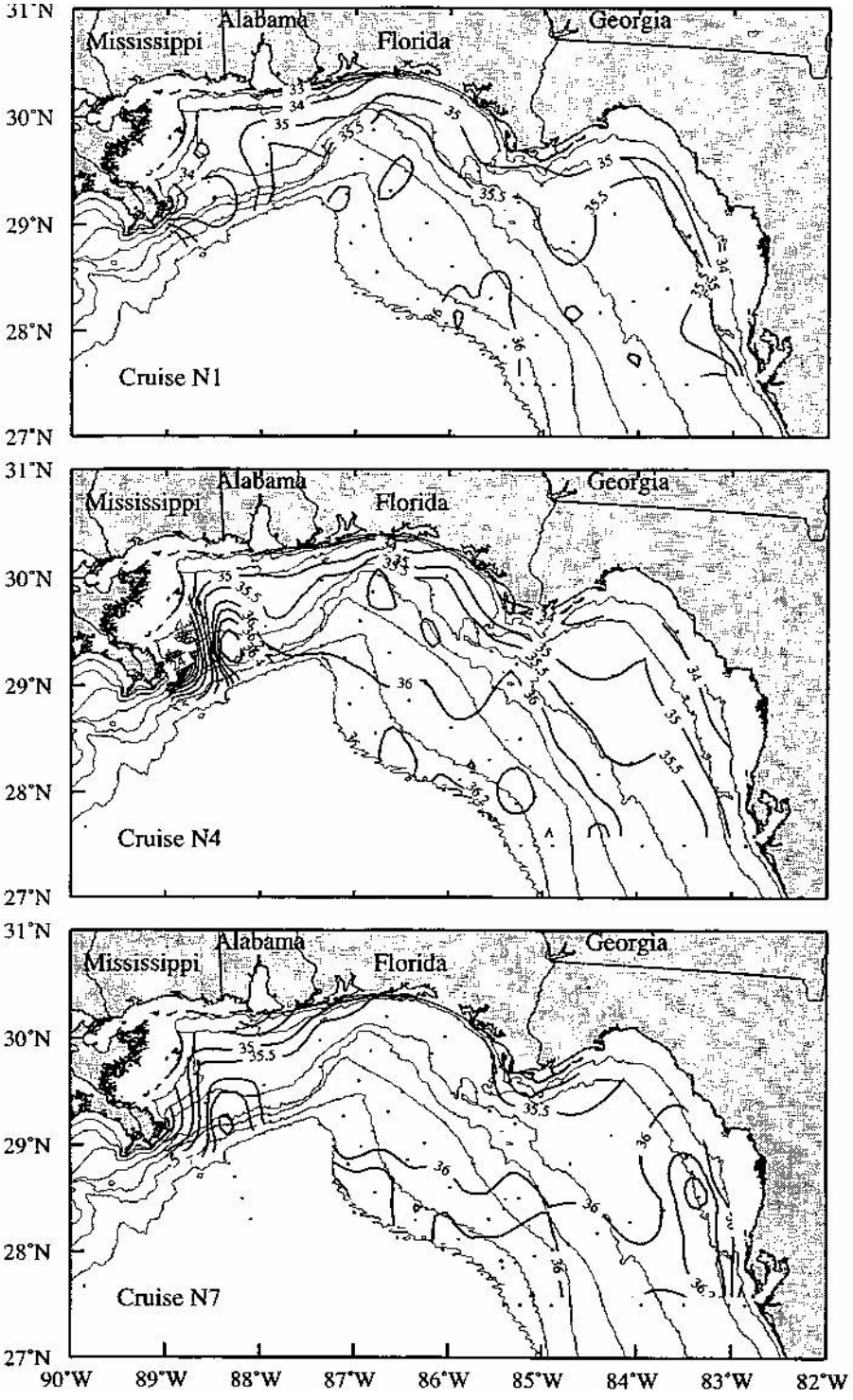

Figure 3. Sea surface salinity contour plots during the winter cruises. NEGOM1: Nov. 16-26, 1997. NEGOM4: Nov. 12-25, 1998. NEGOM7: Nov. 12-23, 1999. Figures from Jochens et al., 2002.

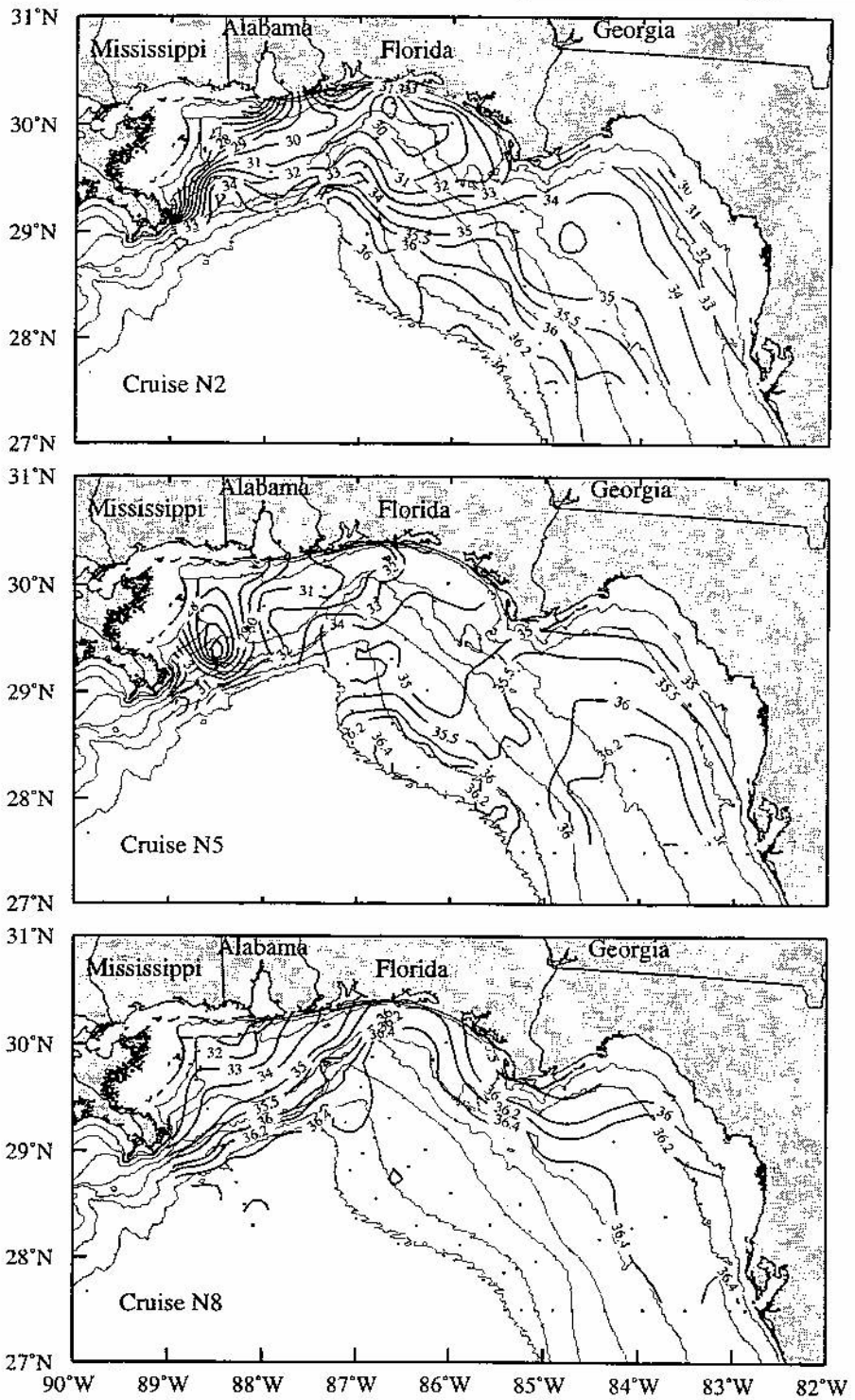

Figure 4. Sea surface salinity contour plots during the spring cruises. NEGOM2: May. 4-15, 1998. NEGOM5: May. 15-28, 1999. NEGOM8: Apr. 14-16, 2000. Figures from Jochens et al., 2002.

2.3.1.3. Spatial Freshwater Distribution for Summer Cruises (NEGOM3, NEGOM6 and NEGOM9)

Freshwater within the NEGOM region was most widely distributed during the summer cruises. There were 76, 72, and 39 stations, respectively, at which the upper water column had >0.33 m^3 of freshwater present. Freshwater was found to extend far offshore as well as showing far eastward distribution for all three of the summer cruises, though the extent of eastward expansion varies interannually between cruises. Freshwater did not, however, dominate in the majority of the nearshore stations extending from line 5 eastward through line 11. Surface salinity contour plots for the summer cruises are given in Figure 5.

For the time periods during these cruises, distribution of freshwater was primarily based upon entrainment of water from the Mississippi River into the NEGOM study area by the presence of anticyclonic (clockwise) slope eddies. The presence of these eddies is established by sea surface height (SSH) (Figure 6) and Acoustic Doppler Current Profiler (ADCP) measurements (Figure 7). These two methods allowed for accurate placement of eddies and their relative strength to be determined. This entrainment of Mississippi River water is the most dominant presence of freshwater in the study area during these cruises. The outflow areas of the other major rivers were either enveloped by the entrained Mississippi River water or did not exhibit the presence of significant amounts of freshwater. The dominance of Mississippi River water entrainment is further supported by the relative amounts of freshwater found within the study area seasonally compared to the overall river outflow for the associated season (Figure 8).

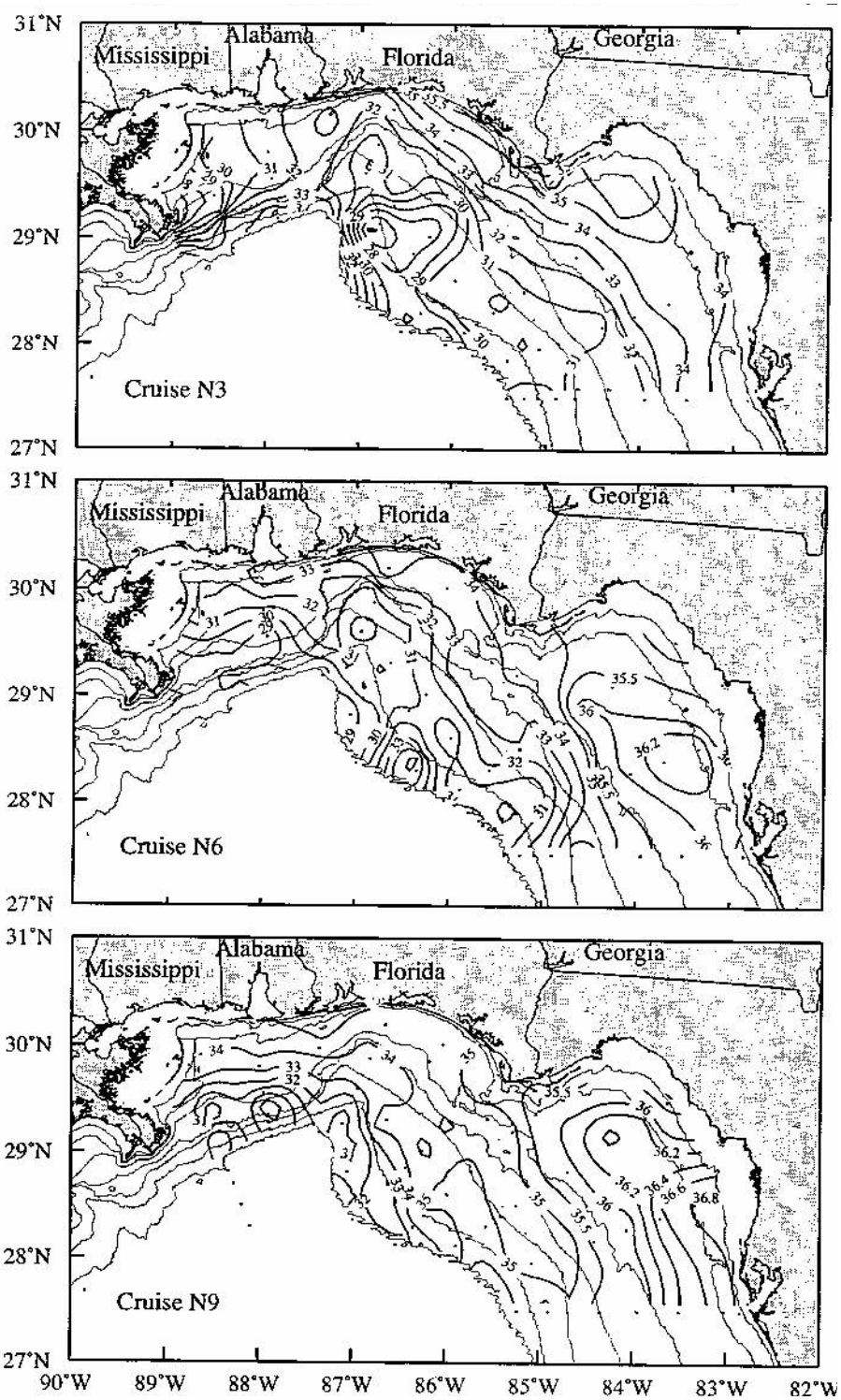

Figure 5. Sea surface salinity contour plots during the summer cruises. NEGOM3: Jul. 25-Aug. 9, 1998. NEGOM6: Aug. 15-28, 1999. NEGOM9: Jul. 28-Aug. 5, 2000. Figures from Jochens et al., 2002.

The extent to which the Mississippi River water is transported eastward depends upon the relative strength and placement of the anticyclonic eddy in the region. While all three summer cruises had anticyclonic eddies within the study area, they were not positioned identically, nor were their current fields of equal intensity and strength. As a result, the eastward extent of freshwater entrainment in the NEGOM area is primarily dependent upon the presence, intensity and positioning of anyticyclonic eddies to the Mississippi River plume.

At stations which had >0.33 m^3 of integrated freshwater, the depth of the 35 psu halocline varied between 4 meters and 27.5 meters, following a general trend of increasing depth with increase in vertically integrated freshwater.

2.3.1.4. Freshwater Abundance for Winter Cruises (NEGOM1, NEGOM4 and NEGOM7)

The three winter cruises measured the least amount of freshwater within the study area for all three years of data recorded. The relative amount of freshwater within the study area during the winter months were as low as one fifth of the following spring and as low as one tenth of the following summer (Figure 8). The low amounts of

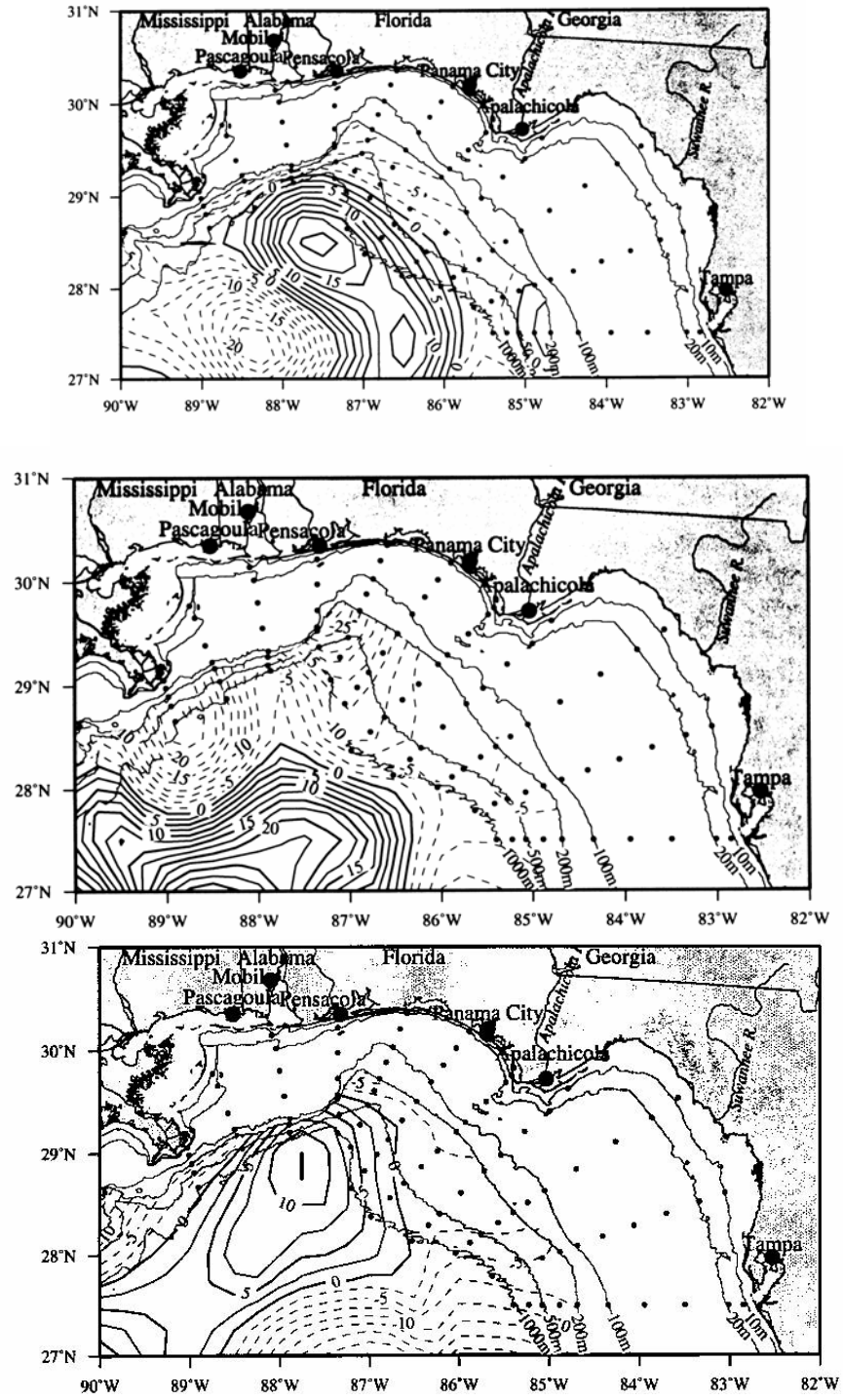

Figure 6. Sea surface height for the summer NEGOM cruises from satellite altimeter data. Units are in +cm SSH for solid lines and –cm SSH for dashed lines. Top figure is NEGOM3, middle figure is NEGOM6, and bottom figure is NEGOM9. Figures from Belabbassi (2001).

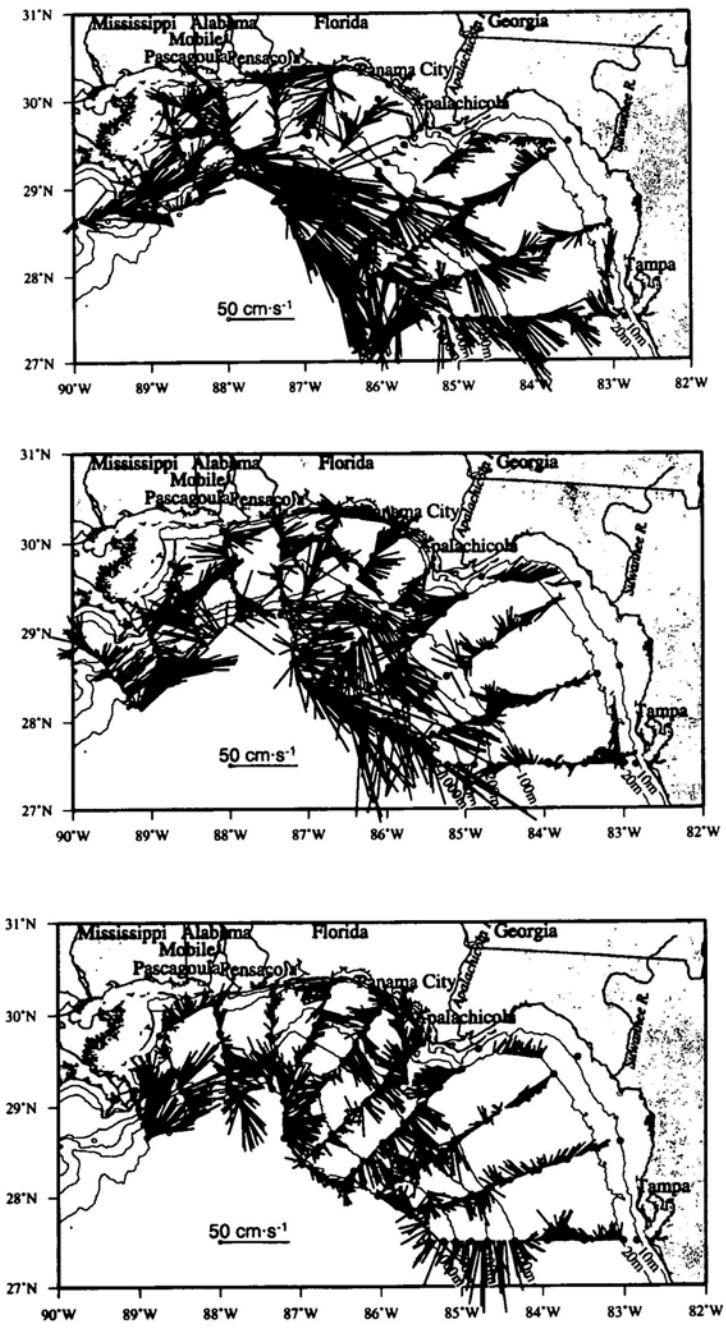

Figure 7. Acoustic Doppler Current Profiler measurements for the NEGOM summer cruises. Top figure is NEGOM3, middle figure is NEGOM6, and bottom figure is NEGOM9. Figures from Belabbassi (2001).

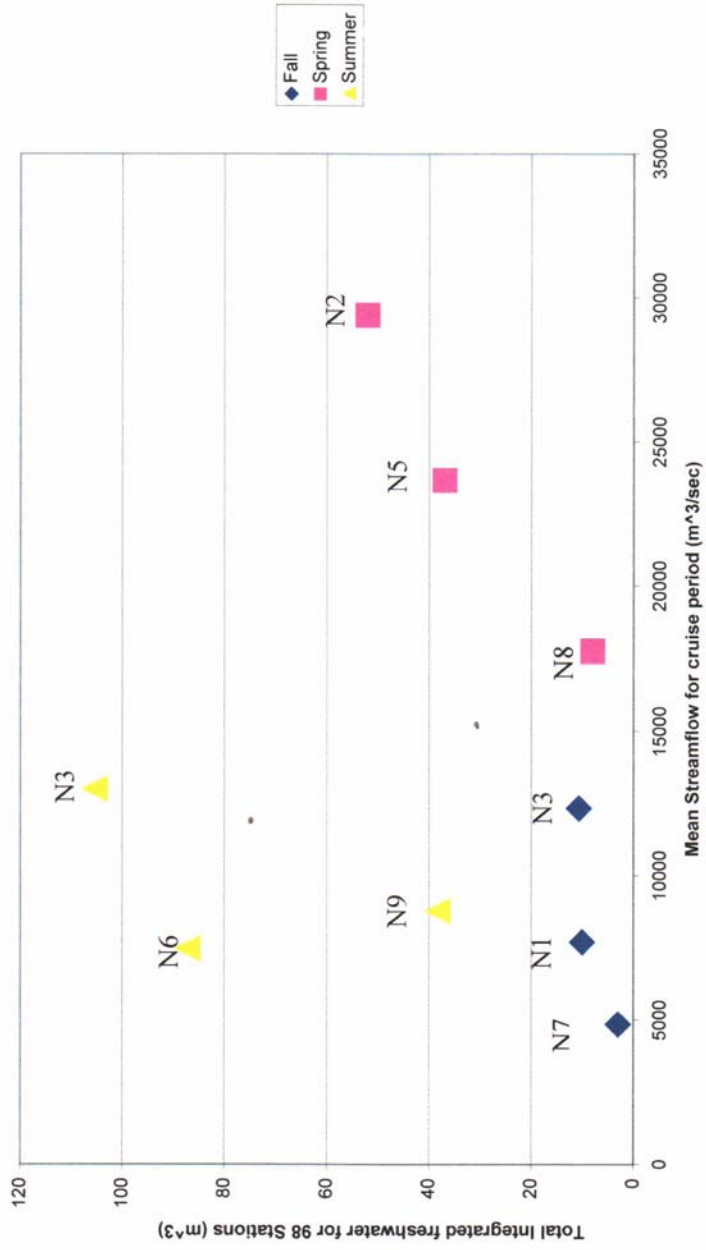

Figure 8. Comparison of mean streamflow during cruise period and relative abundance of freshwater within the NEGOM study area during the cruise period.

freshwater within the study area during the winter period are due to seasonally low river flow from all rivers within the study area (Table. 3).

2.3.1.5. Freshwater Abundance for Spring Cruises (NEGOM2, NEGOM5 and NEGOM8)

The spring cruises had greater freshwater abundance than the winter cruises of the respective year, but lower freshwater abundance than the associated summer cruises. The relative abundance of freshwater within the study area between the spring cruises is correlated to the river flow for that respective cruise period. The river flows during the spring cruises were the highest recorded for all of the cruises (Fig. 8). While the river flow was highest during the spring cruises, this did not translate to the highest abundance of freshwater within the study area. This is due to the lack of lateral transport of river water, particularly from the Mississippi River outflow area.

2.3.1.6. Freshwater Abundance for Summer Cruises (NEGOM3, NEGOM6 and NEGOM9)

The summer cruises had the highest abundance of freshwater within the study area for each respective year. This is the case in spite of the fact that the spring cruise periods had river discharge values that were on average twice the flow of the summer cruises (Figure 8). In the case of the summer cruises, the abundance of freshwater within the study area is caused by the presence of anticyclonic eddies over the slope to the south and southeast of the Birdsfoot Delta (Figure 7). These eddies drive the eastward entrainment of Mississippi River water into the NEGOM study area. This entrainment not only affects nearshore stations, but also strongly affects offshore stations and extends as far eastward as 84^{o}W longitude. There is no direct correlation between river flow and freshwater abundance within the study area for the summer cruises. Summer, 1999 (N6) has a lower river flow rate for the cruise period compared to

summer, 2000 (N9), but the abundance of freshwater in the study area for summer, 1999 (N6) is twice that of summer, 2000 (N9). It is evident that the amount of freshwater within the study area during the summer cruises is dependent upon the presence of slope eddies. The position of these eddies as well as the strength of these features determines how freshwater is redistributed within the study area.

2.3.2. Correlation and Conservation of Physical Parameters of Freshwater

Comparison between several parameters of freshwater distribution demonstrate some overall correlations. Minitab documented a weak yet significant (-0.132, $p<0.05$) correlation found between the measured surface salinity and the depth of the 35 psu halocline for all of the combined cruise data (Figure 9).

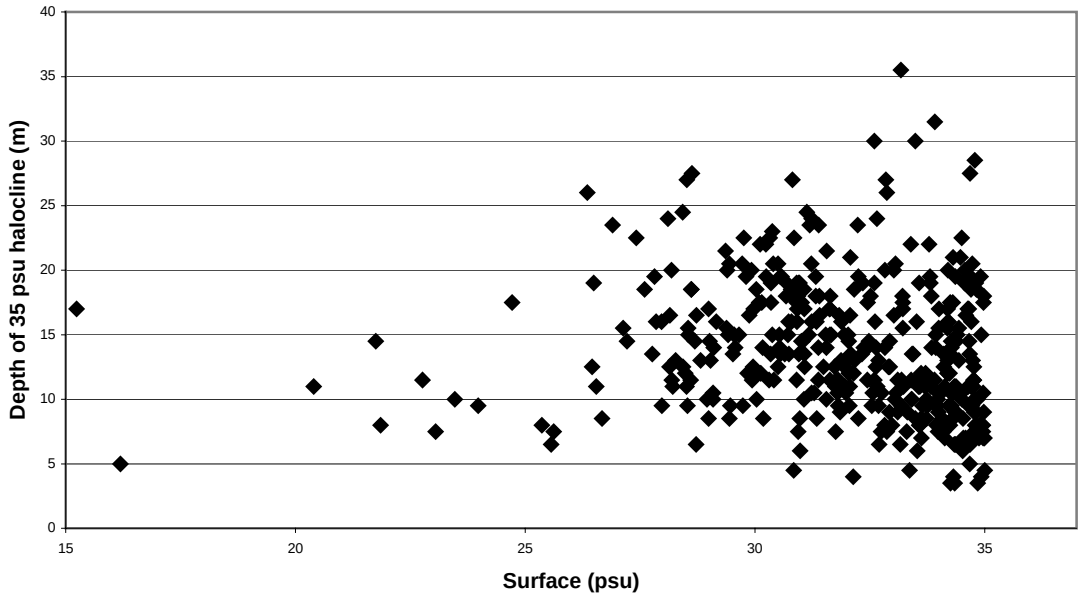

Figure 9. Comparison of surface salinity with depth of 35 psu halocline for all stations of all cruises.

There was slightly stronger significant (0.464, $p<0.05$) positive correlation between integrated freshwater abundance and the depth of the 35 psu halocline for all of the combined cruise data (Figure 10). There was a robust negative correlation (-0.872, $p<0.05$) between the measured surface salinity and the integrated freshwater abundance for all cruises combined (Figure 11). The three winter cruises had only 23 stations with >0.33 m^3/m^2, but the correlation is still robust (-0.928, $p<0.05$) despite the small number of data points (Figure 12).

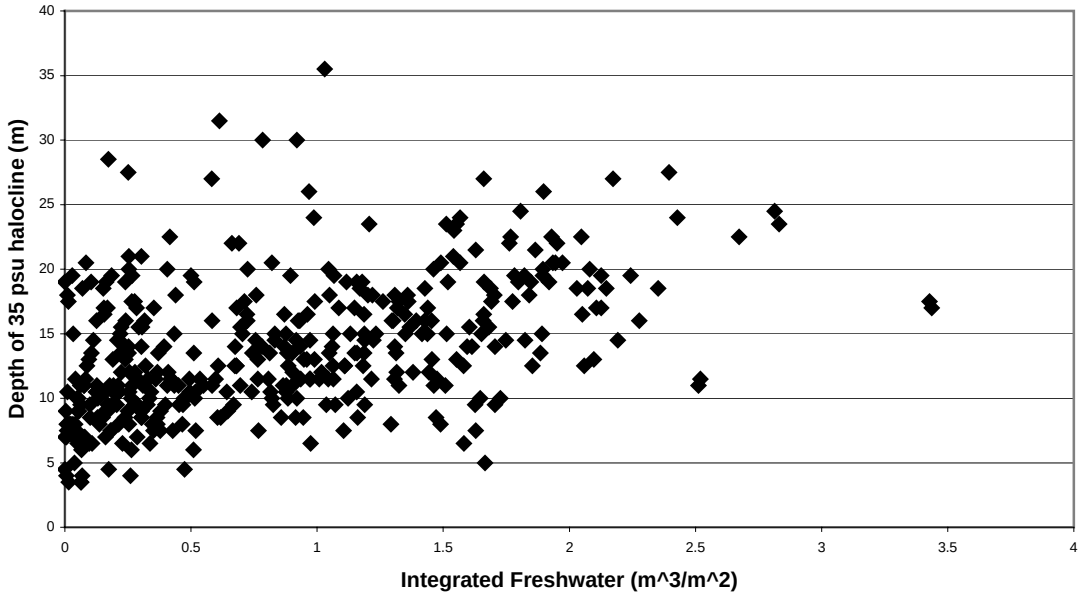

Figure 10. Comparison of integrated freshwater with depth of 35 psu halocline for all stations of all cruises.

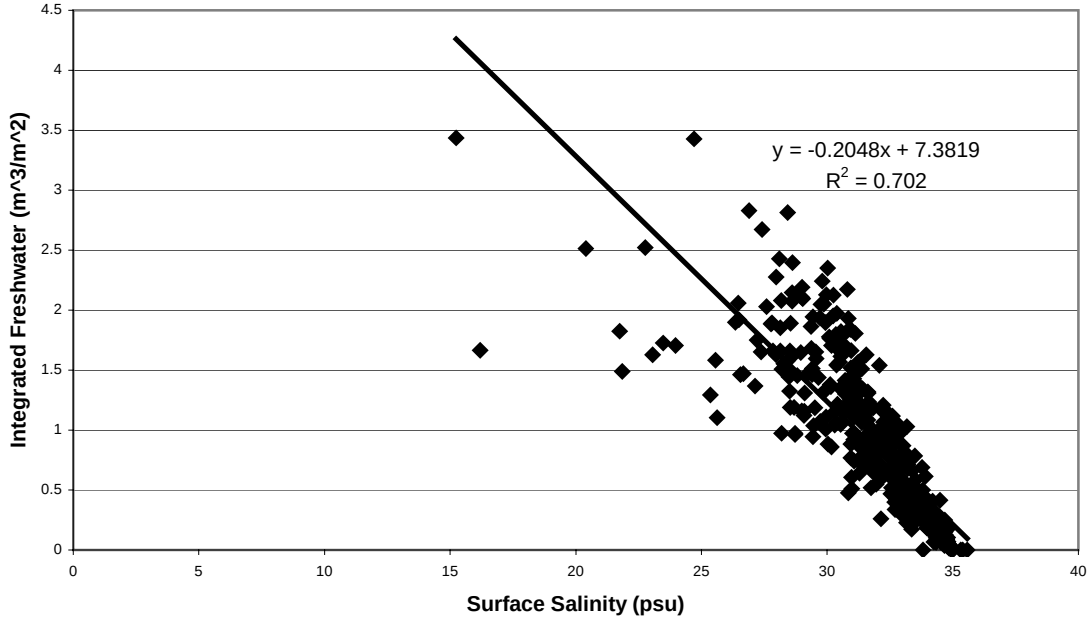

Figure 11. Comparison of integrated freshwater with surface salinity of all stations for all cruises.

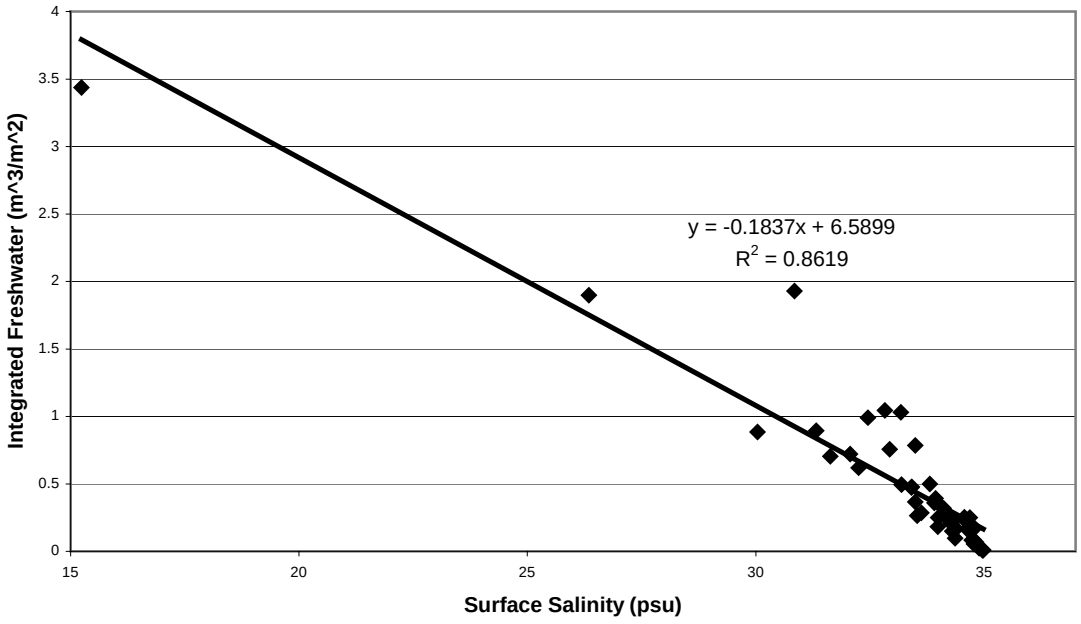

Figure 12. Comparison of integrated freshwater with surface salinity of all stations for all winter cruises.

2.4. Discussion

The abundance of freshwater in the NEGOM area is dependent upon both the amount of river outflow into the region and the incidence of river water entrainment by off shelf circulation, particularly by slope eddies. The overall importance of river discharge in determining the abundance of freshwater is governed by the interannual variation in both of these parameters. Figure 8 shows the relationship between river outflow and total integrated freshwater within the study area. All three years show a decrease in freshwater abundance summed for all 94-98 stations as mean streamflow decreases according to season.

The importance of river water entrainment by slope eddies is shown by the comparison of different seasons from the same year. For all three years of the study, the summer periods show the highest total integrated freshwater, despite that mean streamflow is highest during the spring cruises (Figure8). The relative strengths and placement of slope eddies during the three summer cruises (NEGOM 3, 6 and 9) are described by Belabbassi [2001]. That freshwater abundance is strongly influenced by eastward entrainment of Mississippi River water by anticyclonic eddies has also been reported previous to NEGOM-COH fieldwork [Kelly, 1991; Hamilton et al., 1997; Wiseman and Sturges, 1999; Biggs et al., 2000].

When considering the relative importance of slope eddies in determining the abundance of freshwater in the NEGOM region, it is important to address their periodicity. Eddies are shed from the Loop Current on an average of every 11 months, but the process is stochastic [Sturges, 1994]. For this study, all three summers had anticyclonic eddies near the Mississippi River plume, while these features were absent in the cruises conducted during other seasons. Slope eddies may in fact be typical summertime features in the NEGOM region, for they have also been documented by ship surveys and remote sensing in subsequent summers [Biggs et al., 2002].

Slope eddies likely impact upon the secondary productivity of the NEGOM region [Biggs and Ressler, 2001]. Moreover, the periodic introduction of high nutrient river water into an area that is usually considered to be oligotrophic can lead to increased

fisheries yield [Deegan et al., 1986]. Such biological productivity is likely driven by stochastic processes, rather than simply by seasonal patterns based upon the frequency and timing of river water entrainment into the NEGOM region.

The high variation in the depth of the 35 psu halocline reflects both the relative abundance of freshwater at each particular station as well as the distance from the freshwater source. Stations which were isolated from the Mississippi River outflow but had freshwater present generally showed small quantities of integrated freshwater and shallow 35 psu haloclines. Stations that were distant from the Mississippi River outflow but clearly had their freshwater source from the Mississippi River had high integrated water column freshwater and deep 35 psu haloclines. Stations that were near major freshwater sources and had high abundance of freshwater generally had relatively shallow 35 psu haloclines, but had very sharp and sudden salinity profiles.

This indicates that the depth of the 35 psu halocline is dependent upon both the total integrated freshwater abundance and the length of time that the freshwater has had to mix with the underlying saltwater. This is important in explaining the weak negative correlation between surface salinity and depth of the 35 psu halocline as well as the weak correlation between total integrated freshwater and the depth of the 35 psu halocline.

The strongest correlation between the parameters of integrated freshwater, surface salinity and depth of the 35 psu halocline was the correlation between surface salinity and integrated freshwater abundance (Figure 11). This strong negative correlation between increasing freshwater abundance with decreasing salinity can allow surface salinity to be used as a proxy for the total integrated freshwater in the water column.

Not only is this correlation statistically significant (-0.872, $p<0.05$), a regression analysis shows high enough R^2 values ($R^2>0.7$, see Figure 11) to use surface salinity as a reasonable predictor of water column integrated freshwater abundance. This could allow for reasonable calculations of freshwater abundance using continuous flow through salinity measurements. Using surface salinity as a proxy for integrated water column

freshwater allows for faster, less expensive and more comprehensive coverage of a study area. Given a high enough resolution measurement of surface salinities in an area, it would be possible to make a reasonable estimate of total freshwater volume in a given study area. With an absolute volume of freshwater within a study area, the total mass of nutrients introduced by the freshwater could be estimated based upon nutrient concentrations at the river mouth.

CHAPTER III
SURFACE AND VERTICALLY-INTEGRATED CHLOROPHYLL STOCKS

3.1. Introduction

3.1.1. In Situ Surface Chlorophyll Measurements

The measurement of surface chl-α is widely used as a means of estimating the overall phytoplankton biomass in the oceans. The time rate of change of surface chl-α is a proxy for the rate of primary production, which is an indicator of the overall biological productivity of a marine ecosystem [Qian et al., 2003]. This chapter will examine the overall surface chl-α patterns within the NEGOM study and their differences by season and hydrographic region. The subsurface chl-α profile to several irradiance levels within the euphotic zone will also be analyzed so that comparisons may be made between chl-α dynamics at near surface waters and chl-α dynamics at deeper waters that are still within the euphotic zone.

Studies based upon satellite color data have documented seasonal changes in chl-α abundance over large areas of the Gulf of Mexico, including the NEGOM study region [Muller-Karger et al., 1991; Melo-Gonzalez et al., 2000]. These changes in overall chl-α abundance can be characterized as a minimum level of surface chl-α during the spring/summer months followed by elevated chl-α abundance during the fall/winter months. This cycle is driven by low surface nutrient concentrations during the summer, caused by high stability and strong stratification of the water column. The cooling of the surface waters, coupled with stronger winds during the winter period, allows for better mixing of deeper nutrient rich waters which in turn allows for higher phytoplankton standing stocks [Belabbassi, 2001].

While this seasonal cycle is prominent over the off-shelf waters, it is not strictly the case for continental shelf waters and the inner slope regions, especially in the NEGOM study area. These regions within the NEGOM study area are subject to periodic upwelling events as well as on-shelf flow from deeper slope waters which bring nutrients into the euphotic zone. These periodic nutrient enrichments of the continental

slope and nearshelf waters are driven by shelf circulation and eddy interactions [Gilbes et al., 1996; Belabbassi, 2001; Biggs et al., 2002; Belabbassi et al., 2004 in review].

Further influencing the shelf and upper slope waters of the NEGOM study area is the presence of several freshwater sources, most notably the Mississippi River. These rivers input large amounts of nutrient-rich freshwater onto the inner continental shelf. However, and as shown in Chapter II of this thesis, Loop Current derived slope eddies can entrain large amounts of freshwater and input this water to outer shelf and upper slope regions of the NEGOM study area (see also Hamilton et al., [1997]).

The interaction of all of these factors results in a wide variety of hydrographic regions and ecosystems. Furthermore, these hydrographic regions are not static in time or space; they may persist for limited amounts of time and they may move about in and/or through the NEGOM region. This is particularly true of slope eddies and the freshwater entrainment that they can cause when they interact with the Mississippi River. These factors make the NEGOM study area a highly dynamic region of the ocean and makes studying the surface chl-α within the region both challenging and particularly interesting.

3.1.2. In Situ Water Column Chlorophyll

In addition to the surface chl-α being highly variable in space and time within the study area, the chl-α concentrations through the water column may vary considerably based upon the local conditions of the water, physiological state of the phytoplankton, and the depth rate of change in irradiance [Cullen, 1998; Jochens et al., 2002; Qian et al., 2003]. As such, the surface chl-α concentrations are seldom representative of the overall chl-α abundance within the water column, or overall productivity within the system. As a result, it is useful to determine if surface chl-α concentrations are representative of overall chl-α abundance through the water column.

The NEGOM program of study is a particularly good candidate for this analysis as it contains a large number of sampling stations that encompass a variety of hydrographic conditions. This allows us to observe changes in water column chl-α

abundance according to a wide variety of factors, including depth, light profile, nutrient abundance, and freshwater abundance. This comparison between surface chl-α and water column chl-α is also important in relation to the use of remote sensing techniques to measure chl-α abundance. These techniques are limited to the upper reaches of the water column and cannot infer the abundance of chl-α beyond the first optical depth.

The first section of analysis simply compares the variability of surface chl-α concentrations by season and by hydrographic region. As mentioned above, the hydrographic regions may shift and change from one sampling period to another, and so the cruise by cruise designations for the hydrographic regions described in the previous chapter will be applied to this chapter as well.

The second analysis of this chapter examines the changes in chl-α concentration through the water column to a series of discrete depths based upon surface light penetration. These depths were selected because they represent intervals that are relevant to the other aspects of this study, i.e. the 1st optical depth, secchi disc depth and the estimated bottom of the euphotic zone. The integrated chl-α mass will be compared with the surface chl-α concentrations to determine when and where surface chl-α concentrations can be used to predict overall chl-α abundance through the water column.

3.1.3. Purpose of Research

Because previous studies of seasonal cycle in chl-α in the Gulf of Mexico [i.e. Muller-Karger et al., 1991] had primary emphasis on the outer slope and deepwater regions of the Gulf of Mexico, they did not emphasize regions that have large freshwater inflow. Clearly the proximity of the Mississippi River and other freshwater sources within the NEGOM study area introduce another factor that should influence the observed cycle in surface chl-α concentrations. Because I hypothesized that the seasonal cycle of chl-α concentrations within the NEGOM study area differs from that found in previous studies, in this chapter comparisons are made between mean surface chl-α concentrations of each season and compared to those of the previous study.

Because I further hypothesize that the relationship between surface chl-α concentrations and water column chl-α mass varies based upon the integration depth used and the hydrographic regime present, this chapter also presents station by station comparisons of surface chl-α concentrations with vertically integrated chl-α mass to distinct integration depths. These comparisons are analyzed according to hydrographic region.

3.2. Methods

Subsurface profiles of chlorophyll-α fluorescence were taken at all CTD stations of each cruise, with data being logged at 0.5 meter intervals, using a Chelsea Aquatrakka fluorometer. Continuous profiles of downwelling PAR were measured at those stations occupied during the daytime using a Biospherical Instruments, Inc., Model QSP-200L sensor. Underway measurements of near surface fluorescence were logged once a minute using a continuous-flow Turner Designs model 10 fluorometer. Additional instrument information and sampling methods for chl-α extractions are given in Jochens and Nowlin [1998].

Vertical profiles of PAR were used to calculate the depth of 36.8% surface light penetration (1^{st} optical depth), 18% surface light penetration (traditional secchi depth) and the depth of 1% surface light penetration (assumed compensation depth). Because data logging for the vertical profiles did not always begin at the surface (average depth of 2.5 meters), it was necessary to calculate the inferred surface PAR using the light extinction coefficient (k) for the surface waters. This was done on a station-by-station basis.

Chl-α concentrations at depth were estimated from the fluorescence values (volts) measured by the Chelsea fluorometer based upon the calibration samples collected from water drawn from the hull depth of 3.5m that was pumped into the ship's lab to the continuous flow fluorometer. Surface chl-α concentrations, as determined

from fluorescence values for the continuous flow fluorometer, were plotted against the voltage values for the Chelsea fluorometer at the depth of 3.5 meters and an exponential regression line was drawn for this relationship. Separate regression calculations were done for high chl-α (freshwater influenced) and low chl-α (freshwater absent) regimes. Separate calculations were also done for each individual cruise. An example of the regression equation is given below, representing the summer, 2000 (N9) high chl-α regression equation and Figure 13 shows the regression curve.

$$Y=0.0075e^{3.5946X}$$

Where Y equals the estimated chl-α concentration in mg/m^3, and
X equals the measured Chelsea voltage.

This equation was applied to the Chelsea voltage of each 0.5 meter depth bin of the vertical profile. This allowed the estimation of chl-α concentration for each 0.5 meter depth bin through the water column to the appropriate depth. Next, the mass of chl-α of all depth bins for that CTD station were summed according to the following equation:

$$M_{chl\text{-}\alpha} \quad \sum_{i=1}^{n} C_i V_i$$

Where $M_{chl\text{-}\alpha}$ = Total mass of chl-α in the water column for that station (mg/m^2)
and C_i = Concentration of chl-α in mg/m^3
and V_i = Volume in integration bin i ($0.5\ m^3$)
and n = the number of integrations for depth X

The surface (z=0) PAR value had to be inferred for all CTD stations due to the fact that data logging began at depths significantly deeper than the sea surface (average

of 2.5 meters). To avoid underestimating the integration depths it was necessary to extrapolate the true surface PAR values based upon the shallowest PAR measurements

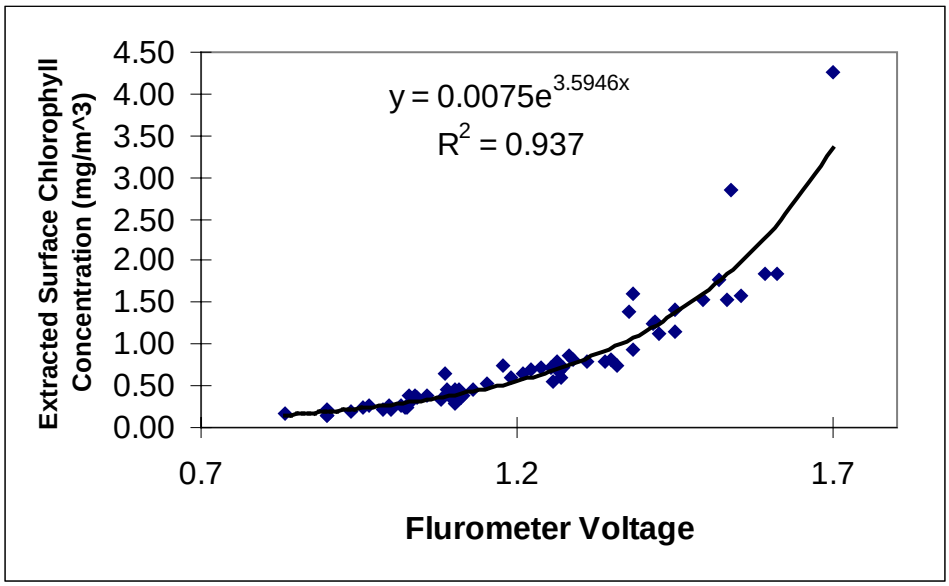

Figure 13. Sample regression curve used to estimate chlorophyll-α concentrations at depth according to CTD fluorometry profiles. Note that the Chelsea fluorometer functions on a logarithmic scale, resulting in the exponential relationship between fluorometer voltage and extracted surface chlorophyll-α concentrations. This regression is from the high chlorophyll-α waters of the summer, 2000 (N9) cruise.

and the light extinction coefficient (k) of the surface waters. Light extinction coefficients (k) were calculated separately for each daytime CTD station that had sufficient light levels by plotting the vertical profiles of PAR on a logarithmic scale. Each of these k values was then used to back-calculate the approximate surface PAR values for each individual station according to the following equation:

$$\text{Log}_{10}(I_0) = ((k*X)+\text{Log } I_x)$$

Where k = the light extinction coefficient
and X = the depth of the shallowest PAR measurement available

The PAR calculations for the 36.8%, 18%, and 1% light penetration depths were done by simply multiplying the inferred surface PAR with 0.368, 0.18 or 0.01 as appropriate. The chl-α mass integration calculations were done to the depth that corresponded with this calculated subsurface PAR for each CTD station.

3.3. Results

3.3.1. Seasonal Trends in Surface Chlorophyll Concentrations and Distribution

This section describes the seasonal patterns of distribution and abundance of chl-α within the NEGOM study area. The emphasis of this section is the description of seasonal patterns of surface chl-α concentration and the seasonal patterns of overall chl-α abundance through the water column. Contour plots of surface chl-α concentrations for each cruise are given in Figure 18.

The integrated chl-α calculations are measured to the 36.8% surface PAR depth (1st optical depth), 18% surface PAR depth (traditional secchi disc depth) and the 1% surface PAR depth (compensation depth). These depths were chosen as being representative of the water depth measured by remote sensing techniques (36.8%), overall phytoplankton abundance in the surface waters (18%) and of the total abundance of photosynthetic plankton through the water column (1%).

The depth to which these integrations are calculated is also given analysis in this section, as this both determines the overall mass of integrated chl-α in the water column and is itself determined by the concentrations of chl-α and other particulates in the surface waters. Attention is also given to the variations in the vertical profiles of chl-α concentrations based upon the three different hydrographic regimes described previously

(freshwater, bluewater and coastal). Each of these hydrographic regimes shows distinct trends in the vertical profile of chl-α concentration, particularly the placement of the depth of chl-α maximum. These differences in the vertical chl-α concentration profiles can influence the total integrated chl-α abundance values depending upon the depth of integration and the placement of the chl-α maximum depth.

3.3.1.1. Surface Chlorophyll Distribution for Winter Cruises (NEGOM1, NEGOM4 and NEGOM7)

The mean surface chl-α concentrations for the all cruises are summarized in Table 4. The mean surface chl-α concentrations for the winter cruises were generally lower than in the other seasons, with the exception of spring, 2000 (N8). The winter mean surface chl-α concentrations were significantly lower (ANOVA, $p<0.01$) than each of the summer cruise periods. In spring and summer, the majority of stations within the study area had chl-α concentrations >0.5 mg/m^3, which reflects both the existence of localized areas of relatively high chl-α concentrations that were restricted to coastal areas and the redistribution of freshwater by slope eddies.

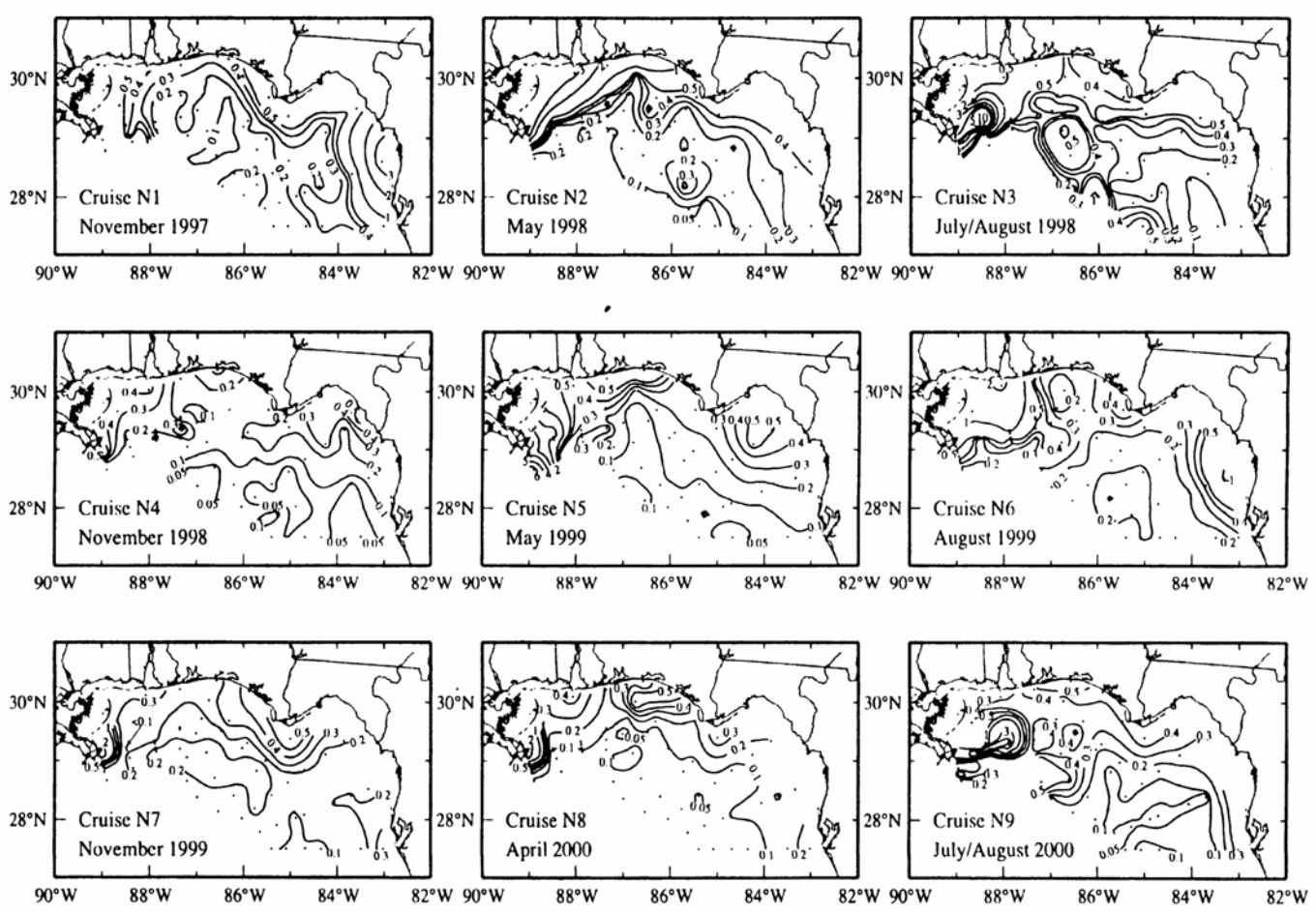

Figure 14. Surface chl-α concentration contour plots for all of the 9 NEGOM cruises. Units are in mg/m^3. Figures from Jochens et al., 2002.

Table 4. Summary of surface chl-α data for the nine NEGOM cruises. Integrated freshwater units are m^3/m^2 for 98 stations combined. All chl-α units are in mg/m^3.

CRUISE	Season	Integrated Freshwater	Mean Surface CHL (all)	Mean Surface CHL (Freshwater)	Mean Surface CHL (Bluewater)	Mean Surface CHL (Coastal)
NEGOM1	winter	10.05	0.50	0.66	0.25	0.22
NEGOM4	winter	10.72	0.42	1.20	0.29	0.79
NEGOM7	winter	3.01	0.38	1.09	0.34	0.48
NEGOM2	spring	52.01	0.84	1.64	0.26	0.70
NEGOM5	spring	36.87	0.64	1.34	0.21	0.81
NEGOM8	spring	7.97	0.25	0.97	0.18	0.30
NEGOM3	summer	105.28	0.90	1.02	0.31	0.99
NEGOM6	summer	87.13	0.88	1.03	0.22	0.63
NEGOM9	summer	38.20	0.89	1.59	0.37	0.67

Because both the amount of river flow and the intensity and location of slope eddies varied in the 1997-2000 period, there is variable placement of these high surface chl-α concentration areas on an interannual basis. In winters though, the high surface chl-α concentrations are primarily restricted to the areas directly adjacent to the river outflow areas. The distribution of these regions can be seen in the surface chl-α contour plots for the winter cruises (Figure 14) and the false color satellite images of surface chl-α concentration for the winter months (Figure 15).

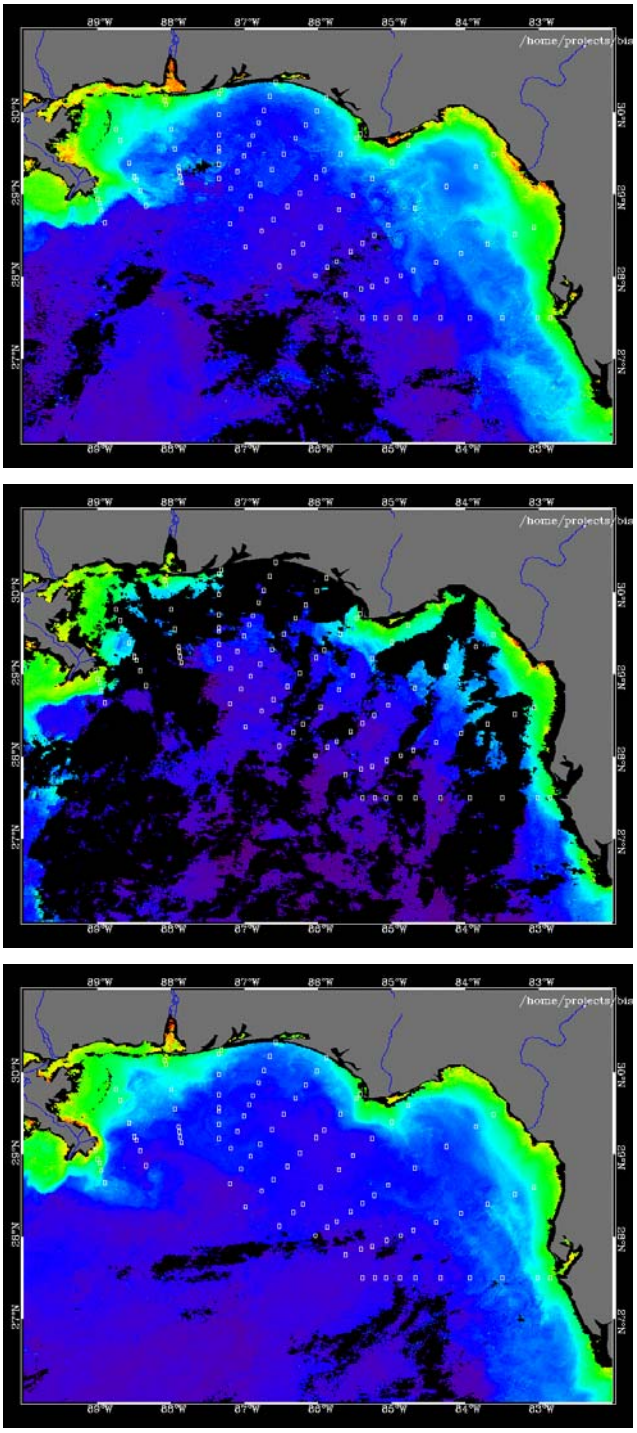

Figure 15. SeaWiFS false color satellite images of surface chlorophyll-α concentrations for the winter NEGOM cruises. Top image is NEGOM1, middle image is NEGOM4, and bottom image is NEGOM7. Images and data processing courtesy of Bisman Nababan and Chuanmin Hu of the University of South Florida.

3.3.1.2. Surface Chlorophyll Distribution for Spring Cruises (NEGOM2, NEGOM5 and NEGOM8)

The mean Surface chl-α concentrations for the spring cruises are summarized in Table 4. The overall surface chl-α concentrations for the spring cruises were higher than the winter cruises, except for spring, 2000 (N8) which had significantly lower overall surface chl-α concentrations than the two other spring cruises. The majority of stations for the spring cruises had surface chl-α concentrations <0.5 mg/m^3.

As was the case for the winter cruises, the regions of highest surface chl-α concentrations are generally restricted to the regions adjacent to the mouths of the major freshwater sources in the region. However, these regions, in general, extend further offshore compared to the winter cruises. The distribution of these regions can be seen in the surface chl-α contour plots for the winter cruises (Figure 14) and the false color satellite images of surface chl-α concentration for the spring months (Figure 16).

3.3.1.3. Surface Chlorophyll Distribution for Summer Cruises (NEGOM3, NEGOM6 and NEGOM9)

The mean surface chl-α concentrations for the summer cruises are summarized in Table 4. Overall, surface chl-α concentrations for the summer cruises were the highest for all of the nine cruises. These surface chl-α concentrations were significantly higher than those of the winter cruises and of the spring, 2000 (N8) cruise. The reason for this high overall surface chl-α concentrations within the study area is due to the redistribution of freshwater within the study area for all three of the summer cruises. The placement of areas with high surface chl-α concentrations are also distinctly different from the winter and spring cruises due to the manner by which the freshwater was introduced into the study area. The presence of large amounts of freshwater within the study area during the three summer cruises is due to the presence of slope eddies south and southeast of the Birdsfoot Delta. These slope eddies entrain Mississippi River

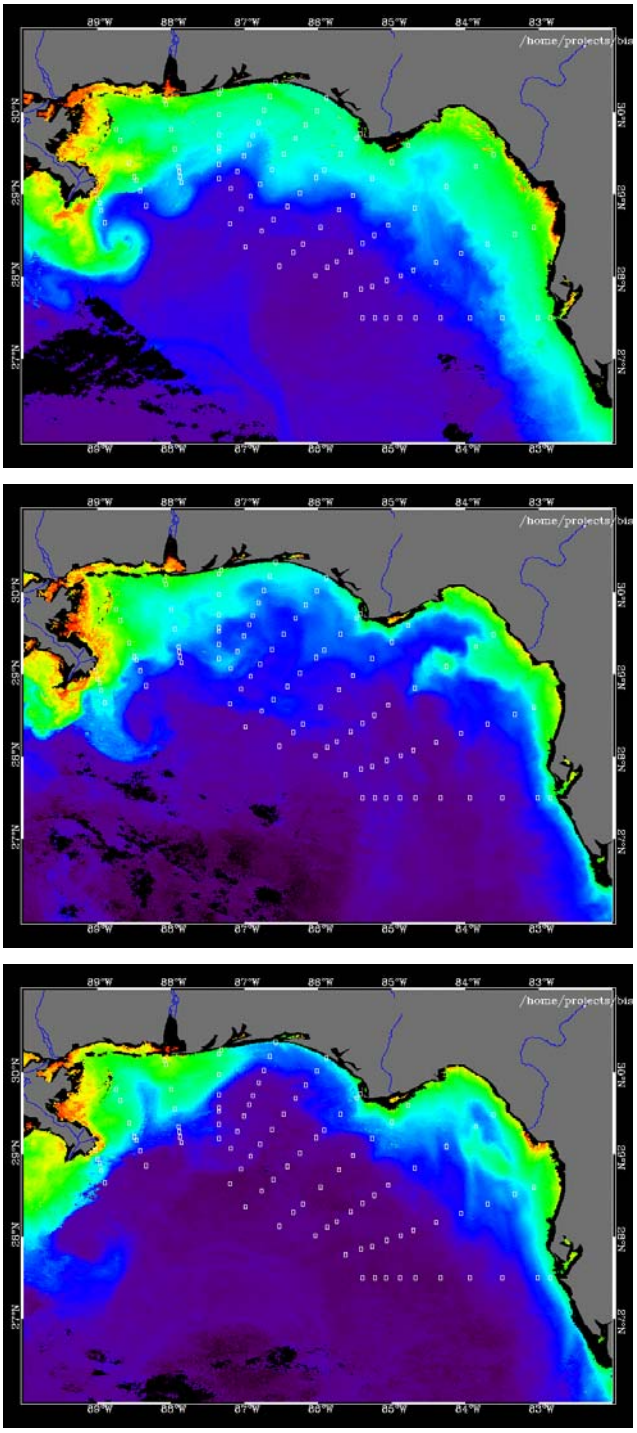

Figure 16. SeaWiFS false color satellite images of surface chlorophyll-α concentrations for the spring NEGOM cruises. Top image is NEGOM2, middle image is NEGOM5, and bottom image is NEGOM8. Images and data processing courtesy of Bisman Nababan and Chuanmin Hu of the University of South Florida.

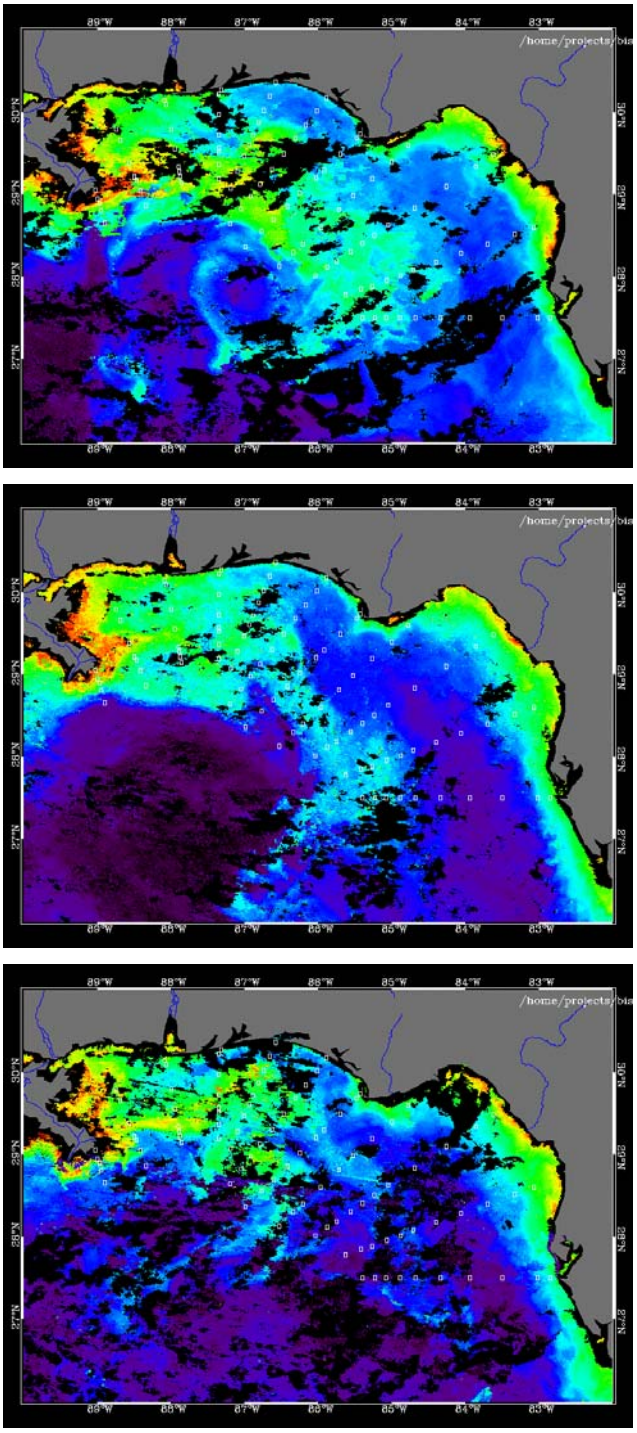

Figure 17. SeaWiFS false color satellite images of surface chlorophyll-α concentrations for the summer NEGOM cruises. Top image is NEGOM3, middle image is NEGOM6, and bottom image is NEGOM9. Images and data processing courtesy of Bisman Nababan and Chuanmin Hu of the University of South Florida.

water and they transport that water within the study area. The extent of the freshwater entrainment and the resulting high surface chl-α regions are clearly seen from the false color satellite images for the summer cruise periods (Figure 17) and in the surface chl-α contour plots for the summer cruises (Figure 14). That substantial amounts of this entrained water get transported into the outer shelf and continental slope areas is evident, nearly half of the stations on each summer cruise had surface chl-α concentrations >0.5 mg/m^3. Many of these stations with high surface chl-α concentration are found far offshore and extending far to the east of the source of entrained water.

Table 5. Summary of chl-α integration data for the nine NEGOM cruises. Integrated freshwater units are m^3/m^2 and integrated chl-α units are mg/m^2.

CRUISE	Season	Integrated Freshwater	Mean 36.8% Light Depth (m)	Mean 18% Light Depth (m)	Mean 1% Light Depth (m)	Mean Integrated CHL at 36.8%	Mean Integrated CHL at 18%	Mean Integrated CHL at 1%
NEGOM1	winter	10.05	6.20	12.26	42.65	2.80	5.27	19.60
NEGOM4	winter	10.72	6.80	14.93	55.88	2.14	4.42	17.50
NEGOM7	winter	3.01	6.51	16.38	57.31	2.00	4.96	17.82
NEGOM2	spring	52.01	6.25	12.10	48.60	2.30	3.87	19.3
NEGOM5	spring	36.87	7.29	15.27	47.08	1.76	4.33	17.30
NEGOM8	spring	7.97	6.91	16.91	50.56	1.18	2.88	8.83
NEGOM3	summer	105.28	5.39	8.54	35.86	4.33	6.64	21.30
NEGOM6	summer	87.13	5.10	8.65	34.31	3.02	6.71	19.92
NEGOM9	summer	38.20	5.12	9.78	36.32	2.86	4.98	17.00

3.3.1.4. Integrated Chlorophyll Abundance at 36.8% Surface Light Penetration Depth for Winter Cruises (NEGOM1, NEGOM4 and NEGOM7)

The last 3 columns of table 5 summarize the mean integrated chl-α (mg/m^2) from the surface to the 36.8%, 18%, and 1% light penetration depth. The vertically integrated chl-α (mg/m^2) to the 36.8% light penetration depth for the winter cruises ranged from 0.75 mg/m^2-11.07 mg/m^2, with a mean of 2.50 mg/m^2. As an overall trend, coastal

stations and freshwater stations had greater integrated chl-α mass than bluewater stations. There is a robust (>0.700, $p<0.05$) positive correlation between surface chl-α concentrations and vertically integrated chl-α to the 1st optical depth (Figure 18). This relationship is statistically significant in all three hydrographic regimes, although the correlation is lowest for the bluewater stations.

3.3.1.5. Integrated Chlorophyll Abundance at 36.8% Surface Light Penetration Depth for Spring Cruises (NEGOM2, NEGOM5 and NEGOM8)

The vertically integrated chl-α (mg/m^2) to the 36.8% light penetration depth for the spring cruises ranged from 0.39 mg/m^2-9.30 mg/m^2, with a mean of 1.70 mg/m^2. There is no discernable overall trend in the distribution of stations with high and low integrated chl-α mass. There is a fairly even distribution of high and low integrated chl-α stations within each of the three hydrographic regimes. However, most of the spring stations in the higher range of integrated chl-α for this integration depth are the shallower stations with high surface chl-α concentrations as opposed to stations with deeper integration depths and lower surface chl-α concentrations. Among the spring cruises, spring, 2000 (N8) had a much lower mean integrated chl-α to the 1st optical depth compared to the other spring cruises, most likely due to the lower amount of freshwater within the study area during this cruise. There is a robust (>0.700, $p<0.05$) positive correlation between surface chl-α concentrations and total integrated chl-α mass to the 1st optical depth (Figure 18). This relationship is conserved for all three hydrographic regimes, though the correlation value is lowest for the bluewater stations.

3.3.1.6. Integrated Chlorophyll Abundance at 36.8% Surface Light Penetration Depth for Summer Cruises (NEGOM3, NEGOM6 and NEGOM9)

The vertically integrated chl-α (mg/m^2) to the 36.8% light penetration depth for the summer cruises ranged from 0.40 mg/m^2-20.50 mg/m^2, with a mean of 3.30 mg/m^2. The freshwater region had the majority of stations that fell within the higher range of integrated chl-α. The higher range of integrated chl-α stations for this integration depth are dominated by stations with shallower integration depths, particularly those stations from the freshwater region that had very high surface chl-α concentrations. There is a robust (>0.600, $p<0.05$) positive correlation between surface chl-α concentrations and vertically integrated chl-α to the 1st optical depth (Figure 18). This relationship is statistically significant in all three hydrographic regimes, although the correlation value is lowest for the bluewater stations. The relative weakness of the bluewater correlation is most likely due to the limited number of stations as well as the limited range of values for these stations as opposed to a weak relationship between surface chl-α and integrated chl-α mass for this integration depth.

3.3.1.7. Integrated Chlorophyll Abundance at 18% Surface Light Penetration Depth for Winter Cruises (NEGOM1, NEGOM4 and NEGOM7)

The vertically integrated chl-α (mg/m^2) at the 18% light penetration depth for the winter cruises ranged from 0.50 mg/m^2-17.60 mg/m^2, with a mean of 4.80 mg/m^2. In general, there are robust (>0.700, $p<0.05$) positive correlations between wintertime surface chl-α concentrations and wintertime vertically integrated chl-α at the 18% light penetration depth for the freshwater and coastal stations (Figure 19).

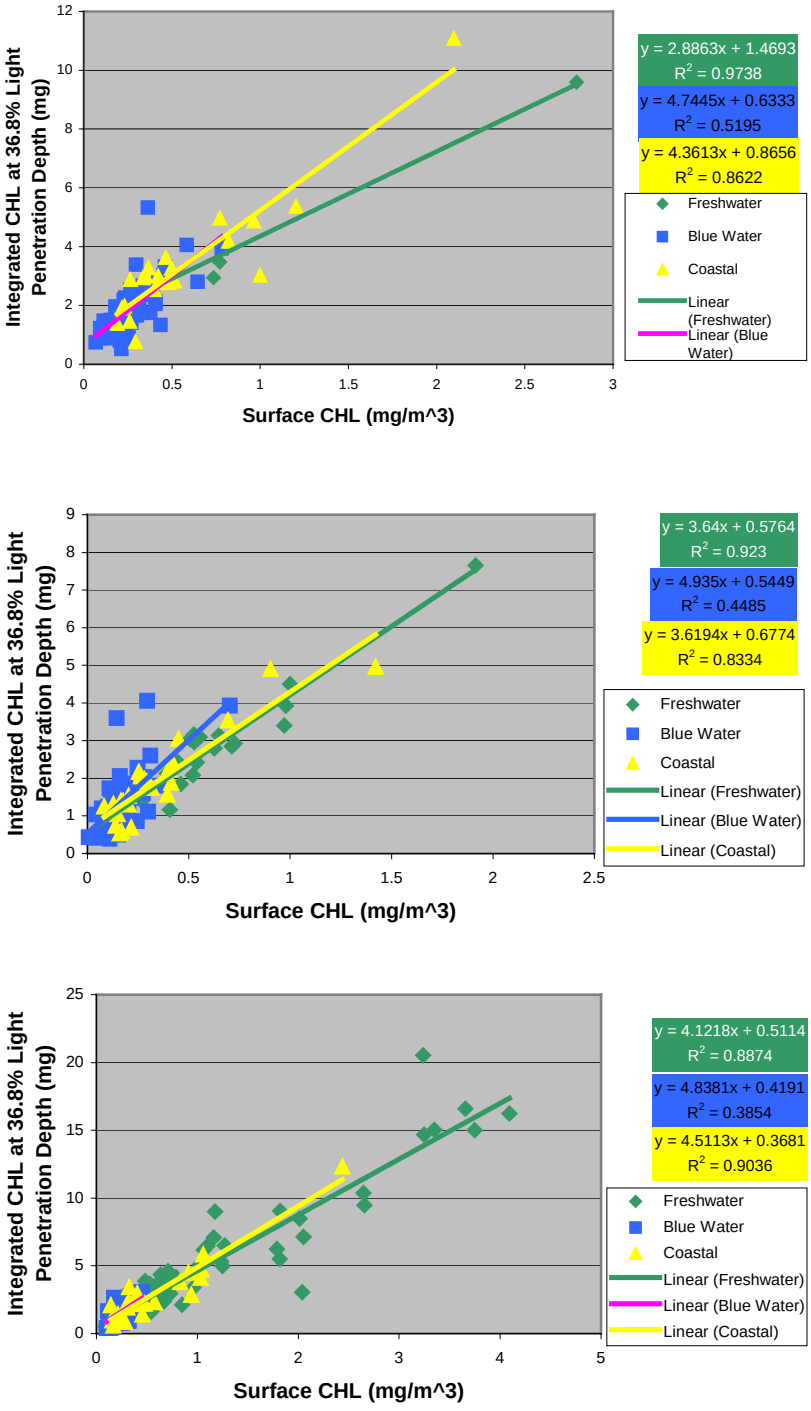

Figure 18. Comparison of surface chlorophyll-α concentration with integrated chlorophyll-α to the 1st optical depth for all cruises. Top figure is winter cruises, middle figure is spring cruises, and bottom figure is summer cruises.

3.3.1.8. Integrated Chlorophyll Abundance at 18% Surface Light Penetration Depth for Spring Cruises (NEGOM2, NEGOM5 and NEGOM8)

The vertically integrated chl-α (mg/m^2) at the 18% light penetration depth for the spring cruises ranged from 0.53 mg/m^2-30.10 mg/m^2, with a mean of 3.70 mg/m^2. Spring, 2000 (N8) had a much lower average integrated chl-α compared to the other spring cruises. The lower values for vertically integrated chl-α for the spring, 2000 (N8) cruise, compared to the other spring cruises, are due to lower chl-α concentrations at the surface and at depth. The integration depths for spring, 2000 (N8) are deeper that the other spring cruises, giving lower values for integrated chl-α is due to a lower volume of water being sampled.

For the spring cruises there is a robust (>0.800, $p<0.05$) positive correlation between surface chl-α concentrations and vertically integrated chl-α mass at the 18% light penetration depth for the freshwater and coastal stations (Figure 19). The highest values of total integrated chl-α at the 18% light penetration depth are found at the stations that have the highest abundance of freshwater, regardless of integration depth. The lower values of total integrated chl-α at the 18% light penetration depth are generally the stations on the outer shelf slope, regardless of integration depth.

3.3.1.9. Integrated Chlorophyll Abundance at 18% Surface Light Penetration Depth for Summer Cruises (NEGOM3, NEGOM6 and NEGOM9)

The vertically integrated chl-α (mg/m^2) at the 18% light penetration depth for the summer cruises ranged from 0.63 mg/m^2-26.93 mg/m^2, with a mean of 6.20 mg/m^2. There is a robust (>0.800, $p<0.05$) positive correlation between surface chl-α concentrations and vertically integrated chl-α mass at the 18% light penetration depth for the freshwater and coastal stations (Figure 19). This correlation does not hold true for the bluewater stations, of which there are very few and among which there are large variations in the integration depth. As with the spring cruises, the highest values of total

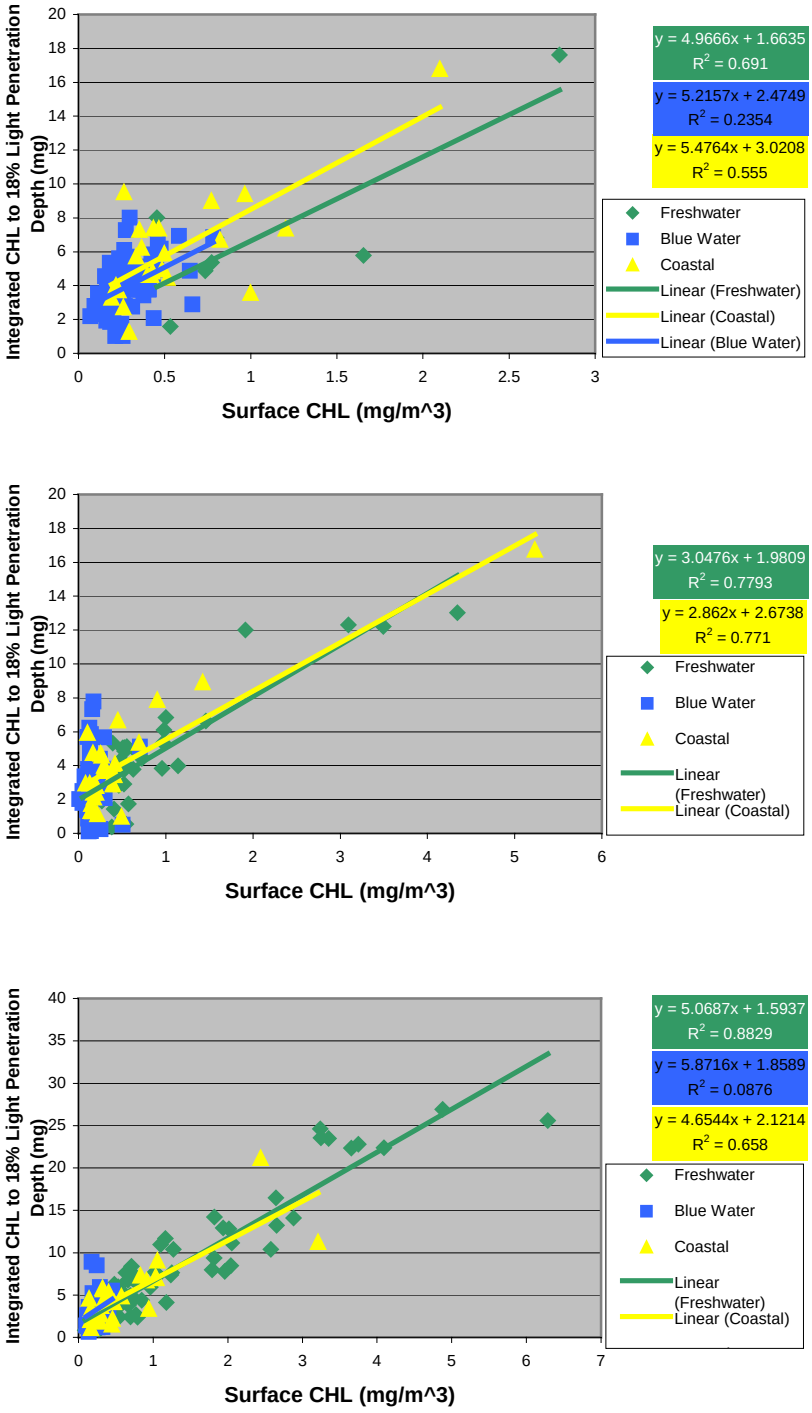

Figure 19. Comparison of surface chlorophyll-α concentration with integrated chlorophyll-α to the secchi disc depth for all cruises. Top figure is winter cruises, middle figure is spring cruises, and bottom figure is summer cruises.

integrated chl-α at the 18% light penetration depth are found at the stations that have the highest abundance of freshwater, regardless of integration depth. Also similar with the spring cruises, the lower values of total integrated chl-α mass at the 18% light penetration depth are generally the stations on the outer shelf slope that do not have freshwater, regardless of integration depth.

3.3.1.10. Integrated Chlorophyll Abundance at 1% Surface Light Penetration Depth for Winter Cruises (NEGOM1, NEGOM4 and NEGOM7)

The vertically integrated chl-α (mg/m^2) at the 1% light penetration depth for the winter cruises ranged from 3.84 mg/m^2-47.07 mg/m^2, with a mean of 18.00 mg/m^2. As an overall trend in the distribution of high values of integrated chl-α, the higher values of integrated chl-α were found at nearshore stations that had high surface chl-α concentrations or at outer shelf slope stations that had deeper integration depths. The majority of the stations had integrated chl-α values that are near the mean value of 18.00 mg/m^2. There is a weak (>0.500, $p<0.05$) correlation between surface chl-α concentrations and vertically integrated chl-α to the 1% light penetration depth for the freshwater and coastal stations (Figure 20).

3.3.1.11. Integrated Chlorophyll Abundance at 1% Surface Light Penetration Depth for spring Cruises (NEGOM2, NEGOM5 and NEGOM8)

The vertically integrated chl-α (mg/m^2) to the 1% light penetration depth for the spring cruises ranged from 3.59 mg/m^2-34.45 mg/m^2, with a mean of 15.00 mg/m^2. The spring, 2000 (N8) cruise showed distinctly different overall values for the vertically integrated chl-α at the 1% light penetration depth compared to the other spring cruises. The mean vertically integrated chl-α is much lower for the spring, 2000 (N8) stations compared to the other spring cruises. This is despite the fact that spring, 2000 (N8) has

deeper integration depths than the other spring cruises. The surface chl-α concentrations and the chl-α concentrations at depth are much lower, as a whole, than those found during the other spring cruises. The reason for the low overall integrated chl-α mass in spring, 2000 (N8) is due to the relative absence of freshwater within the study area compared to the other spring cruises.

The highest values for the vertically integrated chl-α at the 1% light penetration depth for spring, 1998 (N2) and spring, 1999 (N5) are found at the nearshore stations that have a high abundance of freshwater. Aside from these high values found at a few stations, the majority of the stations from these two cruises have relatively deep integration depths and have integrated chl-α mass values that are consistently near the mean value of 18.00 mg/m^2 for the two cruises. The comparison of surface chl-α with vertically integrated chl-α to the 1% light penetration depth (Figure 20) shows a weak (>0.300, $p<0.05$) positive correlation between the two parameters for the stations from all three hydrographic regions.

3.3.1.12. Integrated Chlorophyll Abundance at 1% Surface Light Penetration Depth for summer Cruises (NEGOM3, NEGOM6 and NEGOM9)

The vertically integrated chl-α (mg/m^2) at the 1% light penetration depth for the summer cruises ranged from 3.80 mg/m^2-51.96 mg/m^2, with a mean of 19.00 mg/m^2. There is a robust (>0.700, $p<0.05$) positive correlation between surface chl-α concentrations and the vertically integrated chl-α at the 1% light penetration depth for the coastal and freshwater stations (Figure 20). It should be noted, however, that several stations do not follow this trend due to special circumstances. Several of the coastal stations had relatively low surface chl-α concentrations with high vertically integrated chl-α to the 1% light penetration depth. These particular stations have very high chl-α concentrations at or near the ocean floor. These near bottom chl-α layers are not predicted based upon the surface chl-α concentrations for these stations. At these stations, the unpredicted high total integrated chl-α at the 1% light penetration depth is

due to the very high near bottom chl-α concentrations that are not included in the 36.8 % and 18% light penetration depth integrations. The lowest values of vertically integrated chl-α were found at the stations that had little or no freshwater present and had low surface chl-α concentrations. These stations were generally on the outer shelf slope and did not contain entrained freshwater form the Mississippi River.

3.4. Discussion

The overall seasonal cycle for surface chl-α concentrations in the NEGOM region is atypical for what is expected to be an oligotrophic open ocean system. The general seasonal trend in surface chl-α concentrations expected for oligotrophic waters of a subtropical continental margin is a minima during summer periods and maximum during spring [Cullen, 1982; Muller-Karger et al., 1991; Conkright et al., 2000; Psarra et al., 2000]. In contrast, mean surface chl-α concentrations on the NEGOM cruises were highest during the summer months (Table 4).

As shown here and in Chapter II, chl-α concentrations in the near surface waters of the NEGOM area reflect both the input and the redistribution of low salinity green water. In all three of the summer NEGOM cruises, there were anticyclonic slope eddies south and southeast of the Mississippi River delta that resulted in entrainment of low salinity green water eastward and offshore [Qian et al., 2003; Bellabbassi et al., 2004 in review; Nababan et al., 2004 in review]. So the high surface chl-α concentrations observed during these summer cruises is directly linked to the amount of freshwater being redistributed within the NEGOM area.

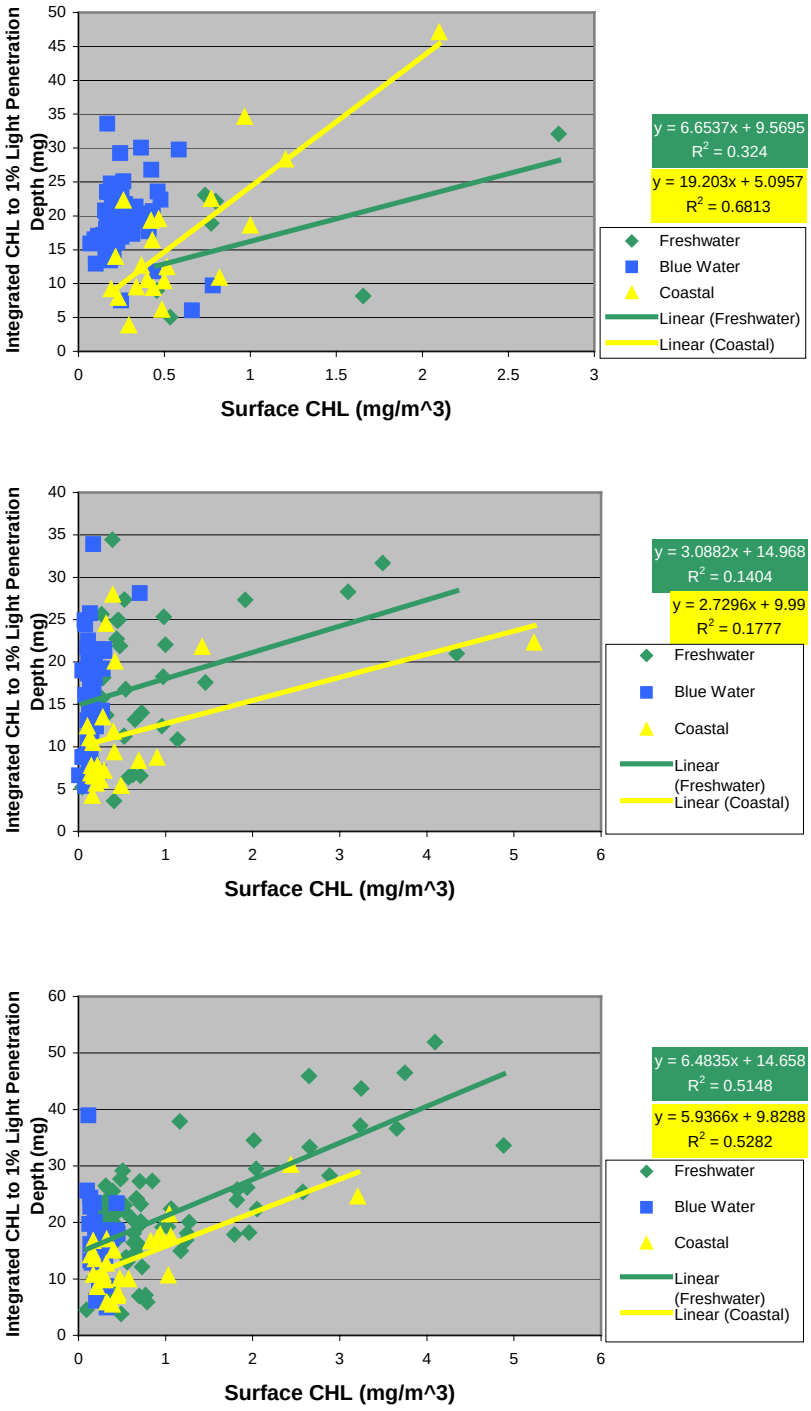

Figure 20. Comparison of surface chlorophyll-α concentration with integrated chlorophyll-α to the estimated depth of the base of the euphotic zone for all NEGOM cruises. Top figure is winter cruises, middle figure is spring cruises, and bottom figure is summer cruises.

The study by Muller-Karger et al. [1991] reported the mean surface chl-α concentrations for an area encompassing the entire Gulf of Mexico. By averaging the entire Gulf of Mexico surface, that study emphasized conditions in the offslope, deep water regions because these account for the majority of area of the Gulf of Mexico. Had a reversed seasonal cycle (i.e. high surface chl-α in summer and low surface chl-α in winter) been present in the NEGOM region, during the period (1978-1985) covered by Muller-Karger et al. [1991], that cycle would likely have been overshadowed by the off-shelf seasonal cycle which dominates the Gulf of Mexico surface area.

The determination of integrated water column chl-α to the three depths described is strongly determined by the depth of integration (Table 5). On a cruise by cruise basis there are large amplitudes in the variation of these integration depths, particularly that of the 1% light penetration depth. This is especially true when the integration depths are calculated separately for each of the three hydrographic regimes, as can be seen by the correlation analyses in appendix A and the figures in appendix B.

For example, a comparison of the integration depths with the associated integrated chl-α mass demonstrates the importance of water depth (Appendix A, Figures A1-A8). One of the most notable trends is that freshwater stations in depths shallower that 100m have no correlation between integration depth and integrated chl-α mass to any of the depths. In contrast, the freshwater stations in depths exceeding 100m have significant ($p<0.05$) positive correlation between integration depth and integrated chl-α mass to the 1st optical depth and the secchi disc depth. Such lack of correlation in water depths <100 m could be caused by several factors associated with the freshwater outflow. The shallower stations will typically be closer to the freshwater source, which can have two separate effects. First is that the closer to the freshwater source the higher the turbidity will be, thus decreasing the light penetration and integration depth. Similarly, the surface chl-α concentrations should be highest near the freshwater source. This condition could lead to very shallow integration depths with simultaneously very high water column chl-α mass in the shallower integration depths.

The river water stations have consistently shallower integration depths than the other hydrographic regimes, but there is high variation in the integration depths between different stations that are considered to be river water stations. The stations that have the shallowest of integration depths are consistently those that are directly adjacent to river outflow areas, particularly the Mississippi River outflow. Light penetration in these specific stations is particularly shallow (approximate mean of 6 meters) due to a combination of plankton biomass, CDOM and suspended sediments [Nababan et al., in review 2004]. While these stations are characterized by very high surface chl-α concentrations (>5mg/m^3) they frequently had relatively low vertically integrated chl-α abundance compared to fresh water stations with lower surface chl-α concentrations.

At stations with freshwater abundance >0.33m^3 that were relatively distant (outer shelf) from the freshwater sources showed surface chl-α concentrations that were higher by an order of magnitude than adjacent blue water stations. Yet frequently these off-margin freshwater stations had deep integration depths compared to freshwater stations closer to shore. In these cases, the relatively high chl-α concentrations were found from the surface through much of the water column, which gave these stations the highest integrated water column chl-α values compared to the majority of other stations for all cruises. This is due to deep integration depth compared to nearshore freshwater stations with much higher surface chl-α values and much higher chl-α concentrations through the water column than blue water stations that have much deeper integration depths. As such, the stations with the highest overall integrated chl-α values were the freshwater stations that were far enough from freshwater sources to allow deeper light penetration yet still maintained high chl-α concentrations in surface waters and at depth.

The bluewater stations for all cruises showed very high variability in the integration depths, particularly at the 18% surface light and 1% surface light penetration depths. This wide range of integration depths led to a wide range of integrated chl-α mass totals for the blue water stations. For example, a bluewater station that is integrated to a 30m depth may have a similar chl-α and light profile as that of a station that is integrated to a depth of 80m, but the two will have very different total integrated

chl-α mass. If at both stations the full euphotic zone has similar chl-α concentrations through depth, the amount of water column chl-α mass is nevertheless greatly affected by the shallow versus deep depth of water column.

In the case of most of these bluewater stations the deep chl-α maximum was included in the 1% surface PAR integration depth. This remains true for the stations that had relatively shallow integration depths as well as those that had very deep integration depths. This further supports the likelihood that these depths were fully representative of the full euphotic depth, regardless of variations between the integration depths between stations.

The inclusion of the deep chl-α maximum for the bluewater stations limited the occasions on which there was significant correlation between surface chl-α concentrations and integrated chl-α mass to the compensation depth. This was true for both shallower bluewater stations (<100m) and deeper stations. There was very strong correlation between surface chl-α concentrations and integrated chl-α mass to the 1st optical depth and the secchi disc depth for bluewater stations of any depth. This indicates that, under conditions where freshwater is not present and surface chl-α concentrations are low (as bluewater stations are defined in this study), surface measurements will not wholly reflect the overall chl-α mass through the euphotic zone.

Care was taken to exclude stations that might affect integration depth due to factors other than light absorption within the water column. Stations that were sampled during early morning and late afternoon frequently had insufficient surface PAR to make effective calculations of integration depth, particularly at the deeper integration depths. As such, these stations were excluded from the chl-α integration analysis, as were any stations that had strikingly different downcast versus upcast light extinction profiles. Excluded stations generally accounted for one third of the total daytime stations per cruise.

An example would be a station where the light profile shows the typical exponential decrease in PAR with depth, and then has a sudden increase of PAR at depth. This could be caused by the shadow of the ship intersecting the path of the sensor

package, or by sudden changes in the surface PAR, such as cloud cover changing the amount of light striking the ocean surface during the CTD deployment. Any stations which had unreliable light profiles were removed from the analysis, so those that were included in the analysis are assumed to be accurate profiles of light extinction and thus accurate measurements of the appropriate integration depth.

Similar steps were also taken to exclude integration depths that were found at light levels that were beyond the reliable range of sensor measurements. In many cases the surface PAR was such that the 1% PAR value was below the signal-to-noise threshold of the sensor's sensitivity. In these cases, that particular depth integration was excluded from the analysis.

Another methods variable that may become important when integrating to deeper depths, particularly for the bluewater stations, is the fact that chl-α concentration is not always an accurate gauge of phytoplankton biomass or overall primary productivity. The relative concentration of chl-α within phytoplankton cells can vary with the type of phytoplankton, the ambient light intensity, nutrient concentrations, and the overall physiological health of the shade-adapted organism [Cullen, 1982; Muller-Karger et al., 1991; Qian et al.,2003; Wawrik et al., 2003].

This variability between phytoplankton biomass and chl-α concentrations is particularly prominent at lower light intensities where increased chl-α concentrations are needed to effectively utilize all available light [Cullen, 1982]. This is quite likely the case for the chl-α maximum at the bluewater stations, which is almost exclusively found at the lower boundary of the euphotic zone for these stations. As such, the inclusion of these chl-α maximum depth bins may cause the overall measurements of total integrated chl-α mass to overestimate phytoplankton biomass (and overall productivity) through this integration depth.

The coastal stations for all cruises had a wide variety of integrated chl-α mass measurements caused by several different factors. First is different bottom depth at these coastal stations. In many cases at the bottom depth, light intensities generally exceeded the 1% and sometimes even 18% of surface PAR intensities. In these cases the

chl-α mass totals were integrated to the bottom depth of the station. As some inner stations were at water depths of 10-20 m, this resulted in low total integrated chl-α mass when compared with adjacent stations in middle-shelf water depths, especially if both had high chl-α concentrations through the entire water column.

Another factor that increased the variability in total integrated chl-α mass at the coastal stations was the geographically variable presence of near bottom high chl-α layers. These near bottom high chl-α layers were typically found on the west Florida shelf in depths ranging from 20m to 30m, but they were also found at other coastal stations of different locations and depths. These near bottom high chl-α layers were characterized by sudden increases in chl-α concentration within a depth interval of only a few meters off bottom. This was often a chl-α increase of up to three times the concentrations found a few meters higher in the water column. Such near bottom high chl-α concentrations frequently doubled the 18% surface PAR and 1% surface PAR integrated chl-α masses, compared to integrations at adjacent stations lacking such near bottom high chl-α concentrations.

While these near bottom chl-α layers have a similar effect upon the integrated chl-α mass as does the deep chl-α maximum of the bluewater stations, the nature of these near bottom chl-α concentrations is likely different from the deep chl-α maximum in the bluewater stations. The deep chl-α maximum of the bluewater stations is typically found at the lower reaches of the euphotic zone and as such it is most likely representative of increase chl-α concentration per phytoplankton biomass [Cullen, 1982; Cullen and Lewis, 1995]. However, the near bottom high chl-α layers within the coastal stations are typically found at light intensities greater than those that contain the lower limits of the euphotic zone. As a result, it is not likely that the increase in chl-α concentration is due to increased chl-α concentrations per phytoplankton biomass. It seems apparent that these near bottom chl-α layers represent actual increases in phytoplankton biomass at depths that are not included in the shallower integration depths. Furthermore, if these depths are not measured by remote sensing techniques, then estimates of coastal water

column productivity based upon satellite measurements may underestimate productivity because of the exclusion of these near bottom chl-α layers.

Chl-α stocks integrated to the 36.8% surface light depth correlated best with surface chl-α concentrations. This was true for all three hydrographic regimes, regardless of season. However, the correlation between vertically integrated chl-α and surface chl-α concentrations was less robust for the bluewater stations than for coastal or freshwater stations, in all of the seasons. A weak correlation at the bluewater stations may arise from the limited number of bluewater stations, particularly the summer cruises.

Another factor that might limit the degree of correlation between these two parameters for the bluewater stations is the relatively small dynamic range of values found within the bluewater data values compared to the other two hydrographic regimes.

A rather unexpected consequence of using the 36.8% surface light integration depth was found during the initial processing of the data. This limitation involved the integration of freshwater stations with very high light extinction coefficients in the upper water column. These stations were typically those nearest the major sources of freshwater. Because data logging for PAR frequently did not begin until the sensors were deeper than 2.5 meters, PAR measurements were not available for these very shallow waters. While this was not an issue for the majority of stations, at some stations the calculated 36.8% surface light integration depths computed to be shallower than the shallowest data point available. In these cases, the 36.8% surface light depth is doubtless underestimated.

Chl-α stocks integrated to the 18% surface light depth were in general positively correlated with the surface chl-α concentrations for all of the seasons and for all hydrographic regions other than the bluewater stations. The correlation between surface chl-α and vertically integrated chl-α was in general strongest for the freshwater stations. The correlation was weakened somewhat for the coastal stations, especially at stations that had uncharacteristically large integrated chl-α masses compared to the surface chl-α concentrations. Upon closer examination, these stations were found to be those that had

near bottom chl-α maxima shallower than the 18% surface light depths. Such near bottom high chl-α layers were responsible for these stations deviating from the trend established by the other coastal stations.

Chl-α stocks integrated to the 1% surface light depth correlated poorly with surface chl-α concentrations, for all of the hydrographic regimes. The coastal stations, as above, had several cases where near bottom high chl-α layers gave stations very high integrated chl-α masses compared to the low surface chl-α concentrations. At bluewater stations, a wide range of vertically integrated chl-α occurred for a very small range of surface chl-α concentrations, largely depending on how much of the deep chl-α maximum was included in the integration.

CHAPTER IV
REMOTE SENSING OF OCEAN COLOR

4.1. Introduction

4.1.1. Remote Sensing Data

The availability of remote sensing technologies allows for a more complete and synoptic coverage of the study area than is practical using ship based measurements. Remote sensing techniques allow for high resolution data collection over a much larger area than is possible from ship based data collection. Furthermore, remote sensing techniques allow for a more continuous data series than can be practically accomplished by other methods. All these advantages make remote sensing technologies an invaluable tool for analyzing how well ships, with their limited temporal and spatial sampling, represent the overall conditions within a study area.

Moreover, because most ship based measurements cover a period no longer than a few weeks, rapidly forming or rapidly moving mesoscale features can be missed completely, or in contrast, they may dominate the study area during the period of the cruise. The use of satellite imagery aids in determining whether the cruise conditions are indicative of the overall area of study as well as the overall seasonal conditions within the study area. The emphasis of this chapter will be to describe the mean condition of surface chl-α abundance based upon satellite ocean color measurements. In chapter V, I will discuss how representative cruise conditions are of overall seasonal conditions between cruise periods.

4.1.2. SeaWiFS Satellite Imagery

The remote sensing data used in this study were obtained from the Institute of Marine Remote Sensing at the University of South Florida (USF), which is a regional data center for ocean color data collected by the Sea-viewing Wide Field-of-View Sensor (SeaWiFS). At USF, chl-α values are routinely computed from the SeaWiFS ocean color data for the eastern Gulf of Mexico region, within the area from 24^{o}-31^{0}N,

91°-85°W. For this thesis, I have reviewed SeaWiFS data from this area for a four year period (Oct 1997-Sep 2001) in order to include all nine of the NEGOM cruises, along with the periods between cruises and a subsequent 12 months of data post summer, 2000 (N9). This allows for a comparison of cruise conditions with the ocean conditions outside of the cruise boundaries, both spatially and temporally.

Now that the advantages of remote sensing have been summarized, however, it is useful to list some of the limitations of using the SeaWiFS data. The first of these limitations is that of temporally overlapping satellite measurements with those of in situ measurements. This problem arises primarily from the need to average data over a period of time so as to reduce loss of spatial coverage due to cloud cover and to reduce noise [Hu et al., 2000]. Thus, a cruise which may cover a study area over a two week period may have some collection sites represented by satellite data several days before or after ship sampling. This presents the quandary of averaging satellite data so that it has the highest possible temporal resolution, while maximizing the spatial coverage. These two aspects must be balanced to gain the most accurate image of ocean conditions, while simultaneously being able to have a comprehensive spatial image of the study area.

A second limitation of the SeaWiFS technology is represented by discrepancies between in situ chl-α measurements and those measured by the satellite. These discrepancies are most often encountered in inshore waters and those areas with high colored dissolved organic matter (CDOM). Bottom reflectance from shallow waters may affect measurements taken by the SeaWiFS sensor, thus potentially overestimating surface chl-α concentrations. High CDOM concentrations may also contribute to overestimation of surface chl-α as measured by the SeaWiFS satellite. This is particularly relevant for areas affected by relatively undiluted river runoff, which thus carry highest concentrations of CDOM. River water typically also contains chl-α concentrations higher than the coastal waters into which it flows. This complicates the interpretation of high chl-α measurements by satellite imagery, as it is potentially difficult to distinguish how much of the chl-α signal is due to CDOM or actual chl-α.

For both of these issues, correction algorithms have been proposed to help reduce inaccuracies in satellite measurements [Carder et al., 1999 and Hu et al., 2000].

4.1.3. Correlation of Satellite Measurements with Ship Data

While the above mentioned limitations of the satellite measurements must be addressed, there was generally strong agreement between in situ chl-α measurements and those of the SeaWiFS sensor, particularly at low concentrations (<1.5 mg/m^3). Hu et al. [2000] report mean relative error (MRE) of the satellite chl-α measurements averaged < ±35% for the winter cruises and < ±50% for the spring and summer cruises. Hu et al. [2003] further showed that with the application of an appropriate bio-optical algorithm, the MRE for the spring and summer cruises could generally be reduced to < ±39%. Such MRE values permit good estimates of surface chl-α concentrations under most conditions for the study area. Hu et al.'s [2003] summary of this study's comparison between satellite measured surface chl-α and in situ surface chl-α for the first six NEGOM cruises is shown as Figure 21.

4.1.4. Purpose of Research

All of the aforementioned complications associated with satellite measurements of surface chl-α concentrations bring into question the reliability of these satellite measurements under certain conditions. Because eddies can redistribute freshwater inflow within the NEGOM regions, this contributes to the difficulty in accurately measuring surface chl-α concentrations by satellite. The convergence of in situ surface chl-α measurements and satellite surface chl-α measurements allows for a determination of how accurate the satellite measurements are by an in situ method. I have hypothesized that the satellite measured surface chl-α concentrations will be influenced by the hydrographic region of each station. This hypothesis was tested by comparing the mean satellite measured chl-α with ship-measured surface chl-α concentrations for each of hydrographic regions.

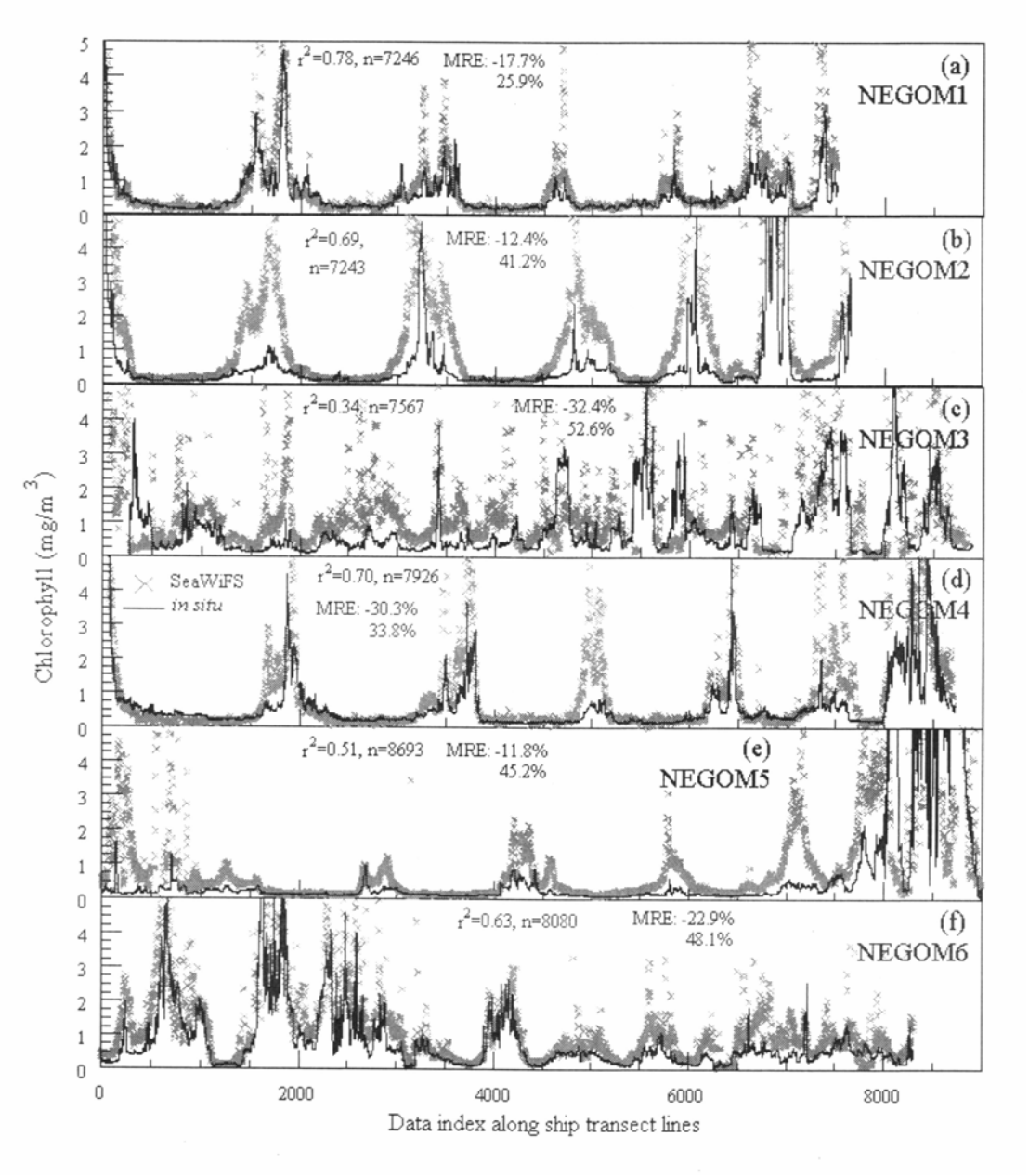

Figure 21. Comparison of satellite measured surface chl-α concentrations with in situ measured surface chl-α concentrations for six of the NEGOM cruises. Solid lines represent in situ measurements while "x"'s represent satellite measurements. Figure from Hu et al., [2003].

4.2. Methods

4.2.1. Data Processing

At USF, the ocean color algorithm OC2, (O'Reilly et al., 1998) was used to filter remote sensing reflectance data at 490 nm and 555 nm, to estimate surface chl-*a* concentrations from the ocean color backscatter data. For a further expansion of the SeaWiFS sensor methods used, refer to Hu et al. [2000]. SeaWiFS data were averaged for one week periods to reduce the loss of spatial coverage due to cloud cover. Each data point represented a weekly average chlorophyll-*a* value for a 5x5 km square centered upon each of the 98 NEGOM CTD stations. These data points include all nine NEGOM cruises in addition to the periods between each cruise, for a total time period of over 4 years. All of the data processing was done by Dr. Chuanmin Hu and his graduate student, Bisman Nababan, at the University of South Florida.

4.3. Results

4.3.1. Mean Chlorophyll Concentrations

This section overviews the mean satellite surface chlorophyll-*a* concentrations. The first analysis comprises the mean remotely sensed with ship measured surface chl-α values for each cruise, inclusive of all stations regardless of hydrographic regime. For the second analysis within this section, the mean surface chl-α values for each cruise are partitioned by hydrographic regime.

4.3.1.1. Mean Surface Chlorophyll by Cruise

The overall mean satellite measured surface chl-α for each cruise is shown compared to the overall mean in situ measured surface chl-α in Figure 22. Using a Spearman rank order comparison between the mean satellite measurements and the mean in situ measurements shows a positive relationship (r_s=0.82) between the mean

measurements from the two methods. The data used for this analysis include a large variation in surface chl-α concentrations, ranging from 0.3 mg/m^3 to as much as 28 mg/m^3. These averages also include water from all three of the previously described hydrographic regions. To limit the impact of this variation on the overall means, high surface chl-α measurements at inshore stations were subsequently removed as outliers. A more specific explanation of this process is given in the following discussion.

4.3.1.2. Weekly Mean Surface Chlorophyll

Figure 23 shows the weekly overall surface chl-α means for the study area for a four year period. A general trend can be observed of low surface chl-α in the fall/winter period, with increasing surface chl-α through the spring and chl-α peaks being reached during the summer months. These weekly mean values include stations from all three of the previously designated hydrographic regimes.

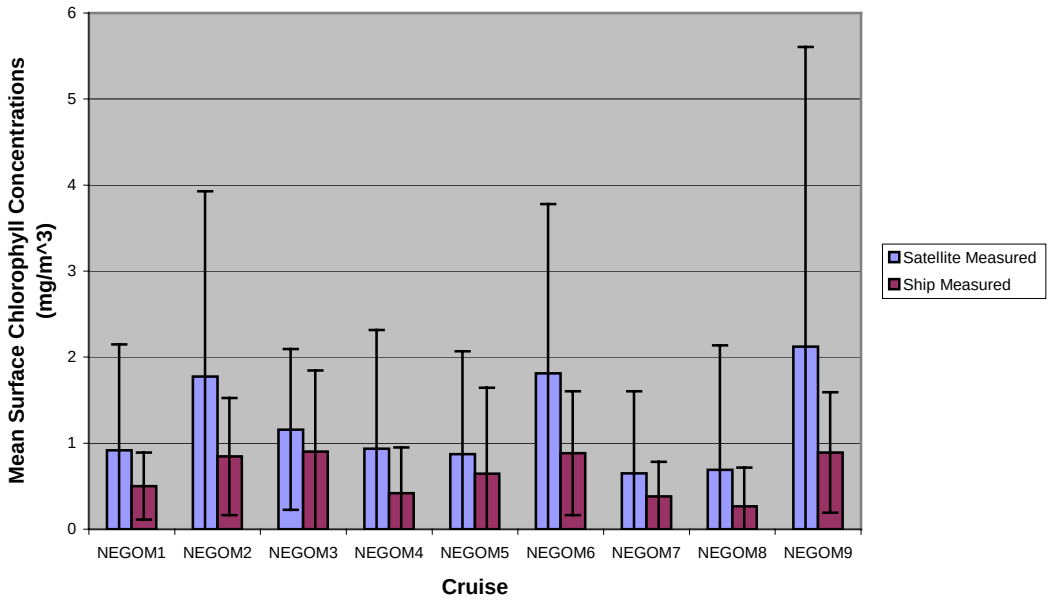

Figure 22. Mean satellite and ship measured surface chlorophyll-α concentrations for all nine NEGOM cruises. Each cruise is composed of 94-98 data points and error bars represent one standard deviation.

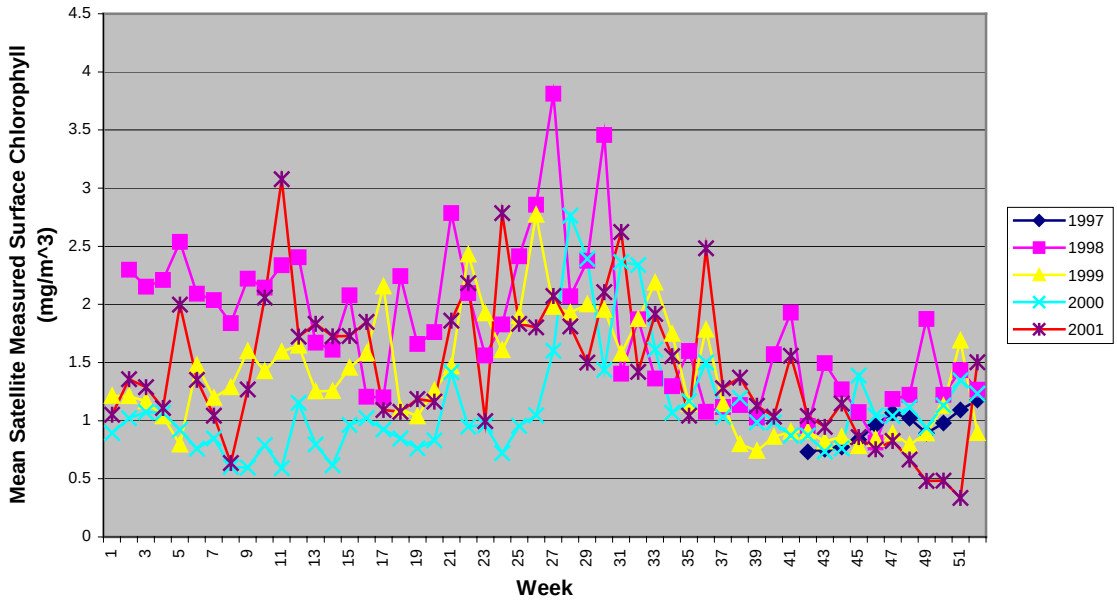

Fig. 23. Mean weekly satellite surface chlorophyll-α measurements throughout the study area for a four year period. Each data point represents the mean value for 98 stations.

4.3.1.3. Mean Surface Chlorophyll by Region

The mean surface chl-α concentrations averaged higher at the fresh water stations than at bluewater stations (Figure 24). This difference is statistically significant (ANOVA, $p<0.05$) for all cruises except summer, 1998 (N3), for which there were too few blue water stations to allow meaningful testing.

The fresh water stations (Figure 24) also had significantly (ANOVA, $p<0.05$) higher surface chl-α concentrations than the coastal stations (Figure 24) for all of the winter cruises (NEGOM1, 4, 7) as well as spring, 2000 (N8) and summer, 2000 (N9). Spring, 1998 (N3) was again an exception in the trend of freshwater stations having higher mean surface chl-α than the coastal stations, though there was no statistical difference between these two means. Spring, 1998 (N3) is also notable as having the lowest mean surface chl-α at the fresh water stations for all of the cruises (Figure 24).

The coastal stations (Figure24) had higher surface chl-α means compared to the blue water stations (Figure 24) for all nine of the cruises. This difference was statistically significant (ANOVA, $p<0.05$) for all winter cruises (NEGOM1, 4, 7) as well as spring, 1999 (N5), summer, 1999 (N6) and summer, 2000 (N9) cruises.

4.3.2. Comparison of Chlorophyll Distribution

The grand mean analysis of satellite measured surface chl-α is limited by the large variation in measurements within each data set. This variation is a combination of different hydrographic regimes influencing surface chl-α concentrations as well as by potential overestimation of surface chl-α concentrations by the satellite methods.

The following section discusses the satellite data based upon the distribution of different chl-α concentration intervals. Three intervals are used for this analysis; low chl-α concentrations (chl-α <1 mg/m^3), high chl-α concentrations (1 mg/m^3< chl-α <5 mg/m^3) and very high chl-α concentrations (chl-α > 5 mg/m^3).

4.3.2.1. Surface Chlorophyll Differences by Season

The overall seasonal trend in satellite measured surface chl-α concentrations is an increase in the number of high (1 mg/m^3< chl-α <5 mg/m^3) chl-α stations for the summer cruises compared to the other seasons. The winter cruises have fewer stations falling under the very high (chl-α > 5 mg/m^3) chl-α range compared to spring and summer. These trends are summarized in Appendix B, Figures B1-B3 and Figures B4-B12 show graphical representations of the surface chl-α distribution for the all cruises.

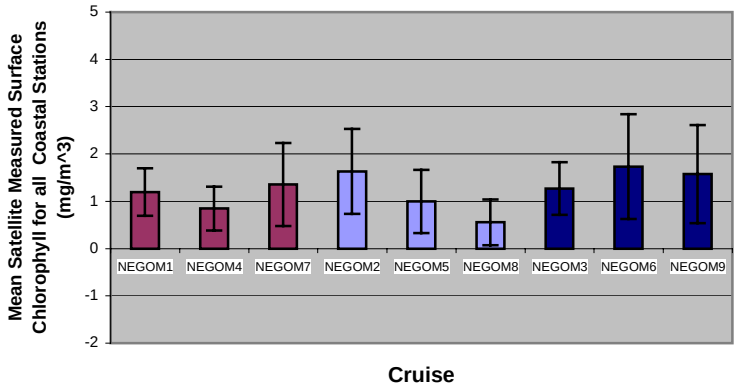

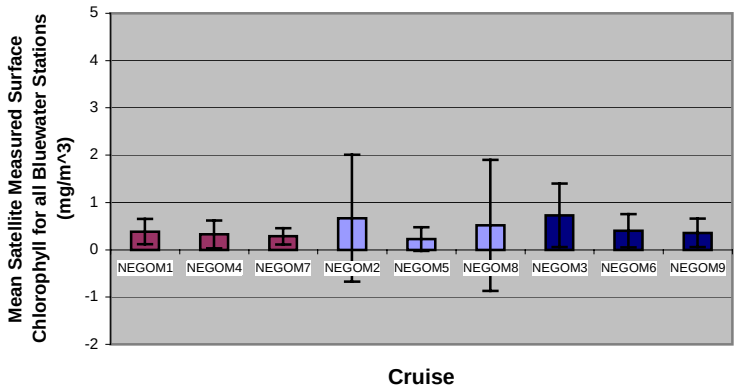

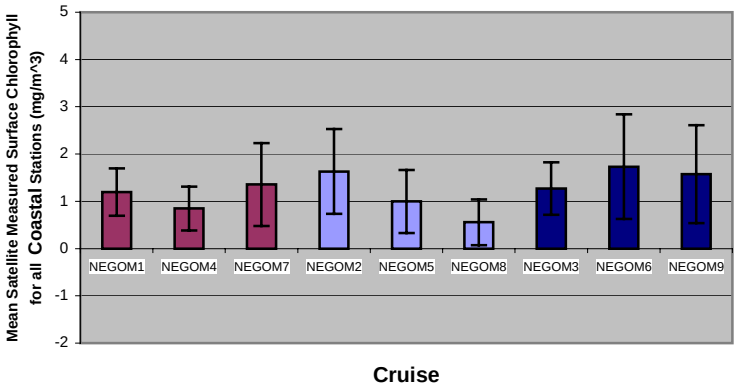

Figure 24. Mean satellite measured surface chlorophyll-α concentrations for each NEGOM cruise separated by hydrographic regions. Error bars represent one standard deviation. Top figure is freshwater stations, middle figure is bluewater stations, and bottom figure is coastal stations.

4.3.2.2. Surface Chlorophyll Differences by Region

Surface chl-α distributions are similar within the freshwater regions for the winter and spring seasons. Summer cruises have a higher proportion of low (chl-α <1 mg/m^3) chl-α freshwater stations compared to the other seasons. These trends are summarized in Appendix B, Figures B13-B15 and Figures B4-B6 show graphical representations of the surface chl-α distribution for winter cruises.

The surface chl-α distributions for the bluewater regions follow a similar trend for all three seasons. For all cruises the majority of the bluewater stations fell under the low (chl-α <1 mg/m^3) chl-α designation, as would be expected of blue water stations. However, some of these stations have satellite measured surface chl-α concentrations in the high and very high ranges. Stations are categorized based upon in situ measured properties, and as such bluewater stations should by definition not have surface chl-α concentrations in the high and very high ranges. The presence of these high and very high surface chl-α concentrations at designated bluewater stations is addressed in the following discussion. These trends are summarized in Appendix B, Figures B16-B18 and Figures B7-B9 show graphical representations of the surface chlorophyll-α distribution for the winter cruises.

Coastal stations for all cruises contain a combination of low surface chl-α stations and high surface chl-α stations with an absence of very high surface chl-α stations. These trends are summarized in Appendix B, Figures B19-B21 and Figures B10-B12 which show graphical representations of the surface chlorophyll-α distribution for the winter cruises.

4.3.3. In Situ Chlorophyll and Satellite Chlorophyll

This final section of results compares ship measurements with SeaWiFS measurements of surface chl-α. The first comparison utilizes the overall mean surface chl-α for each of the nine cruises. Further comparison is done by separating the stations according to hydrographic regime and season.

4.3.3.1. Mean in Situ Chlorophyll and Mean Satellite Chlorophyll

As shown by Spearman rank test of the means for the 9 cruises, in Figure 22, an overall correlation exists between the between the mean satellite measured surface chl-α concentrations and the mean in situ surface chl-α concentrations. However, Figure 22 also shows that satellite measurements tend to overestimate mean surface chl-α concentrations compared to the in situ measurements of surface chl-α concentrations. Further comparisons of these same parameters (Appendix B, Figures B22-B24), when partitioned cruise-by-cruise by hydrographic regime, indicate that on most cruises the bluewater means chl-α values are all relatively low compared to the coastal means, and the coastal means are low compared to the freshwater means. However, the more stations representing each hydrographic regime, the higher was the overall impact on mean surface chl-α concentrations as measured by either ship or SeaWiFS. That is, the higher the proportion of freshwater stations that are present, the higher will be the mean surface chl-α concentrations for the entire study area.

The winter cruises have the overall strongest positive correlation (>0.500, $p<0.05$) between ship and satellite chl-α measurements (Appendix B, Figure B25), reflecting the mostly bluewater condition of chl-α concentration values for the winter cruises. The cruises from the other seasons (Appendix B, Figures B26-B27) show more scatter, but they all show significant (0.300-0.600, $p<0.05$) positive correlation between satellite measured surface chl-α concentrations and in situ surface chl-α concentrations.

4.4. Discussion

The use of mean surface chl-α concentration per cruise in assessing overall trends in surface chl-α is greatly hindered by the large variation in surface chl-α data. Each cruise encompasses a large area over a variety of depths extending from inshore stations to the outer slope which introduces a wide variety of hydrographic regimes. This, compounded with the influences of inputs and redistributions of fresh water into the study area at different times, makes an overall analysis of the surface chl-α concentrations within the study area particularly difficult. For an analysis of the mean satellite measured surface chl-α to be relevant, it must be carried out on a scale smaller than that of the entire NEGOM study area.

The mean satellite measured surface chl-α of all stations for each cruise tends to be higher in summer but shows no marked differences with season or year. This reflects the high variation within the data of each cruise, most notably from stations with very high satellite-measured surface chl-α.

Most of this variation can be pinpointed to the four most inshore stations of Line 1, i.e. those closest to the Mississippi River birdsfoot belta. During several of the cruises, these four stations had satellite measured surface chl-α concentrations apparently greater than 20 mg/m^3. These measured chl-α concentrations were twenty times those of the surface chl-α concentrations for over half of the total stations. Not only does the presence of such stations skew the mean chl-α value for the entire study area, but this also drastically increases the variance of the mean, making any relevant statistical analysis difficult.

To cull these stations that occasionally have very high surface chl-α measurements, a series of criteria were used. First, stations were dropped from the data analysis if they were unreliable outliers. The first of these considerations was only used when the station was shallower than the first optical depth, based upon the light profile for that individual station. This represented the fewest number of data points removed as most shallow water stations with very high chl-α were more likely to be removed according to the second criteria. The second criteria was applied to stations that were

likely to have a strong CDOM signal, i.e. those with significant fresh water abundance. The final criteria for the removal of a data point was whether the measurements were suspected of being asynchronous with in situ measurements as might occur because satellite data are formed from one week averages, with the chronology of the weeks not necessarily coinciding exactly with that of the cruise dates.

If a station passed one of these criteria for eligibility, it was then analyzed according to a second parameter to confirm the removal of the data point from the analysis. This final parameter was a comparison of the satellite chl-α measurements with that of the in situ chl-α measurements. After removal of outliers, a useful comparison between the number of stations with high surface chl-α concentrations and the number of stations with low surface chl-α concentrations could be made. This difference is most notable in the summer season where the number of low surface chl-α stations is by far the lowest of all the seasons. The relatively low number of low surface chl-α stations for the summer cruises can be attributed to the widespread redistribution of fresh water within the study area, particularly at the outer slope stations.

The influence that slope eddies have on the redistribution of freshwater within the NEGOM region is of particular relevance to satellite measurements of surface chl-α concentrations. Occurrence of these entrainment events can be on a time scale that would be easily missed by ship based measurements, making satellite measurements particularly useful. One of the greatest advantages of remote sensing methods is the large spatial covered and comprehensive temporal coverage possible. With these advantages in mind, it is possible to observe the frequency, location and persistence of freshwater redistributions within the NEGOM study area.

By taking several sample stations that are representative of conditions typical to each hydrographic regime, we can observe surface chl-α concentration cycles through interannual and seasonal cycles. This can also be done with shorter time scales in mind, particularly the time scales associated with mesoscale features and their influences. By observing the trends at these representative stations, we can make some observations

about how strongly these features affect the state of these locations and for what proportion of a season or year that these effects persist.

To examine the temporal variation in the local conditions for each of the three hydrographic regions, a sample of four "typical" stations for each region were taken and the weekly mean satellite measurements of surface chl-α concentrations were plotted for each station. From temporal patterns in the surface chl-α concentrations we can make inferences in the timing of mesoscale influences and the relative importance of these influences for each region. These weekly means satellite measured surface chl-α plots are given in Figure 25.

Figure 25 shows that the different hydrographic regions are influenced to different extents by factors such as streamflow and freshwater redistribution. The freshwater stations are most strongly impacted by the streamflow from the adjacent rivers, which results in frequent and persistent levels of very high surface chl-α concentrations. In contrast, the bluewater stations do not show a trend of frequent increases in surface chl-α concentrations. The influence of the freshwater redistribution by the slope eddies of the summer NEGOM cruises is plainly seen in the three high surface chl-α spikes for the sample bluewater stations. These three freshwater redistribution events cause a fourfold increase in the satellite measured surface chl-α concentrations for these bluewater stations.

These increases in surface chl-α concentrations only persist on a time scale of a few weeks. This implies that either the high surface chl-α waters move away from these stations during this time or that the chl-α is removed from the surface waters at this time scale. This large increase in surface chl-α concentrations is only observed in association with the redistribution of freshwater by the slope eddies and that these periods represent a small proportion of the overall number of days being observed.

The coastal stations tend to show a more consistent level of surface chl-α concentrations compared to the other two hydrographic regions. The incidences of high surface chl-α concentrations are not as frequent as the freshwater stations nor as drastic as the bluewater stations. However, local areas of high streamflow can strongly

influence nearby coastal waters as is shown by the spike in surface chl-α concentrations in the first spring of the data series. This spike in surface chl-α concentrations coincides with abnormally high (greater than one standard deviation above the mean) streamflows for the Apalachicola and Suwannee Rivers during this period. The stations that area closest to these river mouths show the highest increase in surface chl-α concentrations while the more distant coastal stations show little effect.

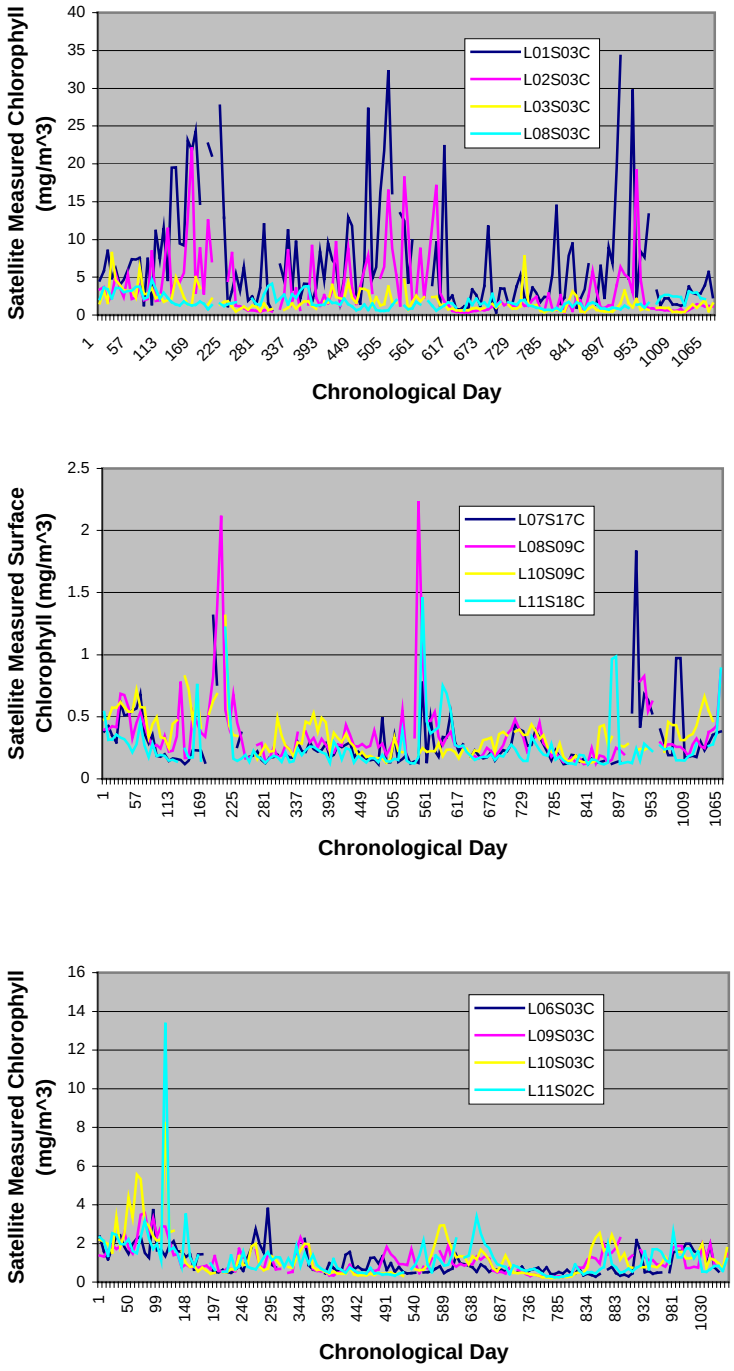

Figure 25. Weekly mean satellite measured surface chl-α concentrations for sample stations from each hydrographic region. Top figure is four freshwater stations, middle figure is four bluewater stations, and bottom figure is four coastal stations.

CHAPTER V
SYNTHESIS

5.1. Introduction

5.1.1. Synthesis of Parameters

This chapter is a synthesis and comparison of parameters addressed within the previous three chapters. Input and redistribution of fresh water within the study area determines the localized surface chl-α concentrations as well as the regional surface chl-α abundance. In Chapter II, freshwater was inventoried according to both surface salinity and total integrated freshwater at each station. In this chapter, these parameters are compared to the in situ surface chl-α measurements as well as the integrated water column chl-α values at varying depths. Freshwater is particularly important in analyzing satellite surface chl-α estimates, as it is a major source of CDOM and other pigments that may affect the satellite measured signal [Cullen and Lewis, 1995;Warwik et al., 2003; Nababan et al., in review 2004]. In this chapter, a follow-on analysis has been made to look at effects of surface salininty and total integrated freshwater upon the integration depths used in the chl-α analysis.

5.1.2. Comparing in Situ Chlorophyll with Satellite Chlorophyll

The second section of this chapter involves the comparison of in situ measured chl-α parameters with the measurements derived from the SeaWiFS satellite. Because the presence of freshwater can have a major effect upon the satellite measurement of surface chl-α, comparisons of in situ measurements with satellite measurements are necessary to ground-truth the satellite data as well as to refine the algorithms used in interpreting ocean color [Hu et al., 2003]. In addition to this, different sources of freshwater can have different compositions of pigments, making regional analysis of the freshwater effects upon satellite measurements important [Nababan et al., in review 2004].

Chapter IV commented on the differences between in situ measurements of chl-α with satellite measurements. In this chapter, satellite data are employed to analyze the overall trends in surface chl-α abundance within the study area. While the NEGOM cruises represented a repeated thorough sampling of the study area, the actual periods of sampling are a small number of the total days from the beginning of the program to the end. We have only nine snapshots of the study area in 3 years, each of which is only a two week window of time. However, the satellite data for this period are continuous through the entire length of the NEGOM program and so allow us to determine how representative each of the NEGOM cruises was of the entire season in which it took place. This is particularly important due to the effects of mesoscale influences, such as slope eddies which can have effects that persist on a scale of a few weeks (Jochens et al., 2002).

5.1.3. Purpose of Research

The periodic introduction of nutrient rich river water into the NEGOM region contributes to increased surface chl-α concentrations. However, this increase in surface chl-α concentrations may be through introduction of pre-existing chl-α from the river water or by new production caused by the influx of nutrients. It is clear that freshwater within the NEGOM region is linked with increased surface chl-α concentrations, but the origins of this chl-α need further study. Is the chl-α derived from new production growth based on the availability of nutrients, or is it imported within the freshwater? This question can be addressed in part by observing the nutrients within the freshwater as it gets entrained farther from the source. Should the chl-α follow conservative mixing patterns within the freshwater, it would follow that no new production is occurring within the freshwater. Conversely, if nutrients are quickly depleted it would follow that no new production is taking place.

The presence of freshwater within the study also presents a challenge for accurate satellite measurements of surface chl-α. I have hypothesized that satellite

measured surface chl-α will have weaker correlation with in situ measured surface chl-α within freshwater and coastal regions, compared to the bluewater region.

5.2. Results

5.2.1. Freshwater and in Situ Chlorophyll

This section details the influences that freshwater abundance have upon in situ measurements of chl-α within the NEGOM study area. The first analysis compares surface salinity with surface chl-α concentration by season. This is followed by a comparison of surface salinity with the vertically integrated chl-α stocks, for each of the three integration depths, and finally by a comparison of surface salinity with integration depth for each of the intervals. Each of these analyses is done separately by season, so that seasonal effects can be partitioned.

5.2.1.1. Surface Salinity and Surface Chlorophyll

There is a strong and significant (>-0.600, $p<0.05$) negative correlation between surface salinity and the in situ measured surface chl-α concentration for the winter cruises (Figure 26). This correlation is weaker for the spring cruises (Figure 26), but is still significant (>-0.550, $p<0.05$). The summer cruises show a slightly weaker significant (>-0.500, $p<0.05$) negative correlation between surface salinity and surface chl-α concentration compared to the winter cruises (Figure 26). In summer there was a large amount of variation of surface chl-α concentrations within the freshwater stations. Several stations had particularly high surface chl-α concentrations. Upon a closer examination of these freshwater stations, it was observed there were two groups of freshwater stations, each with different characteristics. One group was represented by the shallower water stations of the continental shelf. These had relatively shallow and intensely stratified freshwater layers. Others farther offshore had deep freshwater layers that had mixed with the saltwater beneath. The former generally had much higher

surface chl-α concentrations than the latter. This is evident from partitioning the data from Figure 26 by depth range (Figure 27).

5.2.1.2. Surface Salinity and Integrated Chlorophyll

There was a negative significant (>-0.500, $p<0.05$) correlation between surface salinity and vertically integrated chl-α to the 36.8% surface light penetration depth for the winter cruises (Appendix B, Figure B25). This trend did not hold true for the spring cruises, for which there was no discernable correlation between these parameters (Appendix B, Figure B26). But again for summer cruises there was a weak negative significant (>-0.500, $p<0.05$) correlation between surface salinity and vertically integrated chl-α to the 36.8% surface light penetration depth (Appendix B, Figure B27).

There was no correlation between surface salinity and vertically integrated chl-α to the 18% surface light penetration depth for the any of the seasons (Appendix B, Figures B28-B30). In fact, there was great variation in the depths for the 18% surface light penetration level, and this leads to a wide variation in integrated chl-α.

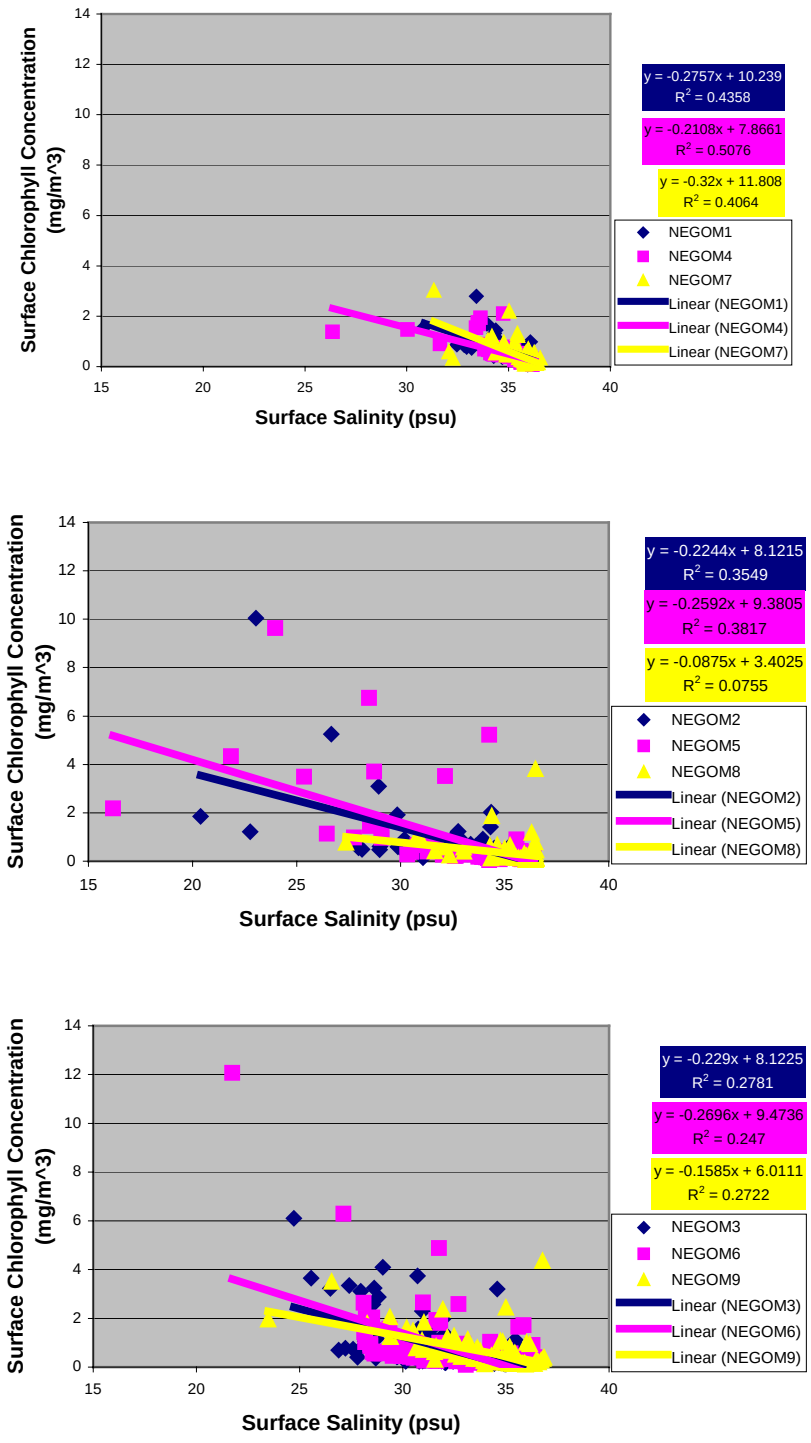

Figure 26. Comparison of surface salinity with in situ measured surface chl-α concentrations for each cruise separated by season. Top figure is winter cruises, middle figure is spring cruises, and bottom figure is summer cruises.

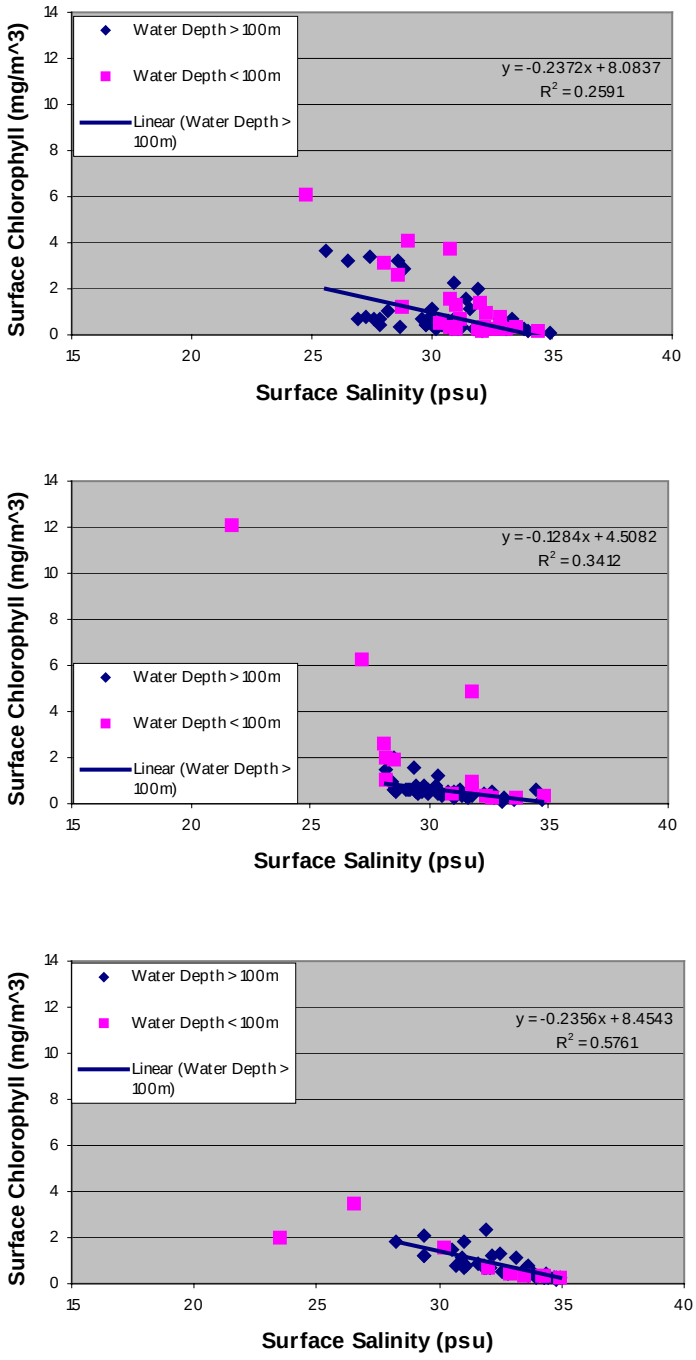

Figure 27. Comparison of surface salinity with in situ measured surface chl-α concentration for all NEGOM cruises separated by season. Top figure is winter cruises, middle figure is spring cruises, and bottom figure is summer cruises. Stations shallower than 100 m depth (in pink) have been removed from statistical analysis

Nor was there a correlation with vertically integrated chl-α to the 1% surface light penetration depth (Appendix B, Figures B31-B33). Once again, there was a wide variation in integration depth that was responsible for the variation in vertically integrated chl-α.

5.2.1.3. Surface Salinity and Integration Depth

Figure 28 shows surface salinity plotted against the integration depths to the 36.8% surface light penetration. A general trend of increasing depth with increasing salinity can be observed for all seasons, though the correlations are not significant for the final three cruises of the study (NEGOM7, 8 and 9). The data also show the general trend that the deepest integration depths are found exclusively at stations that have very high salinity, which are typically outer slope, bluewater stations. Very similar trends are observed for the 18% surface light penetration depth intervals (Figure 29) and the 1% surface light penetration depth intervals (Figure 30), showing an increase in integration depth with increasing salinity. Again, the deepest integration depths are found at highest

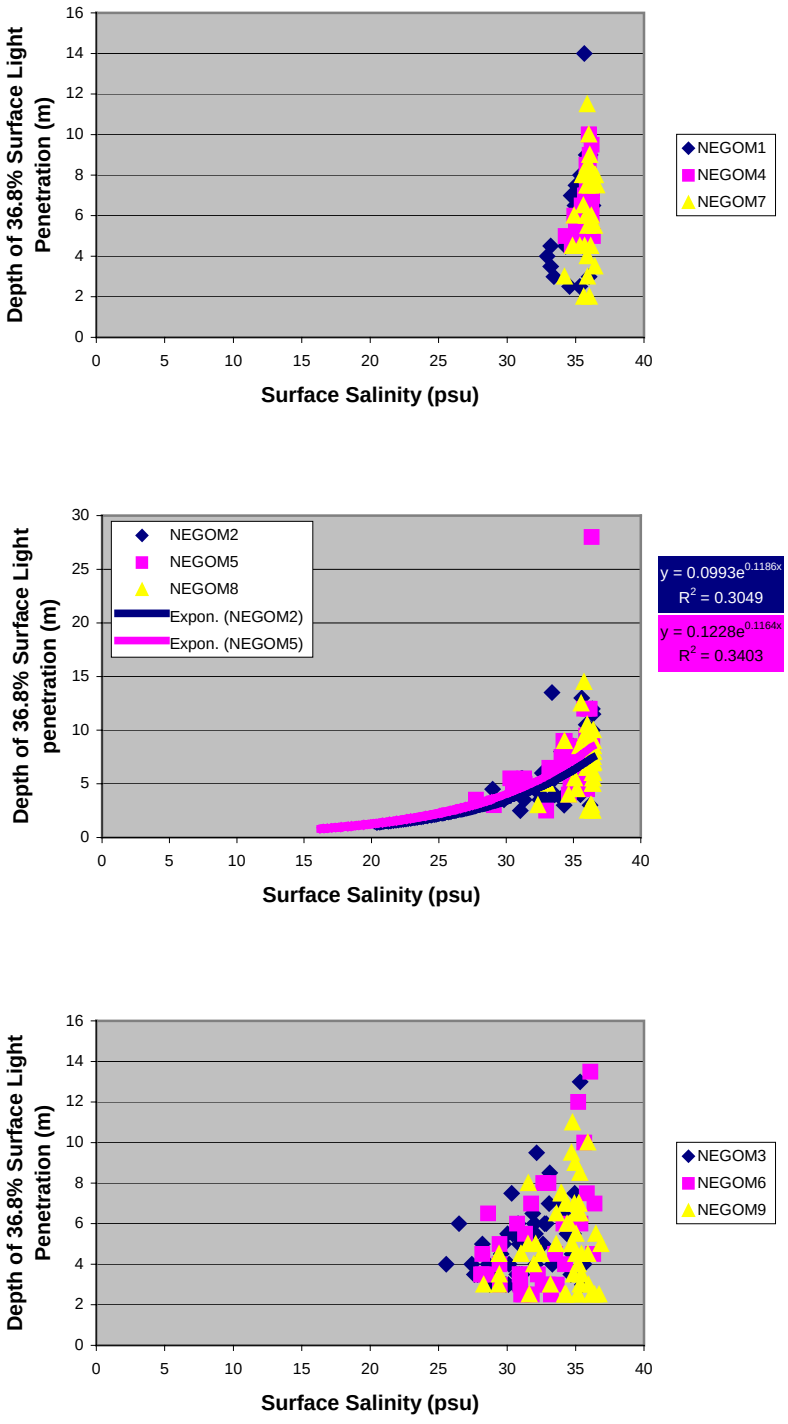

Figure 28. Comparison of surface salinity with integration depth to the 1st optical depth for all NEGOM cruises separated by season. Top figure is winter cruises, middle figure is spring cruises, and bottom figure is summer cruises.

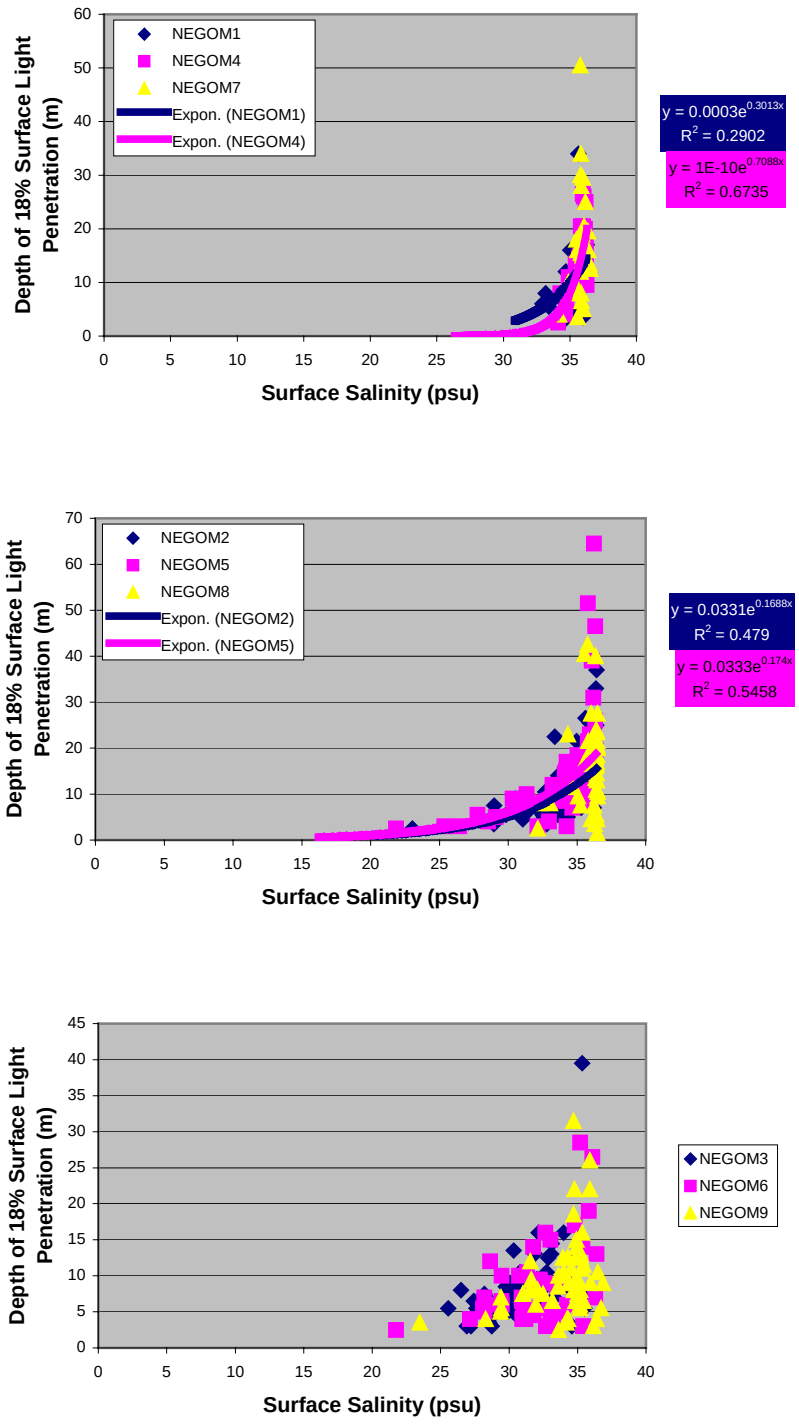

Figure 29. Comparison of surface salinity with integration depth to the secchi disc depth for all NEGOM cruises separated by season. Top figure is winter cruises, middle figure is spring cruises, and bottom figure is summer cruises.

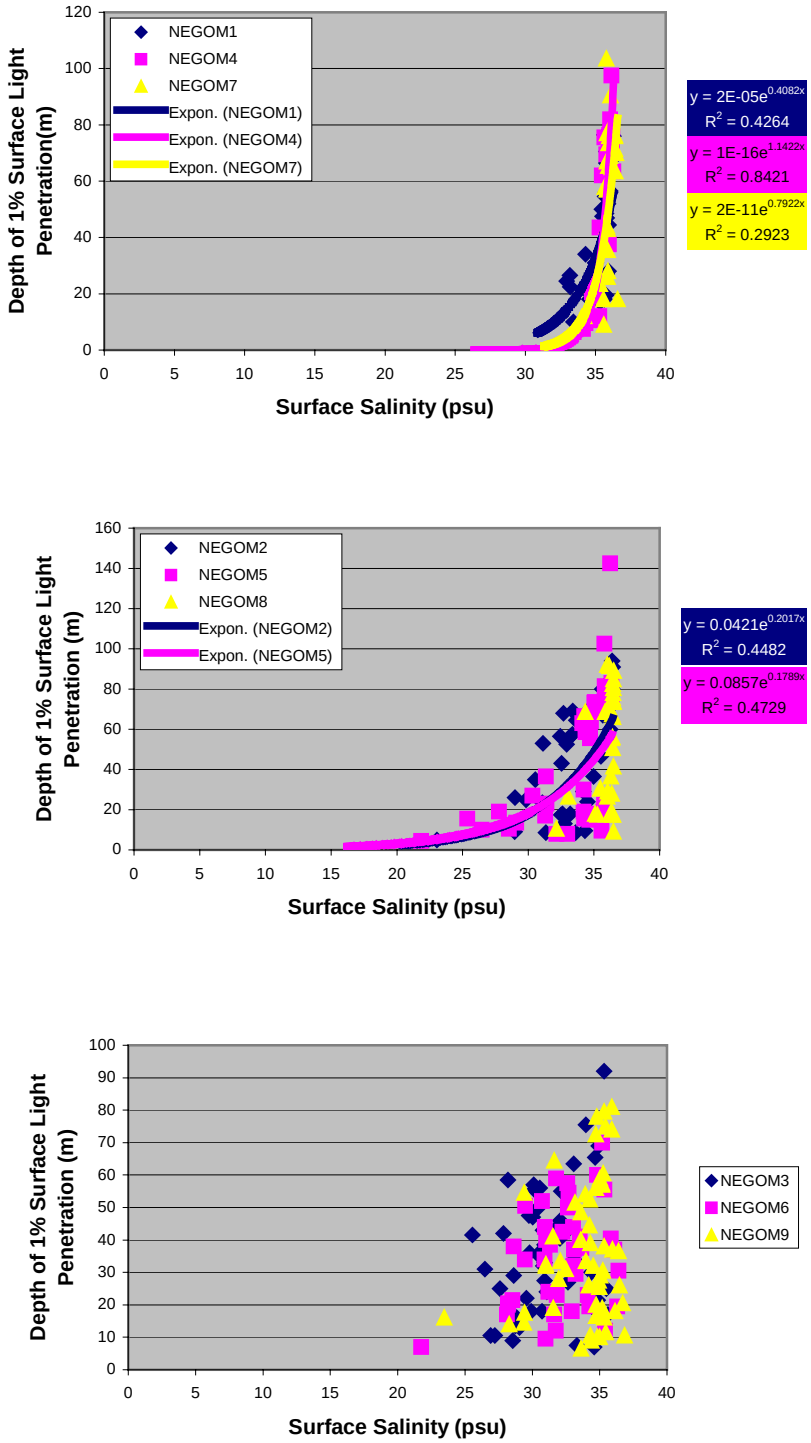

Figure 30. Comparison of surface salinity with integration depth to the estimated euphotic depth for all NEGOM cruises separated by season. Top figure is winter cruises, middle figure is spring cruises, and bottom figure is summer cruises.

salinity stations. The summer cruises show greater scatter than the other seasons for all three of the depths. This seems to be due to a combination of more overall freshwater stations, as well as most of the freshwater stations being located far from the freshwater sources and mixing with the ocean water underneath.

5.2.1.4. Integrated Freshwater and Surface Chlorophyll

There were no evident trends when comparing vertically integrated freshwater with surface chl-α concentrations. In all three seasons (Appendix B, Figures B34-B36), there was no distinct correlation between the two parameters. However, the winter cruises showed a smaller range of surface chl-α values as well as having a much smaller number of overall freshwater stations.

5.2.1.5. Total Freshwater and Mean Satellite Chlorophyll

Mean satellite measured chl-α is positively correlated with vertically integrated freshwater (Figure 31). This correlation holds true on a cruise by cruise basis, as well as seasonally.

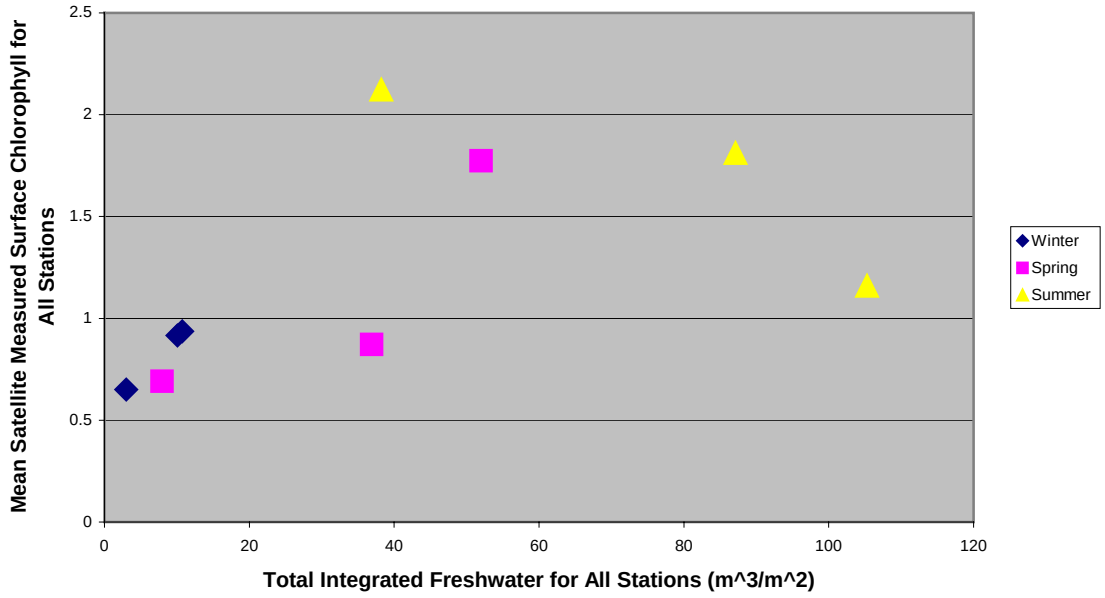

Figure 31. Comparison of total integrated freshwater within the NEGOM study area and mean satellite measured surface chl-α for the NEGOM study area.

5.2.1.6. Surface Salinity and Satellite Chlorophyll

The winter cruises show a robust significant (>-0.600, $p<0.05$) negative correlation between increasing satellite measured surface chl-α concentrations and decreasing surface salinity (Figure 32). The spring cruises (Figure 32) also show significant (>-0.500, $p<0.05$) negative correlation between the surface salinity and the satellite measured surface chl-α concentrations. The summer cruises (Figure 32), however, showed weak significant (>-0.300, $p<0.05$) negative correlations due to the number of stations that have relatively low surface salinity and low surface chl-α concentrations, particularly the Spring, 1998 (N3) cruise which had no significant correlation (-0.007, $p>0.05$). The majority of these stations are found on the outer shelf at some distance from the freshwater sources.

5.2.1.7. Integrated Freshwater and Satellite Chlorophyll

In none of the three seasons was there a strong correlation between integrated freshwater and satellite measured surface chl-α concentrations (Appendix B, Figures B37-B39). One of the variables that may be masking a correlation are coastal stations with a small amount of integrated freshwater but with very high surface chl-α concentrations. Such coastal stations are evident in the winter and spring cruises, for they have high surface chl-α concentrations but little vertically integrated freshwater.

5.2.1.8. Satellite Chlorophyll and in situ Chlorophyll by region

When ship versus satellite comparisons were done using only the freshwater stations, the correlations between these two parameters were generally weak (Appendix B, Figures B40-B42). This was not surprising, though, as the freshwater stations had the largest dynamic range of surface chl-α concentration values as well as the greatest variation of these values for either method of chl-α concentration measurement. NEGOM cruises 7 and 8 are noteworthy in that they are the only cruises that do not have significant ($p>0.05$) correlation between the two measurements due to their low number of freshwater stations.

At bluewater stations, there was in general a wide range of scatter for the satellite measured surface chl-α compared to the more limited range of in situ measured surface chl-α values for all three seasons (Appendix B, Figures B43-B45). The best overall agreement between ship and satellite means was during winter cruises, which had both the largest number of bluewater stations as well as the lowest range of satellite surface chl-α measurements.

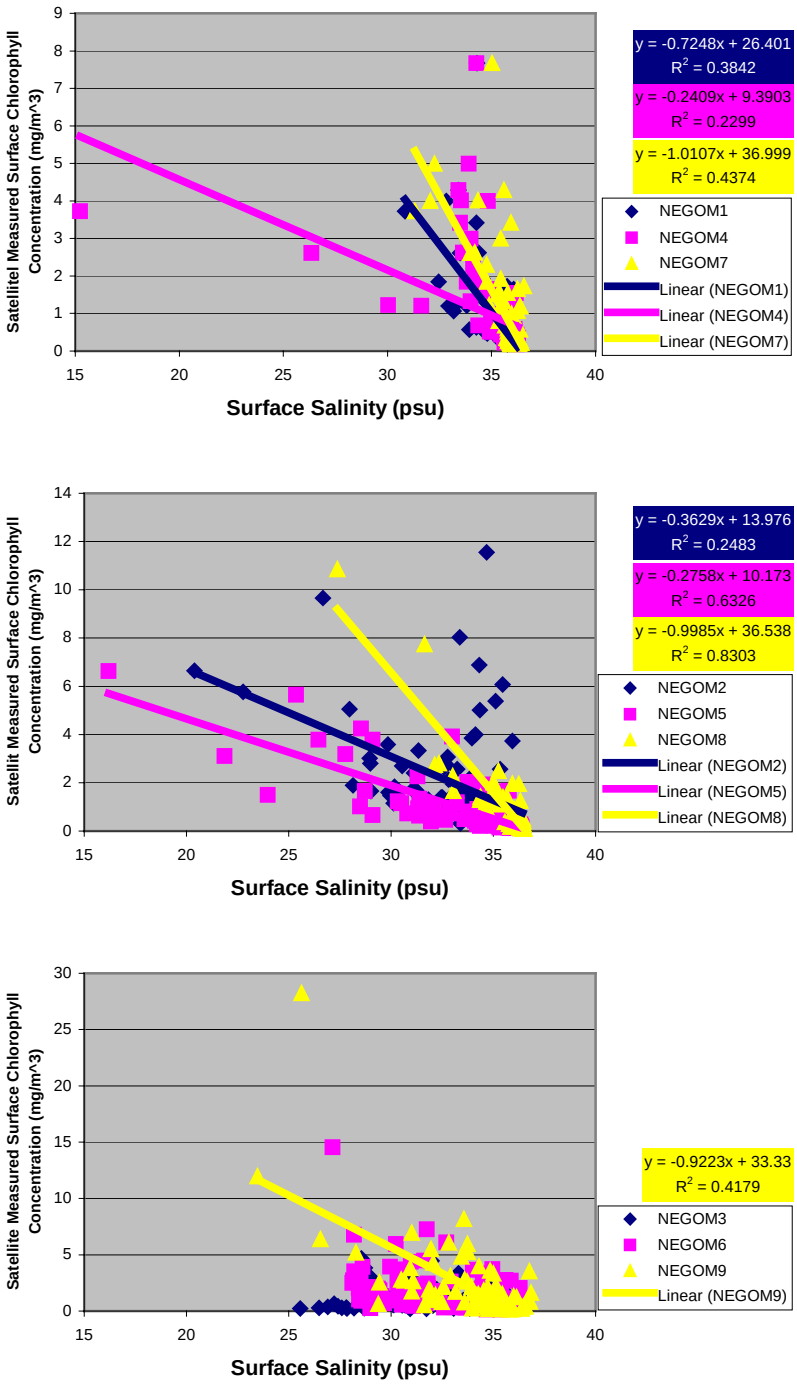

Figure 32. Comparison of surface salinity and satellite measured surface chl-α concentration for all cruises separated by season. Top figure is winter cruises, middle figure is spring cruises, and bottom figure is summer cruises.

Coastal stations showed the highest overall positive correlation between ship and satellite chl-α measurement methods (Appendix B, Figures B46-B48). On all cruises, at coastal stations there was a strong significant (>0.500, $p<0.05$) correlation between satellite measured surface chl-α concentrations and in situ measured surface chl-α concentrations. On the other hand, the coastal stations were generally the minority of the total number of stations on any cruise, with the majority being either freshwater stations or bluewater stations. The relatively low dynamic range of surface chl-α values is likely responsible for much of the improved overall correlation for these cruises.

5.3. Discussion

Direct comparisons of surface salinity and surface chl-α concentration over the entire NEGOM region are difficult to make without separating these stations according to their hydrographic region. Stations that have low salinity tend to have a respectively high surface chl-α concentration, and this is the case for the majority of the freshwater stations. However, the presence of numerous shallow water coastal stations within the NEGOM study frequently leads to many stations having high surface chl-α concentrations at high surface salinities.

Belabbassi [2001] showed that in the freshwater region nutrients were very quickly depleted by the time the freshwater reached the outer slope. This is shown particularly well by Qian et al. [2003] in a comparison of surface salinity and surface nutrients (Figure 33). Both studies indicate that any new production derived from riverine input of nutrients takes place very close to the mouth of the Mississippi River and that high surface chl-α concentrations in the freshwater that reaches the outer slope are an artifact of this initial production.

The strong negative correlation observed between surface salinity and the integrated chl-α mass to the 36.8% surface light penetration depth is to be expected due to the similar correlation between surface chl-α and surface salinity. This integration depth is typically so shallow that it is highly representative of surface chl-α

concentrations and will typically parallel the surface chl-α concentration. The only exceptions to this trend are the stations that are very near sources of freshwater or those that have very low light extinction coefficients in the surface waters. The former type of station frequently have 36.8% surface light penetration depths that are shallower than the first data logged by the instrument, making these stations difficult to measure. The latter type of station has deep enough light penetration that the overall volume of water is enough to skew the integrated chl-α mass compared to other bluewater stations.

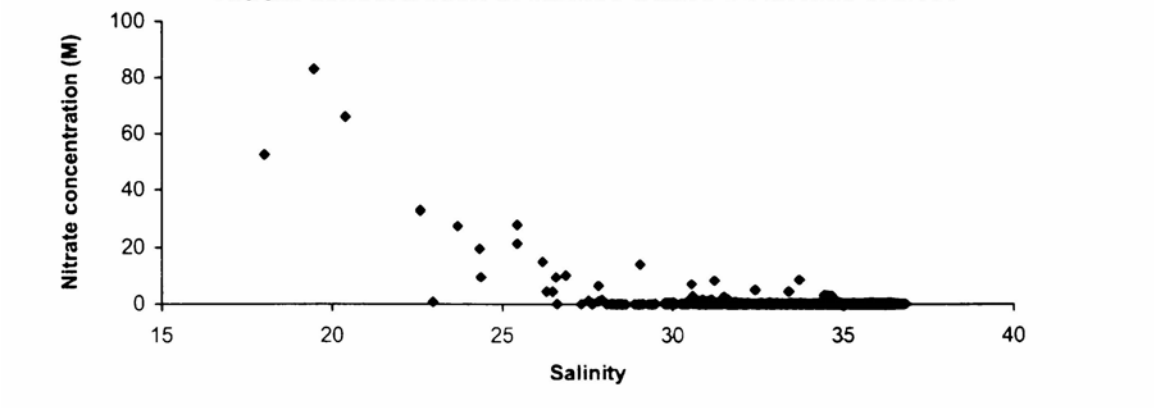

Figure 33. Property plot between surface salinity and near surface nitrate concentrations, showing depletion of surface nitrate at salinity >27 psu. Figure is from Qian et al. [2003].

This is not the case for the 18% surface light penetration and the 1% surface light penetration depth, which are subject to a number of influences that increase the variability of the integrated chl-α mass. The most critical of these factors is the wide variations in the depth at which the 18% surface light penetration and 1% surface light penetration depths are reached. Bluewater stations in particular may have very deep integration depths and the sheer volume of water being integrated skews the total chl-α mass despite low chl-α concentrations through the water column. Another factor that adds to the variability in the integrated chl-α mass is the presence of the near bottom high chl-α layers that were mentioned earlier. In some coastal stations these layers accounted for less than a fifth of the total water column, yet were responsible for two thirds of the total integrated chl-α mass in the water column.

While surface salinity cannot be used to precisely estimate the integration depth for light penetration, it is possible to make some useful generalizations on integration depth based upon surface salinity. The overall trend of decreasing integration depth with decreasing salinity holds true for the different seasons and hydrographic regions, but the reverse is not necessarily the case. A number of high salinity stations have very shallow integration depths due to high surface chl-α concentrations or shallow bottom depth and these stations do not fit the expected curve of decreasing integration depth with decreasing salinity. Another generalization that can be made is that the extremes of integration depth will be found at the extremes of surface salinity. The shallowest integration stations will be those with a great deal of freshwater, as these stations have the most suspended sediments, chl-α and other pigments. The deepest stations will be found in the outer slope regions where light extinction coefficients are the lowest. It is also important to note that the relationship between surface salinity and integration depth is not a linear relationship. This is most likely an artifact of the integration depths being based upon light extinction profiles that follow a logarithmic decrease in light intensity with depth.

Surface chl-α concentrations are not good predictors of total integrated freshwater abundance due to differences in the dispersion rates of the chl-α and the freshwater. Surface chl-α will generally decrease over a much shorter time than it takes for freshwater to disperse through the water column and horizontally along the ocean surface [Wawrik et al., 2003]. While the surface chl-α concentrations may decrease rather quickly due to consumption, settling, or other influences, total integrated freshwater is a more strongly conserved property and can only be reduced by horizontal movement or dispersion of freshwater and by the process of evaporation.

When satellite surface chl-α measurements are compared to in situ measurements on a station by station basis according to season alone, it is clear that the winter season shows the most consistent and strongest agreement in these two methods. This is most likely due to the lower amount of freshwater within the study area during the winter season compared to the spring and summer seasons.

The fact that all three summer NEGOM cruises coincided with slope eddy entrainment events may skew interpretation of what are "typical" summer conditions within the study area. Satellite chl-α maps of the NEGOM study area for the entire summer period for each of the three summers, show that the conditions during NEGOM 3, 6 and 9 were atypical of the majority of the summer period. The large amount of obvious green water being entrained into the NEGOM area was only observed for an approximately 3 week period each summer, which happened to coincide with each of the summer NEGOM cruises. This is shown most plainly seen in the central panel of Figure 25 which shows drastic, short lived elevations in satellite measured surface chl-α which occur during the three summer cruises.

The correlations between the surface chl-α measurements on a station by station basis are much weaker when the analyses are done separately according to hydrographic regime. This indicates that the overall mean chl-α is strongly determined by the number of stations representing the different hydrographic regimes. The greater the number of freshwater stations, the greater the overall mean surface chl-α for the entire study area. At this large scale of analysis the satellite measurements agree well with the in situ measurements of surface chl-α concentration. The fact that the overall satellite measurements agree with the mean in situ measurements and that the individual station comparisons do not agree, indicates that there may be time lag between the in situ measurements and the satellite measurements. This is further complicated by the fact that the satellite data are weekly averages and that these weekly periods do not necessarily coincide with the exact cruise dates.

The timing discrepancy between the satellite measurements and the in situ measurements is of particular concern during the summer NEGOM cruises. These cruises each had freshwater entrained into the study area by slope eddies interacting with the Mississippi River. This entrained water had current speeds exceeding 1 knot in some cases, indicating that the conditions in a single location could change very quickly. When in situ data are collected during a ten day cruise, the conditions at any given station may change drastically over that period of time. Should in situ measurements be

taken at a station before entrained freshwater reaches that station, the in situ measurements will be typically low. With the current speeds measured in the entrained water, a time differential in measurements of only a few days could indicate drastic changes in the conditions for a given station. This was particularly clear when examining the distribution of very high satellite measured surface chl-α stations in what in situ measurements categorized as bluewater stations (Appendix B, Figures B43-B45). As such, any conclusions made about typical summer conditions from the summer NEGOM cruises must take into account the presence of the slope eddies and their influences.

CHAPTER VI

SUMMARY AND PRINCIPAL CONCLUSIONS

The overall patterns of chl-α abundance within the NEGOM study area are strongly affected by the occurrence of freshwater redistribution. This influence is dependent upon volume of flow from freshwater sources, as well as upon the entrainment of river water by slope eddies is also important in determining the amount of freshwater redistributed eastward into the NEGOM region.

The effect of freshwater upon overall surface chl-α distributions can be seen at both annual scales and seasonal scales. Furthermore, satellite observations indicate that the freshwater entrainment can change the overall chl-α abundance in the study area on a scale of several weeks.

The characteristic Gulf of Mexico seasonal chl-α cycle of annual highs in November-February and annual lows from May-August that were described by Muller-Karger et al. [1991] were in each summer of the present study (1998-2000) overshadowed by the summertime high chl-α cycle reflecting freshwater entrainment by slope eddies. The magnitude of entrainment denended on the strength and location of the slope eddies, but usually extended far eastward of the Mississippi River delta, often to 84^0W longitude.

Surface chl-α may be used as a gauge of overall water column chl-α abundance only under certain conditions. Correlation was generally good to the shallowest integration depth (1^{st} optical depth) and to the secchi disc depth as well. However, such estimates must be done on a station-by-station basis and quality assurance/quality control is important, for especially at inner and middle shelf stations single point, near bottom high chl-α concentrations may greatly influence vertical integration calculations.

Tremendous variability in the integration depths for the euphotic zone greatly restricted my ability to forecast vertically integrated chl-α based upon surface chl-α. In fact, the depth of the 1% irradiance level varied widely between stations that were adjacent and seemingly shared the same water properties.

Satellite measurements of surface chl-α were useful for large scale analysis of ocean conditions, but they have limitations when used on fine time and spatial scales. This is particularly true for a continental margin like that in the NEGOM, that contains mesoscale eddies that can drastically redistribute surface chl-α in short time spans.

Cause and effect comparisons between different parameters within such a large and diverse study area were difficult to reliably apply. This reflects the large spatial scales involved in the NEGOM study, as well as the diversity of station types. Future research on freshwater forcing of high summertime chl-α in the NEGOM area should be restricted in scope to smaller spatial scales, so that all stations are occupied as synoptically as possible.

REFERENCES

Belabbassi, L., Importance of physical processes on near-surface nutrient distributions in summer in the Northeastern Gulf of Mexico, 75pp., M.S. thesis, Dept. of Oceanogr., Texas A&M Univ., College Station (2001).

Biggs, D.C., R.R. Leben, and J. Ortega-Ortiz, Ship and satellite studies of mesoscale circulation and sperm whale habitats in the northeastern Gulf of Mexico during GulfCet II, *Gulf Mexico Sci., 18*, 15-22 (2000).

Biggs, D.C., and P.H. Ressler, Distribution and abundance of phytoplankton, zooplankton, ichthyoplankton, and micronekton in the deepwater Gulf of Mexico, *Gulf Mexico Sci., 19*, 7-29 (2001).

Biggs, D.C., R.W. Davis, J.G. Ortega-Ortiz, C.A. Ribic, W.E. Evans, P.H. Ressler, R.D. Cady, R.R. Leben, K.D. Mullin, and B. Warsig, Cetacean habitat in the northeastern oceanic Gulf of Mexico, *Deep-Sea Res. Pt. I, 49(1)*, 121-142 (2002).

Carder, K.L., F.R. Chen, Z.P. Lee, S.K. Hawes, and D. Kamykowski, Semianalytic moderate-resolution imaging spectrometer algorithms for chlorophyll α and absorption with bio-optical domains based on nitrate depletion temperatures, *J. Geophys. Res., 104*, 403-5421 (1999).

Conkright, M.E., W.W. Gregg, S. Levitus, Seasonal cycle of phosphate in the open ocean, *Deep Sea Res. Pt. I, 47(2)*, 159-175 (2000).

Cullen, J.J., The deep chlorophyll maximuim: comparing vertical profiles of chlorophyll α, *Can. J. of Fisheries and Aquatic Sci., 39*, 791-803 (1982).

Cullen, JJ., and M.R. Lewis, Biolgoical processes and optical measurements near the sea surface: some issues relevant to remote sensing, *J. of Geophys. Res., 100*,13,255-13,266 (1995).

Cullen, J.J., R.F. Davis, P.J. Neale, Inhibition of marine photosynthesis by ultraviolet radiation: variable sensitivity of phytoplankton in the Weddell-Scotia Confluence during the austral spring, *Limn. and Oceanogr., 43(3)*, 433-438 (1998).

Deegan, L.A., J.W. Day, Jr., J.G. Gosselink, A. Yanez-Arancibia, G. Soberon-Chavez, and P. Sanchez-Gil, Relationships among physical characteristics, vegetation distribution and fisheries yield in Gulf of Mexico estuaries, in: *Estuaries Variability*, edited by D.A. Wolf, pp. 83-100, Academic Press, Orlando, FL, (1986).

Gilbes, F., C. Tomas, J.J. Walsh, F.E. Muller-Karger, An episodic chlorophyll plume on the West Florida Shelf, *Cont. Shelf Res., 16(9)*, 1201-1207 (1996).

Gonzalez-Rodas, G.E., Physical forcing of the primary productivity in the northwestern Gulf of Mexico, 142 pp., Ph.D. dissertation, Department of Oceanography, Texas A&M University, College Station (1999).

Hamilton, P., E. Waddell, and R. Wayland, Physical environment, in: *Northeastern Gulf of Mexico coastal and marine ecosystem program: data research and synthesis*, Chap. 2, edited by Science applications international corporation, synthesis report, U.S. Dept. of the Interior, U.S. Geological Survey, Biological resources division, USGS/BRD/CR1997-0005, and Minerals Management Service, Gulf of Mexico OCS Region, New Orleans, LA., 313 pp., OCS study/MMS 96- 0014 (1997).

Hu, C., K.L., Carder, F.E. Muller-Karger, Atmospheric correction of SeaWiFS imagery over turbid coastal waters: a practical method, *Remote Sensing of Environment, 74(2)*, 195-206 (2000).

Hu, C., D.C. Biggs, K.L. Carder, F.E. Muller-Karger, B. Nababan, D. Nadeau, J. Vanderbloemen, Comparison of ship and satellite bio-optical measurements on the continental margin of the NE Gulf of Mexico, *Int. J. of Remote Sensing, 24*, 2597-2612 (2003).

Jochens , A.E., W.D. Nowlin, Jr., Northeastern Gulf of Mexico chemical and hydrography study between the Mississippi Delta and Tampa Bay, annual report: year 1, Minerals management Service, Gulf of Mexico OCS Region, New Orleans, LA., pp. 119, MMS contract No. 1435-01-97-CT-30851, OCS Study/MMS 98-0060 (1998).

Jochens, A. E., DiMarco, S. F., Nowlin, W. D., Reid, R. O., and Kennicutt II, M. C. , Northeastern Gulf of Mexico chemical oceanography and hydrography study, New Orleans, LA., 327 pp., MMS contract No. 1435-01-97-CT-30851, OCS Study/MMS 2002-078 (2002).

Kelly, F.J., Physical oceanography, water mass characterization, in: *Mississippi-Alabama continental shelf ecosystem study: data summary and synthesis*, Vol. 2, edited by Brooks J.M., pp. 10-1 to 10-151, Technical Narrative, OCS study MMS 91-0063, U.S. Dept. of the Interior, Minerals Management Service, New Orleans, LA (1991).

Lohrenz, S.E., G.L. Fahnenstiel, D.G. Redalje, G.A. Lang, M.J. Dagg, T.E. Whiledge, and Q. Dortch, The interplay of nutrients, irradiance, and mixing as

factors regulating primary production in coastal water impacted by the Mississippi Rive plume, *Cont. Shelf Res., 19*, 1113-1141 (1999).

Melo-Gonzalez, G.O., F.E. Muller-Karger, S. Cerderira, R. Perez de los Reyes, I. Victoria del Rio, P. Cardenas-Perez, and I. Mitrani-Arenal, Near surface phytoplankton distribution in the western Intra-Americas Sea: the influence of El Nino and weather events, *J. Geophy. Res., 105*, 14,029-14,043 (2000).

Muller-Karger, F.E., J.J. Walsh, R.H. Evens, and M.B. Meyers, On seasonal phytoplankton concentration and sea surface temperature cycles of the Gulf of Mexico as determined by satellites, *J. Geophys. Res., 96(C7)*, 12,645-12,665 (1991).

O'Reilly, J.E., S. Maritorena, B.G. Mitchell, D.A. Siegel, K.L. Carder, S.A. Garver, M. Kahru, and C.R. McClain, Ocean color chlorophyll algorithms for SeaWiFS, *J. Geophys. Res., 103*, 24,937-24,953 (1998).

Parsons, T.R., Y. Maita, and C.M. Lalli, *A Manual of Chemical and Biological Methods for Seawater Analysis*, pp. 173, Prentice-Hall, INC., Elmsford, NY (1985).

Psarra, S., L. Ignatiades, A. Tselepides, Primary productivity in the oligotrophic Cretan Sea (NE Mediterranean): seasonal and interannual variability, *Progress in Oceanogr., 46(2-4)*, 187-204 (2000).

Qian, Y., A.E. Jochens, M.C. Kennicutt II, D.C. Biggs, Spatial and temporal variability of phytoplankton biomass and community structure over the continental margin of the Northeast Gulf of Mexico based on pigment analysis, *Cont. Shelf Res., 23(1)*, 1-17 (2003).

Sturges, W., The frequency of ring separations from the Loop Current, *J. Phys. Oceanogr., 24(7)*, 1647-1651 (1994).

Sturges, W., and R. Leben, Frequency of ring separations from the Loop Current in the Gulf of Mexico, *J. Phys. Oceanogr., 30*, 1814-1819 (2000).

Wawrik, B., J.H. Pahl, L. Campbell, D. Griffin, L.Houchin, A. Fuentes-Ortega, and F.E. Muller-Karger, Vertical structure of the phytoplankton community associated with a coastal plume in the Gulf of Mexico, *Marine Ecology Progress Series, 251*, 87-101 (2003).

Wiseman, W.J. and W. Sturges, *Physical Oceanography of the Gulf of Mexico: Processes that Regulate its Biology, in: Gulf of Mexico Large Marine Ecosystem*,

edited by Kumpf H., K Steidinger, and K. Sheman, pp. 77-92, Blackwell Science Publisher, Molden, MA, (1999).

APPENDIX A

Freshwater Stations of all Depths
Correlation Analysis
Pearson Correlation Coefficients

	SRFSAL	INTFW	L37	L18	L01	ICHL37	ICHL18	ICHL01	DISTS	DMOM	NO3	SIO3	PO4
SRFSAL	1	-0.82	0.33	0.42	0.31	-0.49	-0.46	-0.31	-0.06	0.33	-0.443	-0.58	-0.40
	0	<0.01	<0.01	<0.01	<0.01	<0.01	<0.01	<0.01	0.106	<0.01	<0.01	<0.01	<0.01
	388	388	163	193	173	163	195	172	388	388	381	381	381
INTFW	-0.82	1	-0.36	-0.35	-0.20	-0.37	-0.31	-0.28	0.15	-0.21	0.15	0.32	0.14
	<0.01	0	<0.01	<0.01	<0.01	<0.01	<0.01	<0.01	<0.01	<0.01	<0.01	<0.01	<0.01
	388	388	163	193	173	163	195	172	388	388	381	381	381
L37	0.33	-0.79	1	0.92	0.51	0.15	-0.14	-0.04	0.07	-0.01	-0.14	-0.23	-0.18
	<0.01	<0.01	0	<0.01	<0.01	<0.05	<0.10	0.10<	0.10<	0.10<	<0.10	<0.01	<0.05
	163	163	163	162	145	163	162	144	163	163	157	157	157
L18	0.42	-0.35	0.92	1	0.67	0.24	-0.23	-0.06	0.19	0.13	-0.17	-0.31	-0.27
	<0.01	<0.01	<0.01	0	<0.01	<0.01	<0.01	0.10<	<0.01	<0.10	<0.05	<0.01	<0.01
	193	193	162	193	173	162	193	172	193	193	187	187	187
L01	0.31	-0.20	0.51	0.67	1	0.28	-0.33	-0.03	0.48	0.05	-0.20	-0.35	-0.33
	<0.01	<0.01	<0.01	<0.01	0	<0.01	<0.01	0.10<	<0.01	0.10<	<0.01	<0.01	<0.01
	173	173	145	173	173	145	173	172	173	173	169	169	169
ICHL37	-0.49	0.37	-0.15	-0.24	-0.28	1	0.97	0.67	-0.04	-0.19	0.11	0.19	0.12
	<0.01	<0.01	<0.05	<0.01	<0.01	0	<0.01	<0.01	0.10<	<0.01	0.10<	<0.05	<0.05
	163	163	163	162	145	163	162	144	163	163	157	157	157
ICHL18	-0.46	0.31	-0.14	-0.23	-0.33	0.97	1	0.75	-0.14	-0.29	0.17	0.19	0.25
	<0.01	<0.01	<0.10	<0.01	<0.01	<0.01	0	<0.01	<0.01	<0.01	<0.01	<0.01	<0.01
	195	195	162	193	173	162	195	172	195	195	189	189	189
ICHL01	-0.31	0.28	-0.06	-0.06	-0.03	0.67	0.75	1	-0.06	-0.23	0.05	-0.01	0.10
	<0.01	<0.01	0.10<	0.10<	0.10<	<0.01	<0.01	0	0.10<	<0.01	0.10<	0.10<	0.10<
	172	172	144	172	172	144	172	172	172	172	168	168	168
DISTS	-0.06	0.15	0.07	0.19	0.48	-0.04	-0.14	-0.06	1	0.21	-0.10	-0.20	-0.18
	0.10<	<0.01	0.10<	<0.01	<0.01	0.10<	<0.05	0.10<	0	<0.01	<0.05	<0.01	<0.01
	388	388	163	193	173	163	195	172	388	388	381	381	381
DMOM	0.33	-0.21	-0.01	0.13	0.05	-0.19	-0.29	-0.23	0.21	1	-0.23	-0.34	-0.28
	<0.01	<0.01	0.10<	<0.10	0.10<	<0.01	<0.01	<0.01	<0.01	0	<0.01	<0.01	<0.01
	388	388	163	193	173	163	195	172	388	388	381	381	381
NO3	-0.44	0.15	-0.14	-0.17	-0.20	0.11	0.17	0.05	-0.10	-0.23	1	0.72	0.49
	<0.01	<0.01	<0.10	<0.01	<0.01	0.10<	<0.05	0.10<	<0.05	<0.01	0	<0.01	<0.01
	381	381	157	187	169	157	189	168	381	381	381	381	381
SIO3	-0.58	0.32	-0.23	-0.31	-0.35	0.19	0.19	-0.01	-0.20	-0.34	0.72	1	0.63
	<0.01	<0.01	<0.01	<0.01	<0.01	<0.01	<0.01	0.847	<0.01	<0.01	<0.01	0	<0.01
	381	381	157	187	169	157	189	168	381	381	381	381	381
PO4	-0.40	0.14	-0.18	-0.27	-0.33	0.12	0.25	0.09	-0.18	-0.28	0.49	0.63	1
	<0.01	<0.01	<0.01	<0.01	<0.01	<0.05	<0.01	0.10<	<0.01	<0.01	<0.01	<0.01	0
	381	381	157	187	169	157	189	168	381	381	381	381	381

Figure A1. Correlation analysis for all freshwater stations of all cruises combined. SRFSAL=surface salinity; INTFW=integrated freshwater; L37=depth of 36.8% light penetration; L18= depth of 18% light penetration; L1= depth of 1% light penetration; ICHL37=mass of integrated chl-α to 36.8% light penetration; ICHL18= mass of integrated chl-α to 18% light penetration; ICHL1= mass of integrated chl-α to 1% light penetration; DISTS=distance from nearest shoreline; DMOM=distance from the mouth of the Mississippi; NO3=surface concentration of nitrate in mMol/m^3; SIO3=surface concentration of silicate in mMol/m^3; PO4= surface concentration of phosphate in mMol/m^3.

	Bluewater	Stations of all	Depths										
	Correlation	Analysis											
	Pearson	Correlation	Coefficients										
	SRFSA	**INTFW**	**L37**	**L18**	**L01**	**ICHL37**	**ICHL18**	**ICHL01**	**DISTS**	**DMOM**	**NO3**	**SIO3**	**PO4**
SRFSAL	1		0.18	0.23	0.35	-0.25	-0.13	-0.22	0.28	0.09	-0.14	0.01	-0.04
	0		<0.05	<0.05	<0.01	<0.01	<0.10	<0.01	<0.01	<0.10	<0.01	0.10<	0.10<
	388	388	157	163	135	157	168	134	388	388	383	383	383
INTFW													
	388	388	157	163	135	157	168	134	388	388	383	383	383
L37	0.18		1	0.84	0.48	0.43	0.48	0.18	0.19	-0.01	-0.16	0.02	-0.01
	<0.05		0	<0.01	<0.01	<0.01	<0.01	<0.05	<0.05	0.10<	0.10<	0.10<	0.10<
	157	157	157	154	127	157	154	127	157	157	157	157	157
L18	0.23		0.84	1	0.688	0.28	0.65	0.38	0.20	-0.01	-0.14	-0.02	0.01
	<0.01		<0.01	0	<0.01	<0.01	<0.01	<0.01	<0.01	0.10<	0.10<	0.10<	0.10<
	163	163	154	163	135	154	162	134	163	163	163	163	163
L01	0.35		0.48	0.68	1	-0.15	0.20	0.28	0.54	-0.04	-0.06	0.02	-0.01
	<0.01		<0.01	<0.01	0	<0.10	<0.05	<0.01	<0.01	0.10<	0.10<	0.10<	0.10<
	135	135	127	135	135	127	134	134	135	135	135	135	135
ICHL37	-0.25		0.43	0.28	-0.15	1	0.84	0.54	-0.19	-0.10	-0.01	0.05	0.07
	<0.01		<0.01	<0.01	<0.10	0	<0.01	<0.01	<0.01	0.10<	0.10<	0.10<	0.10<
	157	157	157	154	127	157	154	127	157	157	157	157	157
ICHL18	-0.13		0.48	0.65	0.20	0.84	1	0.64	-0.21	-0.18	0.01	0.05	0.06
	<0.10		<0.01	<0.01	<0.05	<0.01	0	<0.01	<0.01	<0.01	0.10<	0.10<	0.10<
	168	168	154	162	134	154	168	134	168	168	168	168	168
ICHL01	-0.22		0.18	0.38	0.28	0.54	0.64	1	0.13	-0.03	0.08	-0.04	0.17
	<0.01		<0.05	<0.01	<0.01	<0.01	<0.01	0	0.10<	0.10<	0.10<	0.10<	<0.05
	134	134	127	134	134	127	134	134	134	134	134	134	134
DISTS	0.28		0.19	0.20	0.54	-0.19	-0.21	0.13	1	0.41	0.06	-0.16	0.09
	<0.01		<0.05	<0.01	<0.01	<0.01	<0.01	0.10<	0	<0.01	0.10<	<0.01	<0.10
	388	388	157	163	135	157	168	134	388	388	383	383	383
DMOM	0.09		-0.01	-0.01	-0.04	-0.10	-0.18	-0.03	0.41	1	-0.03	-0.22	-0.12
	<0.10		0.10<	0.10<	0.10<	0.10<	<0.05	0.10<	<0.01	0	0.10<	<0.01	<0.01
	388	388	157	163	135	157	168	134	388	388	383	383	383
NO3	-0.14		-0.16	-0.14	-0.06	-0.01	0.01	0.08	0.06	-0.03	1	0.0163	0.21
	<0.01		<0.05	<0.10	0.10<	0.10<	0.10<	0.10<	0.10<	0.10<	0	0.10<	<0.01
	383	383	157	163	135	157	168	134	383	383	383	383	383
SIO3	0.01		0.02	-0.02	0.02	0.05	0.05	-0.04	-0.16	-0.22	0.01	1	0.08
	0.10<		0.10<	0.10<	0.10<	0.10<	0.10<	0.10<	<0.01	<0.01	0.10<	0	0.10<
	383	383	157	163	135	157	168	134	383	383	383	383	383
PO4	-0.04		-0.01	0.01	-0.01	0.07	0.06558	0.17938	0.09	-0.12	0.21	0.08	1
	0.10<		0.10<	0.10<	0.10<	0.10<	0.10<	<0.05	<0.10	<0.01	<0.01	0.10<	0
	383	383	157	163	135	157	168	134	383	383	383	383	383

Figure A2. Correlation analysis for all bluewater stations of all cruises combined. SRFSAL=surface salinity; INTFW=integrated freshwater; L37=depth of 36.8% light penetration; L18= depth of 18% light penetration; L1= depth of 1% light penetration; ICHL37=mass of integrated chl-α to 36.8% light penetration; ICHL18= mass of integrated chl-α to 18% light penetration; ICHL1= mass of integrated chl-α to 1% light penetration; DISTS=distance from nearest shoreline; DMOM=distance from the mouth of the Mississippi; NO3=surface concentration of nitrate in mMol/m^3; SIO3=surface concentration of silicate in mMol/m^3; PO4= surface concentration of phosphate in mMol/m^3.

	Coastal Correlation Pearson	Stations of all Analysis Correlation	Depths Coefficients										
	SRFSA	**INTFW**	**L37**	**L18**	**L01**	**ICHL37**	**ICHL18**	**ICHL01**	**DISTS**	**DMOM**	**NO3**	**SIO3**	**PO4**
SRFSAL	1	-0.58	0.03	0.18	0.32	-0.29	-0.18	-0.21	0.431	0.54	-0.02	-0.08	-0.07
	0	<0.01	0.10<	0.10<	<0.05	<0.05	0.10<	0.10<	<0.01	<0.01	0.10<	0.10<	0.10<
	102	102	52	54	45	52	54	45	102	102	102	102	102
INTFW	-0.58	1	-0.15	-0.21	-0.12	0.01	-0.07	0.15118	-0.21	-0.21	-0.07	0.14	0.04
	<0.01	0	0.10<	<0.10	0.10<	0.10<	0.10<	0.10<	<0.05	<0.05	0.10<	0.10<	0.10<
	102	102	52	54	45	52	54	45	102	102	102	102	102
L37	0.03	-0.15	1	0.86	0.38	0.02	0.20	-0.02	0.11	0.03	-0.10	-0.09	0.23
	0.10<	0.10<	0	<0.01	<0.01	0.10<	0.10<	0.10<	0.10<	0.10<	0.10<	0.10<	<0.10
	52	52	52	52	43	52	52	43	52	52	52	52	52
L18	0.18	-0.21	0.86	1	0.52	-0.04	0.26	-0.04	0.29	0.09	-0.13	-0.11	0.01
	0.10<	<0.10	<0.01	0	<0.01	0.10<	<0.05	0.10<	<0.05	0.10<	0.10<	0.10<	0.10<
	54	54	52	54	45	52	54	45	54	54	54	54	54
L01	0.32	-0.12	0.38	0.52	1	-0.32	-0.19	0.30	0.45	0.13	-0.04	-0.19	-0.34
	<0.05	0.10<	<0.01	<0.01	0	<0.05	0.10<	<0.05	<0.01	0.10<	0.10<	0.10<	<0.05
	45	45	43	45	45	43	45	45	45	45	45	45	45
ICHL37	-0.29	0.01	0.02	-0.04	-0.32	1	0.94	0.60	-0.09	-0.12	0.01	-0.10	0.03
	<0.05	0.10<	0.10<	0.10<	<0.05	0	<0.01	<0.01	0.10<	0.10<	0.10<	0.10<	0.10<
	52	52	52	52	43	52	52	43	52	52	52	52	52
ICHL18	-0.18	-0.07	0.20	0.26	-0.19	0.94	1	0.57	-0.01	-0.09	-0.03	-0.12	-0.01
	0.10<	0.10<	0.10<	<0.05	0.10<	<0.01	0	<0.01	0.10<	0.10<	0.10<	0.10<	0.10<
	54	54	52	54	45	52	54	45	54	54	54	54	54
ICHL01	-0.21	0.15	-0.02	-0.04	0.30	0.60	0.57	1	0.16	-0.01	-0.08	-0.19	-0.23
	0.10<	0.10<	0.10<	0.10<	<0.05	<0.01	<0.01	0	0.10<	0.10<	0.10<	0.10<	0.10<
	45	45	43	45	45	43	45	45	45	45	45	45	45
DISTS	0.43	-0.21	0.11	0.29	0.45	-0.09	-0.01	0.16	1	0.31	-0.07	-0.25	-0.05
	<0.01	<0.05	0.10<	<0.05	<0.01	0.10<	0.10<	0.10<	0	<0.01	0.10<	<0.01	0.10<
	102	102	52	54	45	52	54	45	102	102	102	102	102
DMOM	0.54	-0.21	0.03	0.09	0.13	-0.12	-0.09	-0.01	0.31	1	-0.08	-0.25	-0.14
	<0.01	<0.05	0.10<	0.10<	0.10<	0.10<	0.10<	<0.01	<0.01	0	0.10<	<0.01	0.10<
	102	102	52	54	45	52	54	45	102	102	102	102	102
NO3	-0.02069	-0.07	-0.10	-0.13	-0.04	0.01	-0.03	-0.08	-0.07	-0.08	1	0.43	0.19
	0.10<	0.10<	0.10<	0.10<	0.10<	0.10<	0.10<	0.10<	0.10<	0.10<	0	<0.01	<0.05
	102	102	52	54	45	52	54	45	102	102	102	102	102
SIO3	-0.08	0.14	-0.09	-0.11	-0.19	-0.10	-0.12	-0.19	-0.25	-0.25	0.43	1	0.24
	0.10<	0.10<	0.10<	0.10<	0.10<	0.10<	0.10<	0.10<	<0.01	<0.01	<0.01	0	<0.01
	102	102	52	54	45	52	54	45	102	102	102	102	102
PO4	-0.07	0.04	0.23	0.01	-0.34	0.03	-0.01	-0.23	-0.05	-0.14	0.19	0.244	1
	0.10<	0.10<	<0.10	0.10<	<0.05	0.10<	0.10<	0.10<	0.10<	0.10<	<0.05	<0.01	0
	102	102	52	54	45	52	54	45	102	102	102	102	102

Figure A3. Correlation analysis for all coastal stations of all cruises combined. SRFSAL=surface salinity; INTFW=integrated freshwater; L37=depth of 36.8% light penetration; L18= depth of 18% light penetration; L1= depth of 1% light penetration; ICHL37=mass of integrated chl-α to 36.8% light penetration; ICHL18= mass of integrated chl-α to 18% light penetration; ICHL1= mass of integrated chl-α to 1% light penetration; DISTS=distance from nearest shoreline; DMOM=distance from the mouth of the Mississippi; NO3=surface concentration of nitrate in mMol/m^3; SIO3=surface concentration of silicate in mMol/m^3; PO4= surface concentration of phosphate in mMol/m^3.

Freshwater Stations with Depth > 100m

	Correlation Pearson	Analysis Correlation		Coefficients									
	SRFSAL	INTFW	L37	L18	L01	ICHL37	ICHL18	ICHL01	DISTS	DMOM	NO3	SIO3	PO
SRFSAL	1	-0.86	0.33	0.44	0.30	-0.39	-0.45	-0.33	0.04	0.46	-0.67	-0.65	-0.4744
	0	<0.01	<0.01	<0.01	<0.01	<0.01	<0.01	<0.01	0.10<	<0.01	<0.01	<0.01	<0.01
	177	177	73	91	81	73	93	81	177	177	177	177	17
INTFW	-0.86	1	-0.23	-0.34	-0.16	0.31	0.30	0.30	0.04	-0.40	0.48	0.52	0.30
	<0.01	0	<0.05	<0.01	0.10<	<0.01	<0.01	<0.01	0.10<	<0.01	<0.01	<0.01	<0.01
	177	177	73	91	81	73	93	81	177	177	177	177	17
L37	0.33	-0.23	1	0.92	0.44	-0.31	-0.27	-0.13	0.04	0.14	-0.23	-0.35	-0.25
	<0.01	<0.05	0	<0.01	<0.01	<0.01	<0.05	0.10<	0.10<	0.10<	<0.05	<0.01	<0.05
	73	73	73	73	65	73	73	65	73	73	73	73	7
L18	0.44	-0.34	0.92	1	0.69	-0.40	-0.38	-0.15	0.26	0.33	-0.35	-0.41	-0.37
	<0.01	<0.01	<0.01	0	<0.01	<0.01	<0.01	0.10<	<0.01	<0.01	<0.01	<0.01	<0.01
	91	91	73	91	81	73	91	81	91	91	91	91	9
L01	0.30	-0.16	0.44	0.69	1	-0.33	-0.34	0.03	0.54	0.08	-0.25	-0.42	-0.36
	<0.01	0.10<	<0.01	<0.01	0	<0.01	<0.01	0.10<	<0.01	0.10<	<0.05	<0.01	<0.01
	81	81	65	81	81	65	81	81	81	81	81	81	8
ICHL37	-0.39	0.31	-0.31	-0.40	-0.33	1	0.95	0.69	-0.02	-0.30	0.16	0.15153	0.39
	<0.01	<0.01	<0.01	<0.01	<0.01	0	<0.01	<0.01	0.10<	<0.01	0.10<	0.10<	<0.01
	73	73	73	73	65	73	73	65	73	73	73	73	7
ICHL18	-0.45	0.30	-0.27	-0.38	-0.34	0.95	1	0.76	-0.06	-0.35	0.28	0.18	0.39
	<0.01	<0.01	<0.05	<0.01	<0.01	<0.01	0	<0.01	0.10<	<0.01	<0.01	<0.10	<0.01
	93	93	73	91	81	73	93	81	93	93	93	93	9
ICHL01	-0.33	0.30	-0.13	-0.15	0.03	0.69	0.76	1	0.05	-0.28	0.16	0.05	0.19
	<0.01	<0.01	0.10<	0.10<	0.10<	<0.01	<0.01	0	0.10<	<0.01	0.10<	0.10<	<0.10
	81	81	65	81	81	65	81	81	81	81	81	81	8
DISTS	0.04	0.04	0.04	0.26	0.54	-0.02	-0.06	0.05	1	0.13	-0.09	-0.29	-0.23
	0.10<	0.10<	0.10<	<0.01	<0.01	0.10<	0.10<	0.10<	0	<0.10	0.10<	<0.01	<0.01
	177	177	73	91	81	73	93	81	177	177	177	177	17
DMOM	0.46	-0.40	0.14	0.33	0.08	-0.30	-0.35	-0.28	0.13	1	-0.37	-0.46	-0.34
	<0.01	<0.01	0.10<	<0.01	0.10<	<0.01	<0.01	<0.01	<0.10	0	<0.01	<0.01	<0.01
	177	177	73	91	81	73	93	81	177	177	177	177	17
NO3	-0.67	0.48	-0.23	-0.35	-0.25	0.16	0.28	0.16	-0.09	-0.37	1	0.66	0.63
	<0.01	<0.01	<0.05	<0.01	<0.05	0.10<	<0.01	0.10<	0.10<	<0.01	0	<0.01	<0.01
	177	177	73	91	81	73	93	81	177	177	177	177	17
SIO3	-0.65	0.52	-0.35	-0.41	-0.42	0.15153	0.18	0.05	-0.29	-0.46	0.66	1	0.61
	<0.01	<0.01	<0.01	<0.01	<0.01	0.10<	<0.10	0.10<	<0.01	<0.01	<0.01	0	<0.01
	177	177	73	91	81	73	93	81	177	177	177	177	17
PO4	-0.47	0.30	-0.25	-0.37	-0.36	0.39	0.39	0.19	-0.23	-0.34	0.63	0.61	1
	<0.01	<0.01	<0.05	<0.01	<0.01	<0.01	<0.01	<0.10	<0.01	<0.01	<0.01	<0.01	0
	177	177	73	91	81	73	93	81	177	177	177	177	17

Figure A4. Correlation analysis for all freshwater stations deeper than 100m of all cruises combined. SRFSAL=surface salinity; INTFW=integrated freshwater; L37=depth of 36.8% light penetration; L18= depth of 18% light penetration; L1= depth of 1% light penetration; ICHL37=mass of integrated chl-α to 36.8% light penetration; ICHL18= mass of integrated chl-α to 18% light penetration; ICHL1= mass of integrated chl-α to 1% light penetration; DISTS=distance from nearest shoreline; DMOM=distance from the mouth of the Mississippi; NO3=surface concentration of nitrate in mMol/m^3; SIO3=surface concentration of silicate in mMol/m^3; PO4= surface concentration of phosphate in mMol/m^3.

Freshwater Stations with Depth < 100m

	Correlation Analysis												
	Pearson Correlation Coefficients												
	SRFSAL	**INTFW**	**L37**	**L18**	**L01**	**ICHL37**	**ICHL18**	**ICHL01**	**DISTS**	**DMOM**	**NO3**	**SIO3**	**PO**
SRFSAL	1	-0.77	0.41	0.49	0.52	-0.58	-0.51	-0.33	0.02	0.13	-0.41	-0.57	-0.43
	0	<0.01	<0.01	<0.01	<0.01	<0.01	<0.01	<0.01	0.10<	<0.10	<0.01	<0.01	<0.01
	207	207	86	98	89	86	98	88	207	207	207	207	20
INTFW	-0.77	1	-0.40	-0.43	-0.47	0.43	0.39	0.34	0.07	0.06	0.07	0.22	0.10
	<0.01	0	<0.01	<0.01	<0.01	<0.01	<0.01	<0.01	0.10<	0.10<	0.10<	<0.01	0.10<
	207	207	86	98	89	86	98	88	207	207	207	207	20
L37	0.41	-0.40	1	0.93	0.54	-0.04	-0.03	0.06	-0.08	-0.07	-0.07	-0.21	-0.22
	<0.01	<0.01	0	<0.01	<0.01	0.10<	0.10<	0.10<	0.10<	0.10<	0.10<	<0.05	<0.05
	86	86	86	85	77	86	85	76	86	86	86	86	8
L18	0.49	-0.43	0.93	1	0.65	-0.13	-0.07	0.06	0.01	0.04	-0.15	-0.30	-0.27
	<0.01	<0.01	<0.01	0	<0.01	0.10<	0.10<	0.10<	0.10<	0.10<	0.10<	<0.01	<0.01
	98	98	85	98	89	85	98	88	98	98	98	98	9
L01	0.52	-0.47	0.54	0.65	1	-0.24	-0.29	-0.01	0.13	0.14	-0.25	-0.41	-0.44
	<0.01	<0.01	<0.01	<0.01	0	<0.05	<0.01	0.10<	0.10<	0.10<	<0.05	<0.01	<0.01
	89	89	77	89	89	77	89	88	89	89	89	89	8
ICHL37	-0.58	0.43	-0.04	-0.13	-0.24	1	0.98	0.69	-0.03	-0.10	0.01	0.29	0.09
	<0.01	<0.01	0.10<	0.10<	<0.05	0	<0.01	<0.01	0.10<	0.10<	0.10<	<0.01	0.10<
	86	86	86	85	77	86	85	76	86	86	86	86	8
ICHL18	-0.51	0.39	-0.03	-0.07	-0.29	0.98	1	0.72	-0.13	-0.24	0.18	0.26	0.23
	<0.01	<0.01	0.7231	0.10<	<0.01	<0.01	0	<0.01	0.10<	<0.05	<0.10	<0.01	<0.05
	98	98	85	98	89	85	98	88	98	98	98	98	9
ICHL01	-0.33	0.34	0.06	0.06	-0.01	0.69	0.72	1	-0.05	-0.15	0.05	0.06	0.15
	<0.01	<0.01	0.10<	0.10<	0.10<	<0.01	<0.01	0	0.10<	0.10<	0.10<	0.10<	0.10<
	88	88	76	88	88	76	88	88	88	88	88	88	8
DISTS	0.02	0.07	-0.08	0.01	0.13	-0.03	-0.13	-0.05	1	0.63	-0.19	-0.18	-0.17
	0.10<	0.10<	0.10<	0.10<	0.10<	0.10<	0.10<	0.10<	0	<0.01	<0.01	<0.01	<0.01
	207	207	86	98	89	86	98	88	207	207	207	207	20
DMOM	0.13	0.06	-0.07	0.04	0.14	-0.10	-0.24	-0.15	0.63	1	-0.23	-0.27	-0.30
	<0.10	0.10<	0.10<	0.10<	0.10<	0.10<	<0.05	0.10<	<0.01	0	<0.01	<0.01	<0.01
	207	207	86	98	89	86	98	88	207	207	207	207	20
NO3	-0.41	0.07	-0.07	-0.15	-0.25	0.01	0.18	0.05	-0.19	-0.23	1	0.83	0.48
	<0.01	0.10<	0.10<	0.10<	<0.05	0.10<	0.10<	0.10<	<0.01	<0.01	0	<0.01	<0.01
	207	207	86	98	89	86	98	88	207	207	207	207	20
SIO3	-0.57	0.22	-0.21	-0.30	-0.41	0.29	0.26	0.06	-0.18	-0.27	0.83	1	0.60
	<0.01	<0.01	<0.05	<0.01	<0.01	<0.01	<0.01	0.10<	<0.01	<0.01	<0.01	0	<0.01
	207	207	86	98	89	86	98	88	207	207	207	207	20
PO4	-0.43	0.10	-0.22	-0.27	-0.44	0.09	0.23	0.15	-0.17	-0.30	0.48	0.60	1
	<0.01	0.10<	<0.05	<0.01	<0.01	0.10<	<0.05	0.10<	<0.01	<0.01	<0.01	<0.01	0
	207	207	86	98	89	86	98	88	207	207	207	207	20

Figure A5. Correlation analysis for all freshwater stations with a depth shallower than 100m for all cruises combined. SRFSAL=surface salinity; INTFW=integrated freshwater; L37=depth of 36.8% light penetration; L18= depth of 18% light penetration; L1= depth of 1% light penetration; ICHL37=mass of integrated chl-α to 36.8% light penetration; ICHL18= mass of integrated chl-α to 18% light penetration; ICHL1= mass of integrated chl-α to 1% light penetration; DISTS=distance from nearest shoreline; DMOM=distance from the mouth of the Mississippi; NO3=surface concentration of nitrate in mMol/m^3; SIO3=surface concentration of silicate in mMol/m^3; PO4= surface concentration of phosphate in mMol/m^3.

Bluewater Stations with Depth > 100m

	Correlation Pearson	Analysis Correlation	Coefficients										
	SRFSAL	**INTFW**	**L37**	**L18**	**L01**	**ICHL37**	**ICHL18**	**ICHL01**	**DISTS**	**DMOM**	**NO3**	**SIO3**	**PO**
SRFSAL	1	.	0.10	0.26	0.31	-0.23	-0.08	-0.50	0.18	0.25	-0.19	0.09	-0.19
	0	.	0.10<	0.10<	0.10<	0.10<	0.10<	<0.01	<0.10	<0.05	<0.10	0.10<	<0.10
	91	91	34	35	31	34	35	31	91	91	91	91	9
INTFW	.	.	.	.	.	.	.	.	.	.	.	.	.
	.	.	.	.	.	.	.	.	.	.	.	.	.
	91	91	34	35	31	34	35	31	91	91	91	91	9
L37	0.10	.	1	0.94	0.36	0.66	0.75	0.24	-0.05	0.16	-0.16	-0.20	-0.25
	0.10<	.	0	<0.01	<0.05	<0.01	<0.01	0.10<	0.10<	0.10<	0.10<	0.10<	0.10<
	34	34	34	33	29	34	33	29	34	34	34	34	3
L18	0.26	.	0.94	1	0.48	0.59	0.71	0.18	-0.07	0.17	-0.16	-0.10	-0.23
	0.10<	.	<0.01	0	<0.01	<0.01	<0.01	0.10<	0.10<	0.10<	0.10<	0.10<	0.10<
	35	35	33	35	31	33	35	31	35	35	35	35	3
L01	0.31	.	0.36	0.48	1	0.10	0.27	0.21	0.30	0.07	-0.02	-0.05	-0.31
	<0.10	.	<0.05	<0.01	0	0.10<	0.10<	0.10<	<0.10	0.10<	0.10<	0.10<	<0.10
	31	31	29	31	31	29	31	31	31	31	31	31	3
ICHL37	-0.23	.	0.66	0.59	0.10	1	0.95	0.54	-0.08	0.08	0.03	-0.09	-0.05
	0.10<	.	<0.01	<0.01	0.10<	0	<0.01	<0.01	0.10<	0.10<	0.10<	0.10<	0.10<
	34	34	34	33	29	34	33	29	34	34	34	34	3
ICHL18	-0.08	.	0.75	0.71	0.27	0.95	1	0.52	-0.06	0.11	-0.03	-0.11	-0.10
	0.10<	.	<0.01	<0.01	0.10<	<0.01	0	<0.01	0.10<	0.10<	0.10<	0.10<	0.10<
	35	35	33	35	31	33	35	31	35	35	35	35	3
ICHL01	-0.50	.	0.24	0.18	0.21	0.54	0.52	1	0.25	0.12	0.19	-0.09	-0.02
	<0.01	.	0.10<	0.10<	0.10<	<0.01	<0.01	0	0.10<	0.10<	0.10<	0.10<	0.10<
	31	31	29	31	31	29	31	31	31	31	31	31	3
DISTS	0.18	.	-0.05	-0.07	0.30	-0.08	-0.06	0.25	1	0.57	0.18	-0.08	-0.05
	<0.05	.	0.10<	0.10<	<0.10	0.10<	0.10<	0.10<	0	<0.01	<0.10	0.10<	0.10<
	91	91	34	35	31	34	35	31	91	91	91	91	9
DMOM	0.25	.	0.16	0.17	0.07	0.08	0.11	0.12	0.57	1	-0.11	-0.01	-0.28
	<0.05	.	0.10<	0.10<	0.10<	0.10<	0.10<	0.10<	<0.01	0	0.10<	0.10<	<0.01
	91	91	34	35	31	34	35	31	91	91	91	91	9
NO3	-0.19	.	-0.16	-0.16	-0.02	0.03	-0.03	0.19	0.18	-0.11	1	-0.05	0.11
	<0.10	.	<0.10	<0.10	<0.10	<0.10	<0.10	<0.10	<0.10	<0.10	0	0.10<	0.10<
	91	91	34	35	31	34	35	31	91	91	91	91	9
SIO3	0.09631	.	-0.20	-0.10	-0.05	-0.09	-0.11	-0.09	-0.08	-0.01	-0.05	1	0.10
	0.10<	0.10<	0.10<	0.10<	0.10<	0.10<	0.10<	0.10<	0.10<	0.10<	0.10<	0	0.10<
	91	91	34	35	31	34	35	31	91	91	91	91	9
PO4	-0.19	.	-0.25	-0.23	-0.31	-0.05	-0.10	-0.02	-0.05	-0.28	0.11	0.10	1
	<0.10	.	0.10<	0.10<	<0.10	0.10<	0.10<	0.10<	0.10<	<0.01	0.10<	0.10<	0
	91	91	34	35	31	34	35	31	91	91	91	91	9

Figure A6. Correlation analysis for all bluewater stations with depth greater than 100m for all cruises combined. SRFSAL=surface salinity; INTFW=integrated freshwater; L37=depth of 36.8% light penetration; L18= depth of 18% light penetration; L1= depth of 1% light penetration; ICHL37=mass of integrated chl-α to 36.8% light penetration; ICHL18= mass of integrated chl-α to 18% light penetration; ICHL1= mass of integrated chl-α to 1% light penetration; DISTS=distance from nearest shoreline; DMOM=distance from the mouth of the Mississippi; NO3=surface concentration of nitrate in mMol/m^3; SIO3=surface concentration of silicate in mMol/m^3; PO4= surface concentration of phosphate in mMol/m^3.

Bluewater Stations with Depth < 100m

	Correlation Pearson	Analysis Correlation	Coefficients										
	SRFSAL	**INTFW**	**L37**	**L18**	**L01**	**ICHL37**	**ICHL18**	**ICHL01**	**DISTS**	**DMOM**	**NO3**	**SIO3**	**PO**
SRFSAL	1	.	0.14	0.17	0.34	-0.25	-0.18	-0.19	0.24	0.11	-0.15	-0.02	-0.04
	0	.	0.10<	<0.05	<0.01	<0.01	<0.05	<0.05	<0.01	<0.05	<0.01	0.10<	0.10<
	296	296	123	128	104	123	133	103	296	296	296	296	29
INTFW	.	.	.	.	.	.	.	.	.	.	.	.	.
	.	.	.	.	.	.	.	.	.	.	.	.	.
	296	296	123	128	104	123	133	103	296	296	296	296	29
L37	0.14	.	1	0.81	0.48	0.39	0.40	0.09	0.14	0.01	-0.06	0.04	0.03
	0.10<	.	0	<0.01	<0.01	<0.01	<0.01	0.10<	0.10<	0.10<	0.10<	0.10<	0.10<
	123	123	123	121	98	123	121	98	123	123	123	123	12
L18	0.17	.	0.81	1	0.79	0.22	0.64	0.40	0.13	0.03	-0.05	-0.04	0.04
	<0.05	.	<0.01	0	<0.01	<0.01	<0.01	<0.01	0.10<	0.10<	0.10<	0.10<	0.10<
	128	128	121	128	104	121	127	103	128	128	128	128	12
L01	0.34	.	0.48	0.79	1	-0.35	0.18	0.13	0.38	0.26	-0.18	-0.02	-0.08
	<0.01	.	<0.01	<0.01	0	<0.01	<0.10	0.10<	<0.01	<0.01	<0.10	0.10<	0.10<
	104	104	98	104	104	98	103	103	104	104	104	104	10
ICHL37	-0.25	.	0.39	0.22	-0.35	1	0.79	0.59	-0.24	-0.22	-0.03	0.12	0.19
	<0.01	.	<0.01	<0.01	<0.01	0	<0.01	<0.01	<0.01	<0.01	0.10<	0.10<	<0.05
	123	123	123	121	98	123	121	98	123	123	123	123	12
ICHL18	-0.18	.	0.40	0.64	0.18	0.79	1	0.69	-0.30	-0.28	0.06	0.09	0.12
	<0.05	.	<0.01	<0.01	<0.10	<0.01	0	<0.01	<0.01	<0.01	0.10<	0.10<	0.10<
	133	133	121	127	103	121	133	103	133	133	133	133	13
ICHL01	-0.19	.	0.09	0.40	0.13	0.59	0.69	1	-0.02	0.01	0.07	-0.03	0.21
	<0.05	.	0.10<	<0.01	0.10<	<0.01	<0.01	0	0.10<	0.10<	0.10<	0.10<	<0.05
	103	103	98	103	103	98	103	103	103	103	103	103	10
DISTS	0.24	.	0.14	0.13	0.38	-0.24	-0.30	-0.02	1	0.63	0.05	-0.18	0.07
	<0.01	.	0.10<	0.10<	<0.01	<0.01	<0.01	0.10<	0	<0.01	0.10<	<0.01	0.10<
	296	296	123	128	104	123	133	103	296	296	296	296	29
DMOM	0.11	.	0.01	0.03	0.26	-0.22	-0.28	0.01	0.63	1	-0.03	-0.28	-0.03
	<0.05	.	0.10<	0.10<	<0.01	<0.01	<0.01	0.10<	<0.01	0	0.10<	<0.01	0.10<
	296	296	123	128	104	123	133	103	296	296	296	296	29
NO3	-0.15	.	-0.06	-0.05	-0.18	-0.03	0.06	0.07	0.05	-0.03	1	0.02	0.252
	<0.01	.	0.10<	0.10<	<0.05	0.10<	0.10<	0.10<	0.10<	0.10<	0	0.10<	0
	296	296	123	128	104	123	133	103	296	296	296	296	29
SIO3	-0.02	.	0.04	-0.04	-0.02	0.12	0.09	-0.03	-0.18	-0.28	0.02	1	0.08
	0.10<	0.10<	0.10<	0.10<	0.10<	0.10<	0.10<	0.10<	<0.01	<0.01	0.10<	0	0.10<
	296	296	123	128	104	123	133	103	296	296	296	296	29
PO4	-0.04	.	0.03	0.04	-0.08	0.19	0.12	0.21	0.07	-0.03	0.25	0.08	1
	0.10<	.	0.10<	0.10<	0.10<	<0.05	0.10<	<0.05	0.10<	0.10<	<0.01	0.10<	0
	296	296	123	128	104	123	133	103	296	296	296	296	29

Figure A7. Correlation analysis for all bluewater stations shallower than 100m for all cruises combined. SRFSAL=surface salinity; INTFW=integrated freshwater; L37=depth of 36.8% light penetration; L18= depth of 18% light penetration; L1= depth of 1% light penetration; ICHL37=mass of integrated chl-α to 36.8% light penetration; ICHL18= mass of integrated chl-α to 18% light penetration; ICHL1= mass of integrated chl-α to 1% light penetration; DISTS=distance from nearest shoreline; DMOM=distance from the mouth of the Mississippi; NO3=surface concentration of nitrate in mMol/m^3; SIO3=surface concentration of silicate in mMol/m^3; PO4= surface concentration of phosphate in mMol/m^3.

Coastal Stations with Depth < 100m

	Correlation	Analysis											
	Pearson	Correlation	Coefficients										
	SRFSAL	**INTFW**	**L37**	**L18**	**L01**	**ICHL37**	**ICHL18**	**ICHL01**	**DISTS**	**DMOM**	**NO3**	**SIO3**	**PO**
SRFSAL	1	-0.58	0.03	0.18	0.32	-0.29	-0.18	-0.21	0.43	0.54	-0.05	-0.18	-0.15
	0	<0.01	0.10<	0.10<	<0.05	<0.05	0.10<	0.10<	<0.01	<0.01	0.10<	<0.10	0.10<
	102	102	52	54	45	52	54	45	102	102	102	102	10
INTFW	-0.58	1	-0.15	-0.21	-0.12	0.01	-0.07	0.15	-0.21	-0.21	-0.04	0.20	0.07
	<0.01	0	0.10<	0.10<	0.10<	0.10<	0.10<	0.10<	<0.05	<0.05	0.10<	<0.05	0.10<
	102	102	52	54	45	52	54	45	102	102	102	102	10
L37	0.03	-0.15	1	0.86	0.38	0.02	0.20	-0.02	0.11	0.03	-0.08	-0.08	0.17
	0.10<	0.10<	0	<0.01	<0.01	0.10<	0.10<	0.10<	0.10<	0.10<	0.10<	0.10<	0.10<
	52	52	52	52	43	52	52	43	52	52	52	52	5
L18	0.18	-0.21	0.86	1	0.52	-0.04	0.26	-0.04	0.29	0.09	-0.11	-0.11	-0.04
	0.10<	0.10<	<0.01	0	<0.01	0.10<	<0.05	0.10<	<0.05	0.10<	0.10<	0.10<	0.10<
	54	54	52	54	45	52	54	45	54	54	54	54	5
L01	0.32	-0.12	0.38	0.52	1	-0.32	-0.19	0.30	0.45	0.13	-0.04	-0.16	-0.29
	<0.05	0.10<	<0.01	<0.01	0	<0.05	0.10<	<0.05	<0.01	0.10<	0.10<	0.10<	<0.05
	45	45	43	45	45	43	45	45	45	45	45	45	4
ICHL37	-0.29	0.01	0.02	-0.04	-0.32	1	0.94	0.60	-0.09	-0.12	0.04	-0.09	0.04
	<0.05	0.10<	0.10<	0.10<	<0.05	0	<0.01	<0.01	0.10<	0.10<	0.10<	0.10<	0.10<
	52	52	52	52	43	52	52	43	52	52	52	52	5
ICHL18	-0.18	-0.07	0.20	0.26	-0.19	0.94	1	0.57	-0.01	-0.09	-0.01	-0.12	-0.02
	0.10<	0.10<	0.10<	<0.05	0.10<	<0.01	0	<0.01	0.10<	0.10<	0.10<	0.10<	0.10<
	54	54	52	54	45	52	54	45	54	54	54	54	5
ICHL01	-0.21	0.15	-0.02	-0.04	0.30	0.60	0.57	1	0.16	-0.01	-0.09	-0.15	-0.20
	0.10<	0.10<	0.10<	0.10<	<0.05	<0.01	<0.01	0	0.10<	0.10<	0.10<	0.10<	0.10<
	45	45	43	45	45	43	45	45	45	45	45	45	4
DISTS	0.43	-0.21	0.11	0.29	0.45	-0.09	-0.01	0.16	1	0.31	-0.09	-0.27	-0.10
	<0.01	<0.05	0.10<	<0.05	<0.01	0.10<	0.10<	0.10<	0	<0.01	0.10<	<0.01	0.10<
	102	102	52	54	45	52	54	45	102	102	102	102	10
DMOM	0.54	-0.21	0.03	0.09	0.13	-0.12	-0.09	-0.01	0.31	1	-0.10	-0.28	-0.20
	<0.01	<0.05	0.10<	0.10<	0.10<	0.10<	0.10<	0.10<	<0.01	0	0.10<	<0.01	<0.05
	102	102	52	54	45	52	54	45	102	102	102	102	10
NO3	-0.05	-0.04	-0.08	-0.11	-0.04	0.04	-0.01	-0.09	-0.09	-0.10	1	0.51	0.33
	0.10<	0.10<	0.10<	0.10<	0.10<	0.10<	0.10<	0.10<	0.10<	0.10<	0	<0.01	<0.01
	102	102	52	54	45	52	54	45	102	102	102	102	10
SIO3	-0.18	0.20	-0.08	-0.11	-0.16	-0.09	-0.12	-0.15	-0.27	-0.28	0.51	1	0.48
	<0.10	<0.05	0.10<	0.10<	0.10<	0.10<	0.10<	0.10<	<0.01	<0.01	<0.01	0	<0.01
	102	102	52	54	45	52	54	45	102	102	102	102	10
PO4	-0.15	0.07	0.17	-0.04	-0.29	0.04	-0.02	-0.20	-0.10	-0.20	0.33	0.48	1
	0.10<	0.10<	0.10<	0.10<	<0.05	0.10<	0.10<	0.10<	0.10<	<0.05	<0.01	<0.01	0
	102	102	52	54	45	52	54	45	102	102	102		

Figure A8. Correlation analysis for all coastal stations of all cruises combined. SRFSAL=surface salinity; INTFW=integrated freshwater; L37=depth of 36.8% light penetration; L18= depth of 18% light penetration; L1= depth of 1% light penetration; ICHL37=mass of integrated chl-α to 36.8% light penetration; ICHL18= mass of integrated chl-α to 18% light penetration; ICHL1= mass of integrated chl-α to 1% light penetration; DISTS=distance from nearest shoreline; DMOM=distance from the mouth of the Mississippi; NO3=surface concentration of nitrate in mMol/m^3; SIO3=surface concentration of silicate in mMol/m^3; PO4= surface concentration of phosphate in mMol/m^3.

APPENDIX B

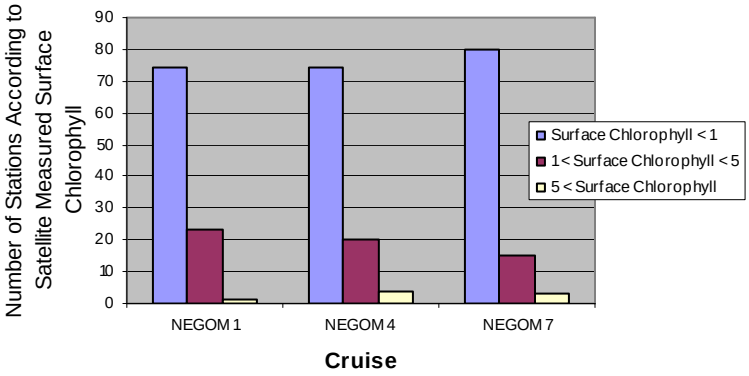

Figure B1: Numerical distribution of stations with different surface chlorophyll concentration ranges for the winter cruises.

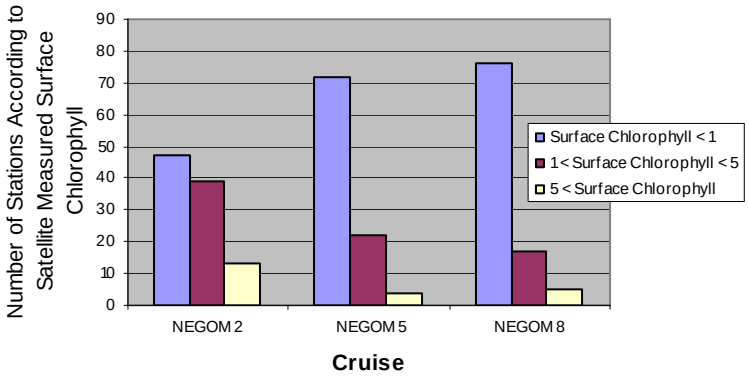

Figure B2: Numerical distribution of stations with different surface chlorophyll concentration ranges for the spring cruises.

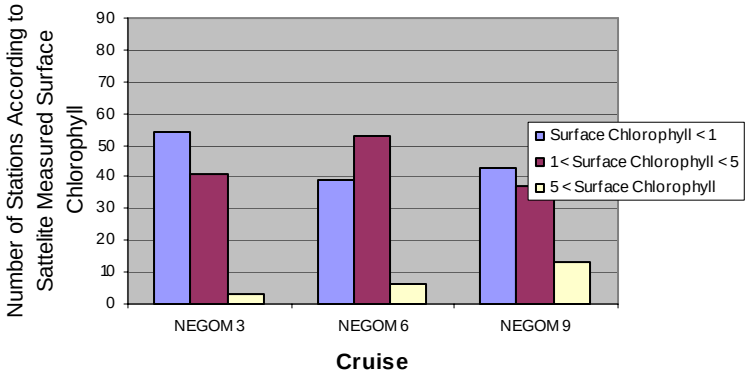

Figure B3: Numerical distribution of stations with different surface chlorophyll concentration ranges for the summer cruises.

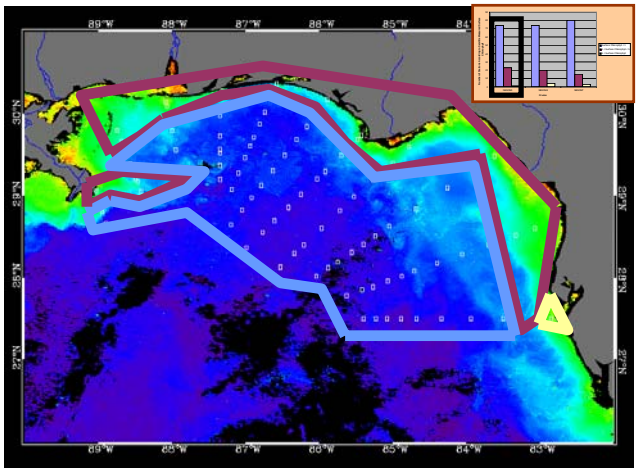

Figure B4. Graphical representation of surface chlorophyll distributions for winter, 1997cruise (N1). Blue box is CHL<1, Red box is 1<CHL<5 and Yellow box is 5<CHL.

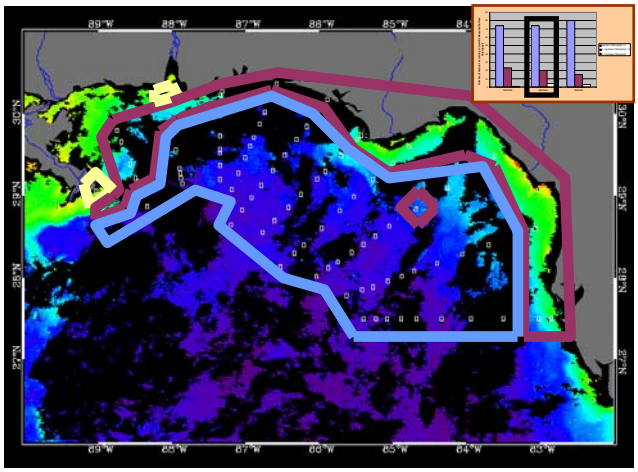

Figure B5. Graphical representation of surface chlorophyll distributions for winter, 1998 cruise (N4). Blue box is CHL<1, Red box is 1<CHL<5 and Yellow box is 5<CHL.

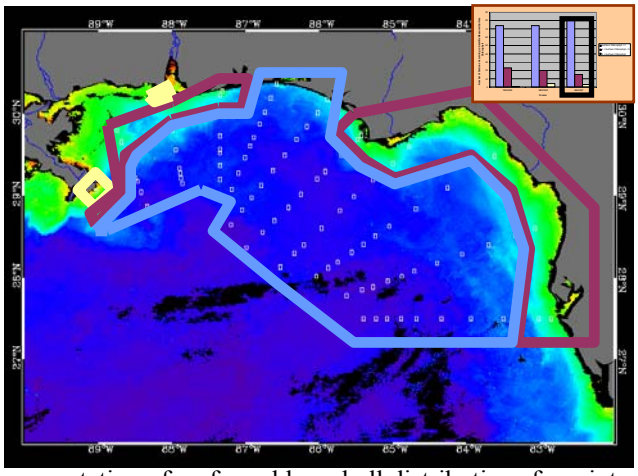

Figure B6. Graphical representation of surface chlorophyll distributions for winter, 1999 cruise (N7). Blue box is CHL<1, Red box is 1<CHL<5 and Yellow box is 5<CHL.

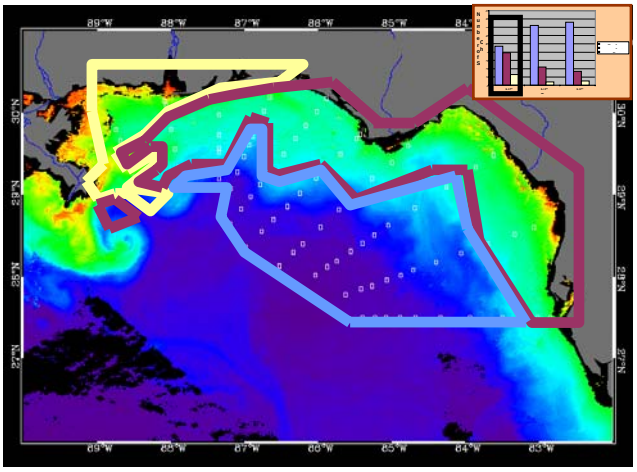

Figure B7. Graphical representation of surface chlorophyll distributions for spring, 1998 cruise (N2). Blue box is CHL<1, Red box is 1<CHL<5 and Yellow box is 5<CHL.

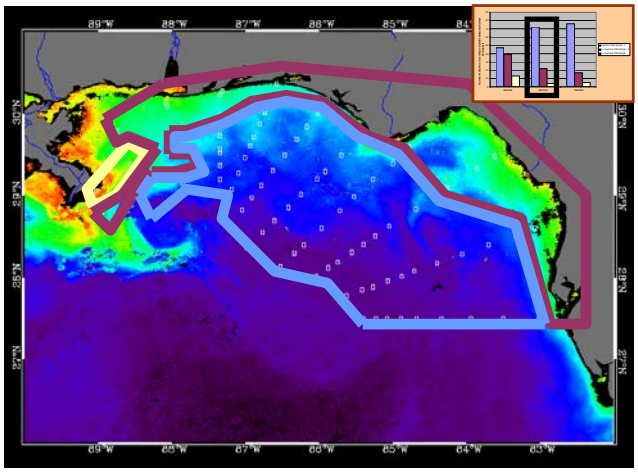

Figure B8. Graphical representation of surface chlorophyll distributions for spring, 1999 cruise (N5). Blue box is CHL<1, Red box is 1<CHL<5 and Yellow box is 5<CHL.

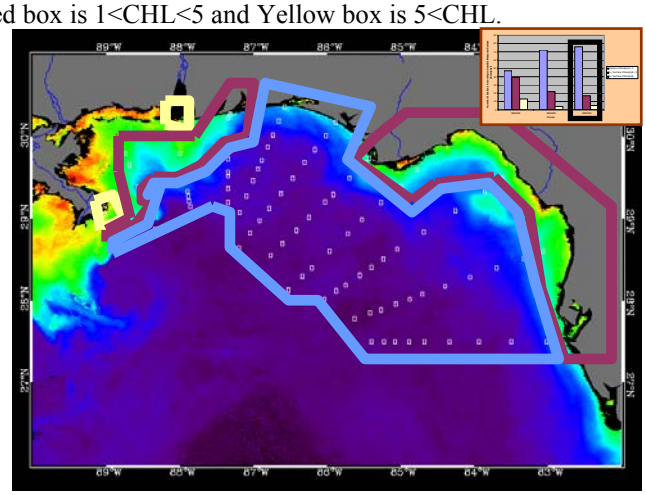

Figure B9. Graphical representation of surface chlorophyll distributions for spring, 2000 cruise (N8). Blue box is CHL<1, Red box is 1<CHL<5 and Yellow box is 5<CHL.

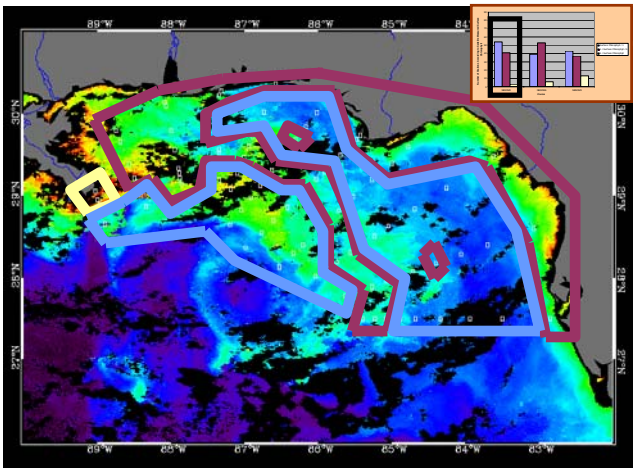

Figure B10. Graphical representation of surface chlorophyll distributions for summer, 1998 cruise (N3). Blue box is CHL<1, Red box is 1<CHL<5 and Yellow box is 5<CHL.

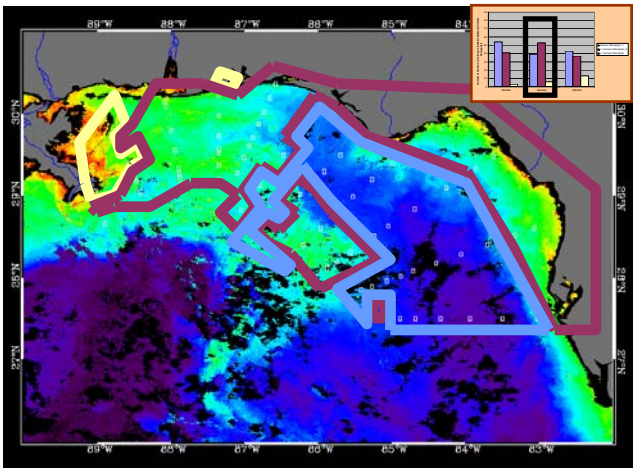

Figure B11. Graphical representation of surface chlorophyll distributions for summer, 1999 cruise (N6). Blue box is CHL<1, Red box is 1<CHL<5 and Yellow box is 5<CHL.

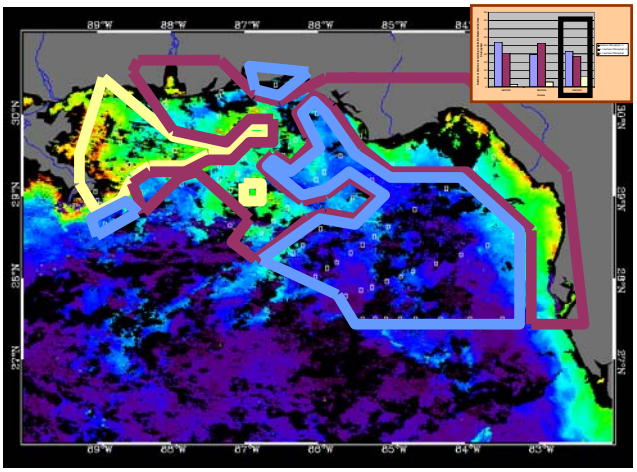

Figure B12. Graphical representation of surface chlorophyll distributions for summer, 2000 cruise (N9). Blue box is CHL<1, Red box is 1<CHL<5 and Yellow box is 5<CHL.

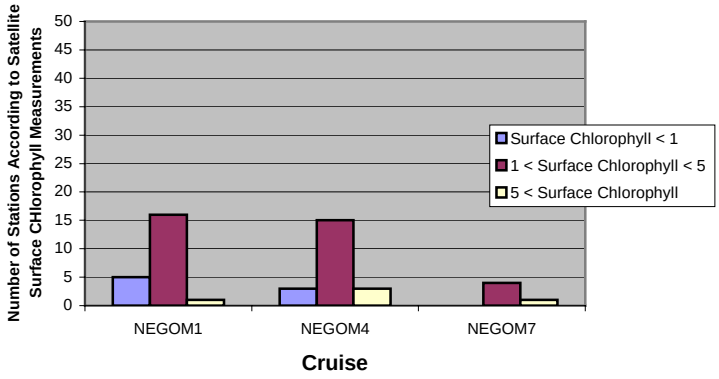

Figure B13. Numerical distribution of freshwater stations with different surface chlorophyll concentration ranges for the winter cruises.

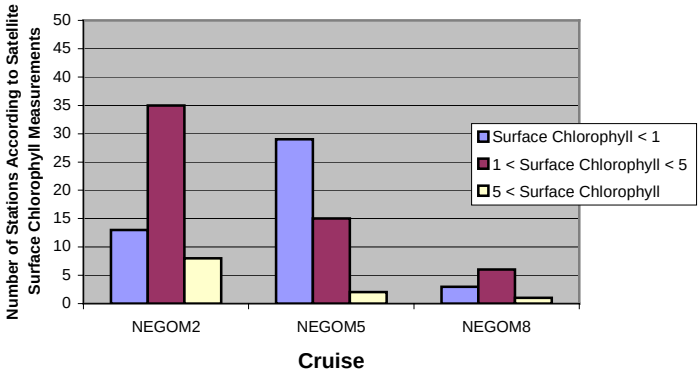

Figure B14. Numerical distribution of freshwater stations with different surface chlorophyll concentration ranges for the spring cruises.

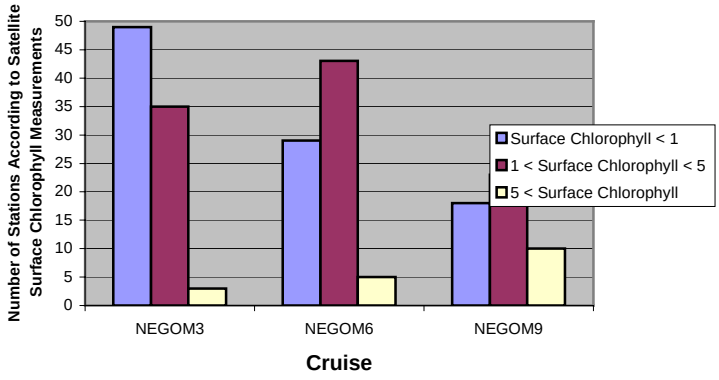

Figure B15. Numerical distribution of freshwater stations with different surface chlorophyll concentration ranges for the summer cruises.

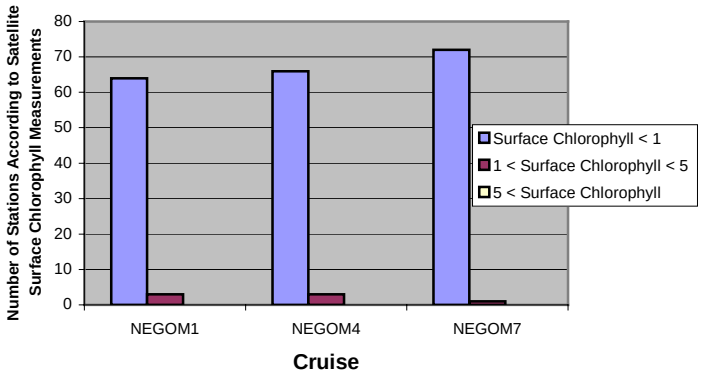

Figure B16. Numerical distribution of bluewater stations with different surface chlorophyll concentration ranges for the winter cruises.

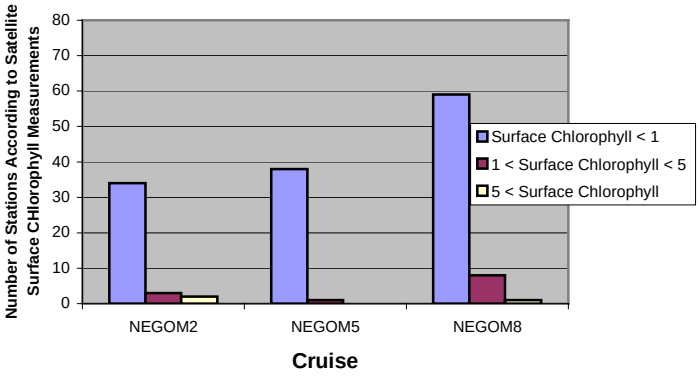

Figure B17. Numerical distribution of bluewater stations with different surface chlorophyll concentration ranges for the spring cruises.

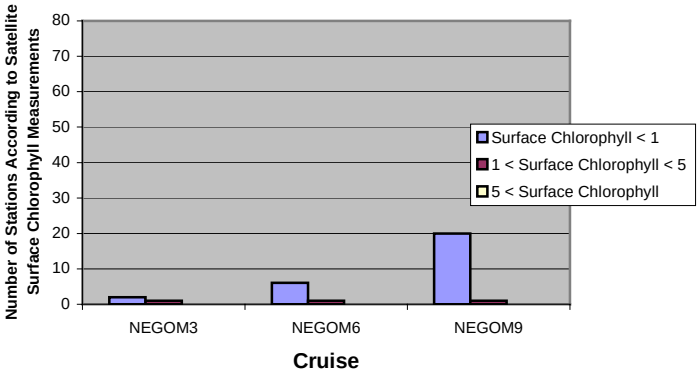

Figure B18. Numerical distribution of bluewater stations with different surface chlorophyll concentration ranges for the summer cruises.

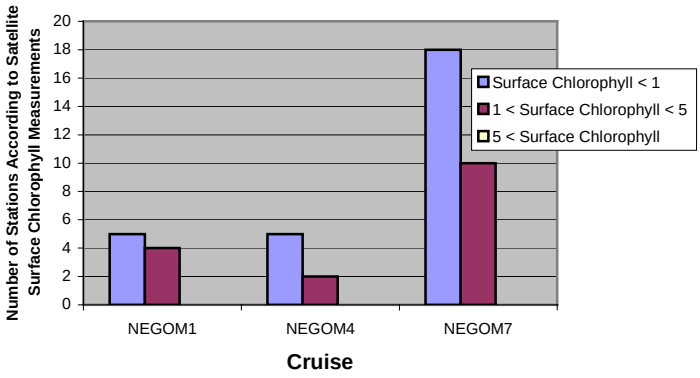

Figure B19. Numerical distribution of coastal stations with different surface chlorophyll concentration ranges for the winter cruises.

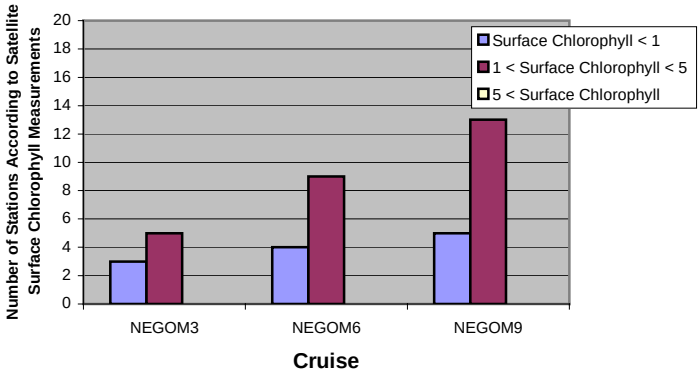

Figure B20. Numerical distribution of coastal stations with different surface chlorophyll concentration ranges for the spring cruises.

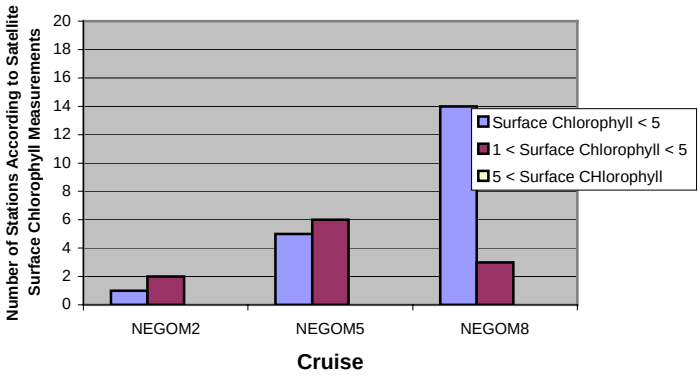

Figure B21. Numerical distribution of coastal stations with different surface chlorophyll concentration ranges for the summer cruises.

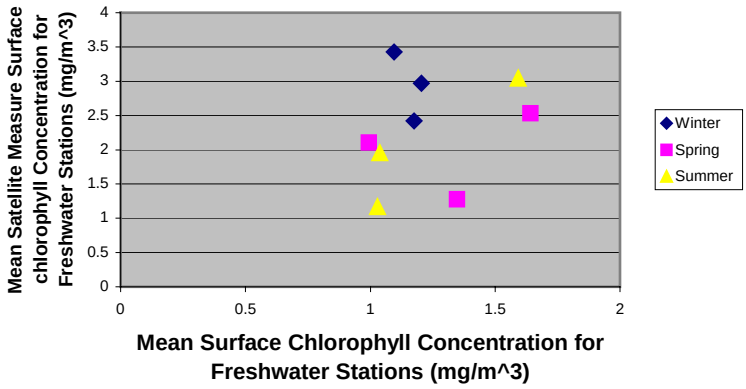

Figure B22. Comparison of mean in situ chl-α concentration with mean satellite measured surface chl-α for all freshwater stations.

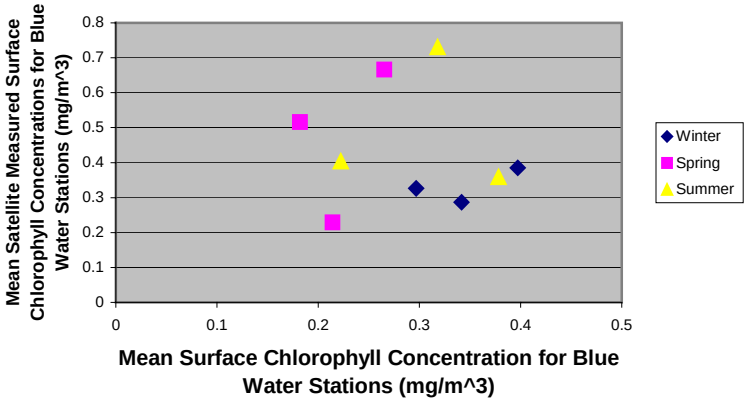

Figure B23. Comparison of mean in situ chl-α concentration with mean satellite measured surface chl-α for all bluewater stations.

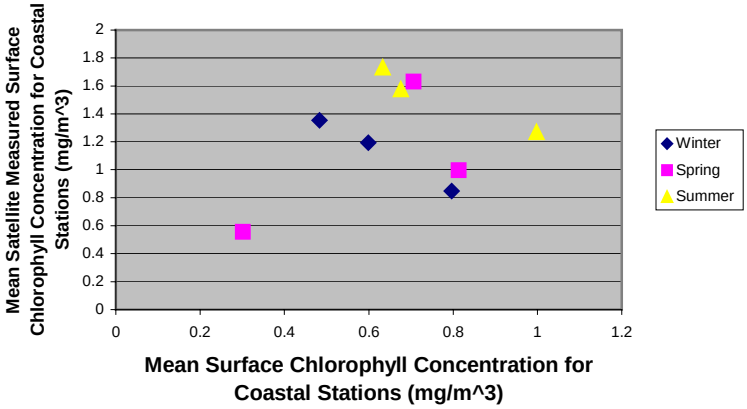

Figure B24. Comparison of mean in situ chl-α concentration with mean satellite measured surface chl-α for all coastal stations.

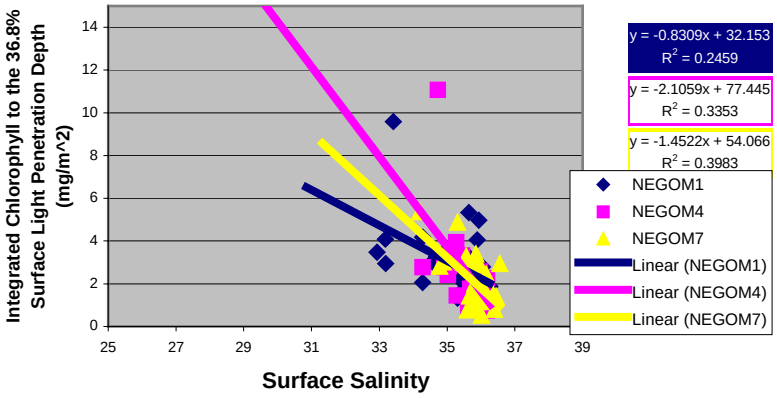

Figure B25. Comparison of surface salinity and integrated chl-α to the 36.8% surface light penetration depth for the winter cruises.

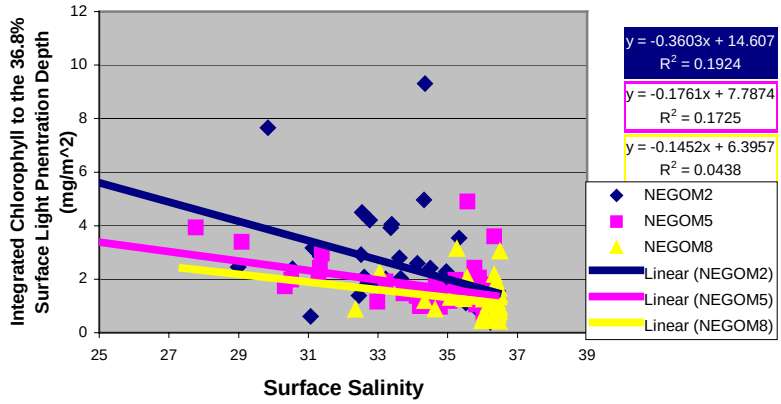

Figure B26. Comparison of surface salinity and integrated chl-α to the 36.8% surface light penetration depth for the spring cruises.

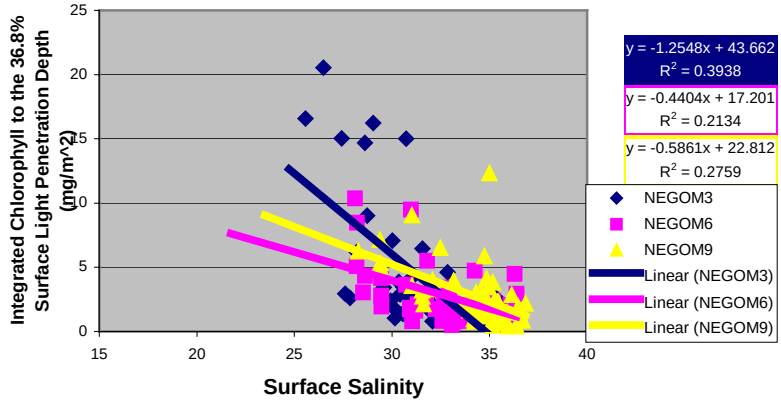

Figure B27. Comparison of surface salinity and integrated chl-α to the 36.8% surface light penetration depth for the summer cruises.

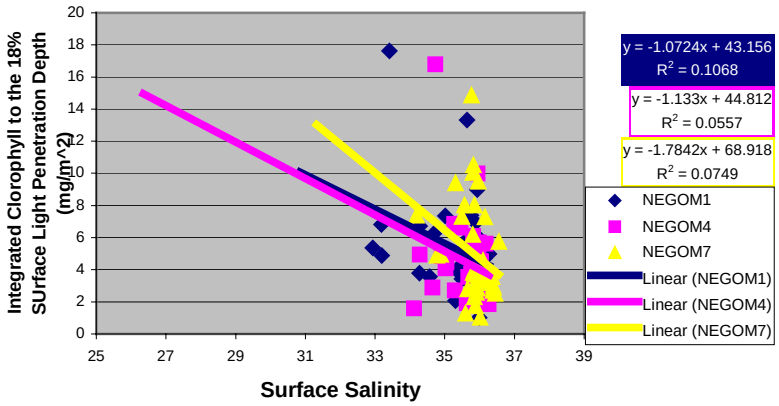

Figure B28. Comparison of surface salinity and integrated chl-α to the 18% surface light penetration depth for the winter cruises.

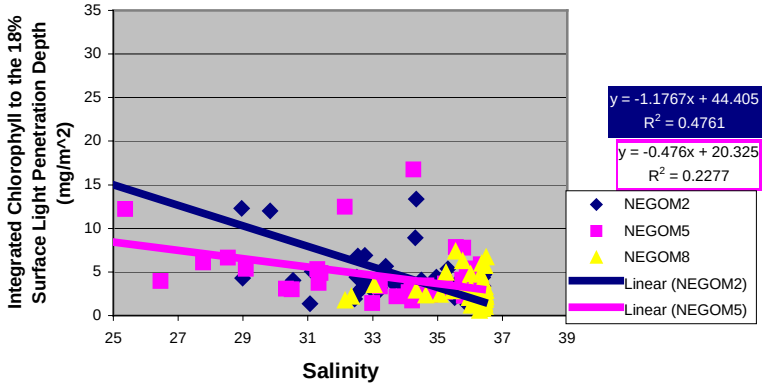

Figure B29. Comparison of surface salinity and integrated chl-α to the 18% surface light penetration depth for the spring cruises.

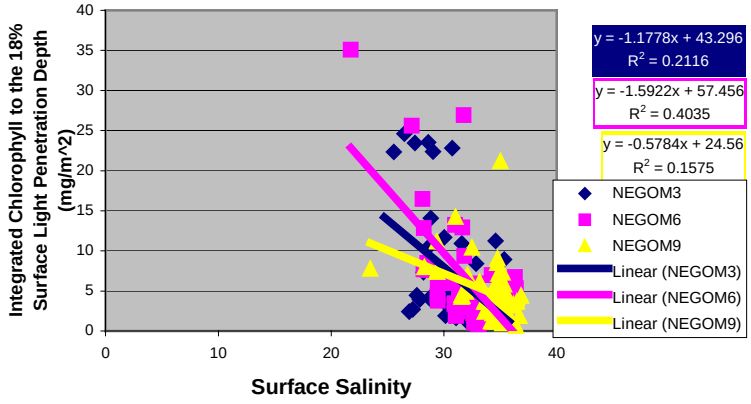

Figure B30. Comparison of surface salinity and integrated chl-α to the 18% surface light penetration depth for the summer cruises.

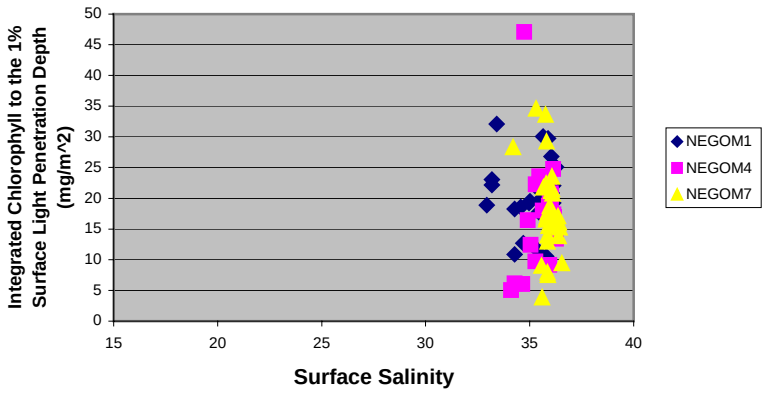

Figure B31. Comparison of surface salinity and integrated chl-α to the 1% surface light penetration depth for the winter cruises.

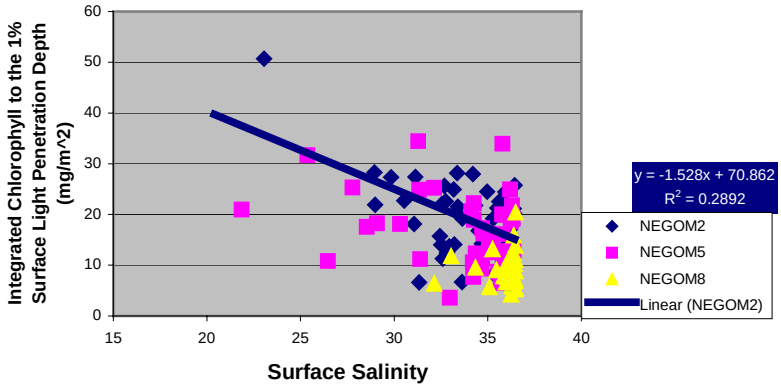

Figure B32. Comparison of surface salinity and integrated chl-α to the 1% surface light penetration depth for the spring cruises.

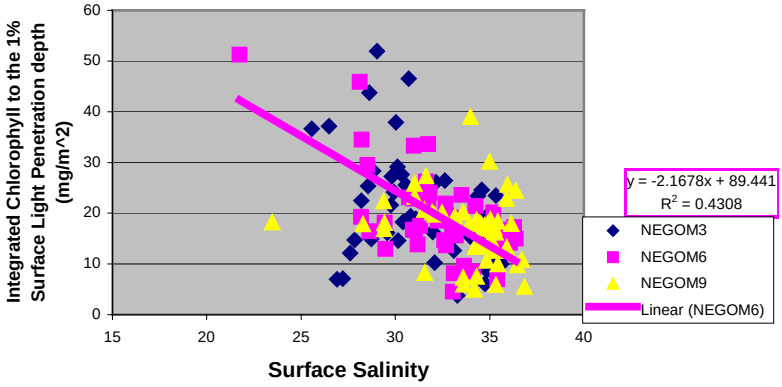

Figure B33. Comparison of surface salinity and integrated chl-α to the 1% surface light penetration depth for the summer cruises.

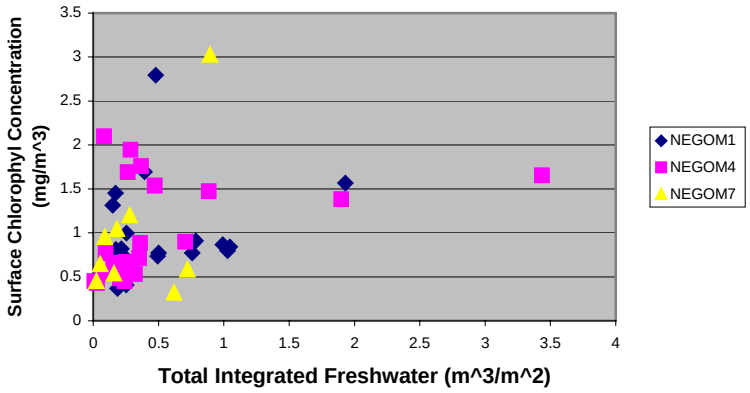

Figure B34. Comparison of vertically integrated freshwater and in situ measured surface chl-α concentration for the winter cruises.

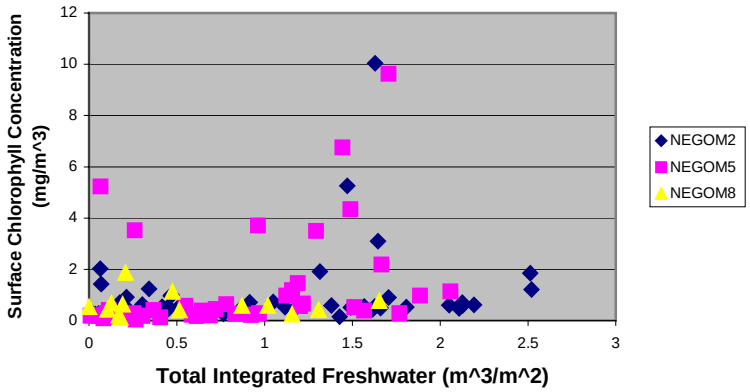

Figure B35. Comparison of vertically integrated freshwater and in situ measured surface chl-α concentration for the spring cruises.

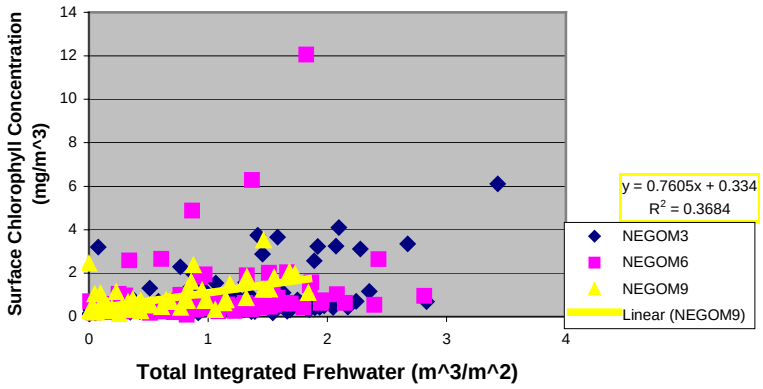

Figure B36. Comparison of vertically integrated freshwater and in situ measured surface chl-α concentration for the summer cruises.

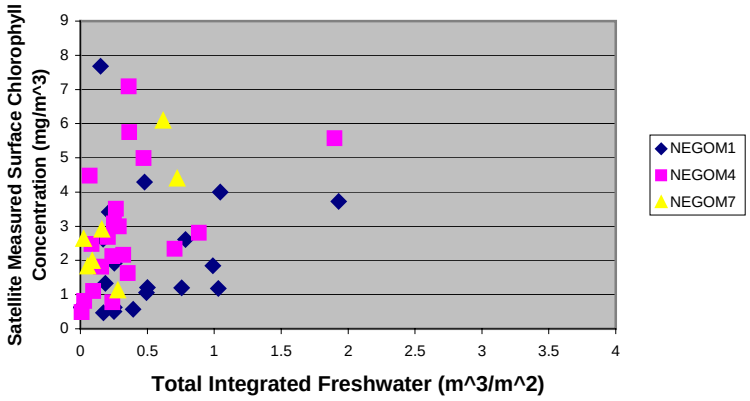

Figure B37. Comparison of vertically integrated freshwater and satellite measured surface chl-α concentration for the winter cruises.

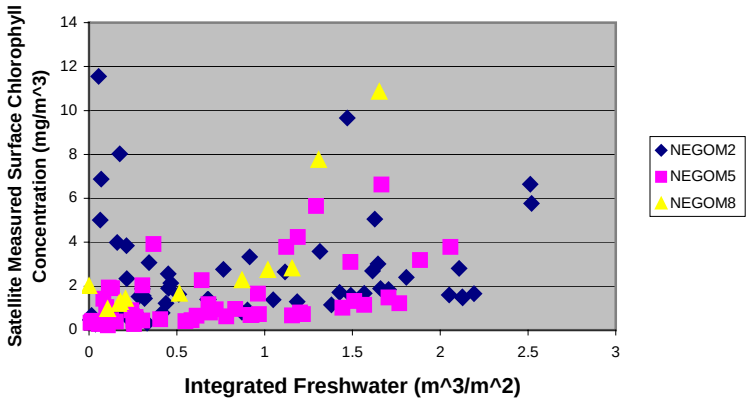

Figure B38. Comparison of vertically integrated freshwater and satellite measured surface chl-α concentration for the spring cruises.

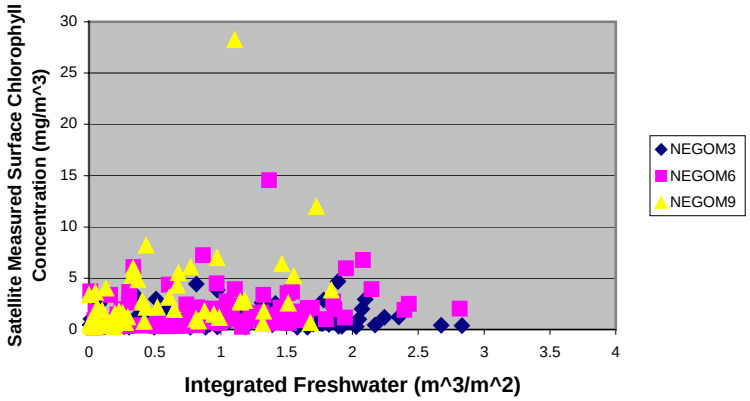

Figure B39. Comparison of vertically integrated freshwater and satellite measured surface chl-α concentration for the summer cruises.

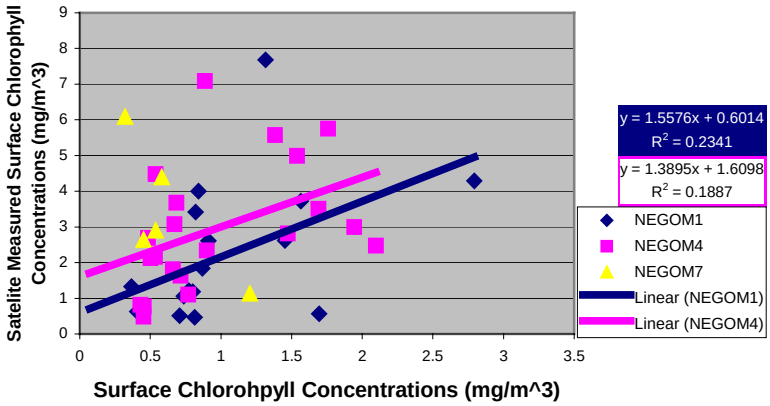

Figure B40. Comparison of in situ measured surface chl-α concentration and satellite measured surface chl-α concentration for freshwater stations of winter cruises.

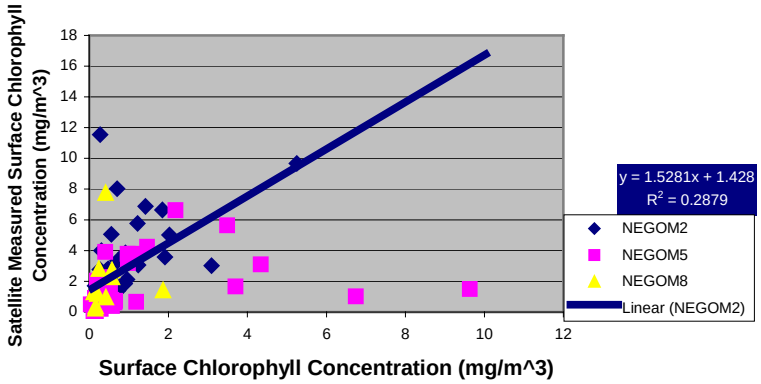

Figure B41. Comparison of in situ measured surface chl-α concentration and satellite measured surface chl-α concentration for freshwater stations of spring cruises.

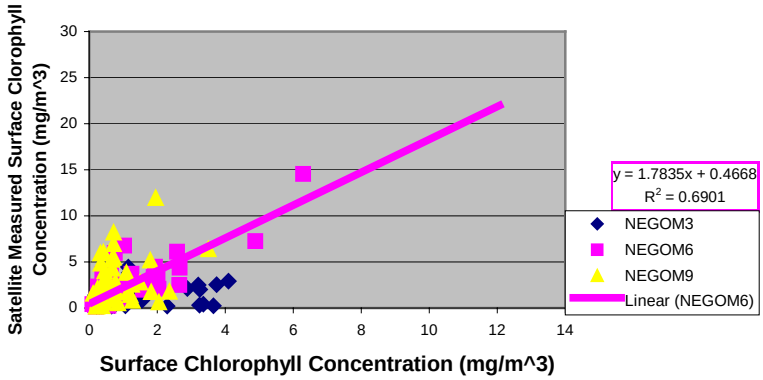

Figure B42. Comparison of in situ measured surface chl-α concentration and satellite measured surface chl-α concentration for freshwater stations of summer cruises.

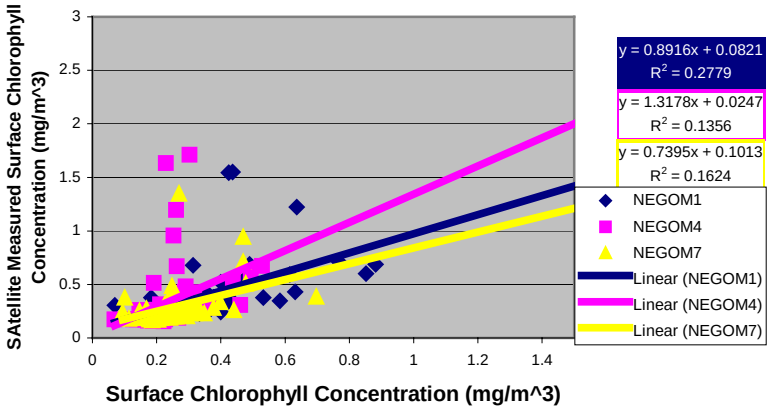

Figure B43. Comparison of in situ measured surface chl-α concentration and satellite measured surface chl-α concentration for bluewater stations of winter cruises.

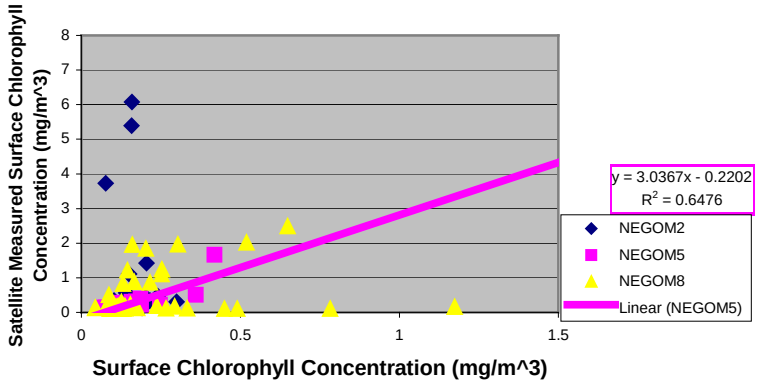

Figure B44. Comparison of in situ measured surface chl-α concentration and satellite measured surface chl-α concentration for bluewater stations of spring cruises.

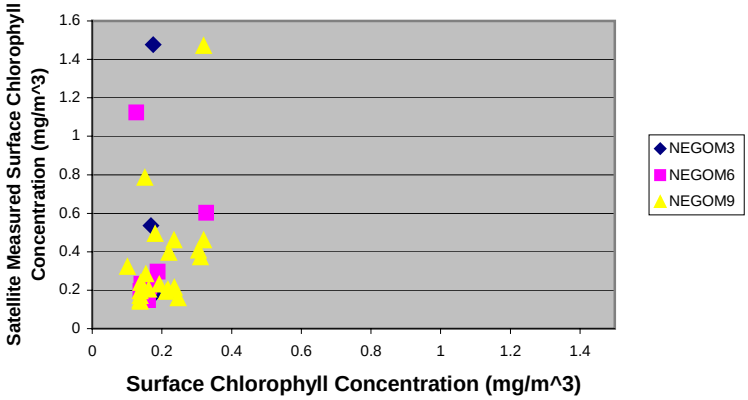

Figure B45. Comparison of in situ measured surface chl-α concentration and satellite measured surface chl-α concentration for bluewater stations of summer cruises.

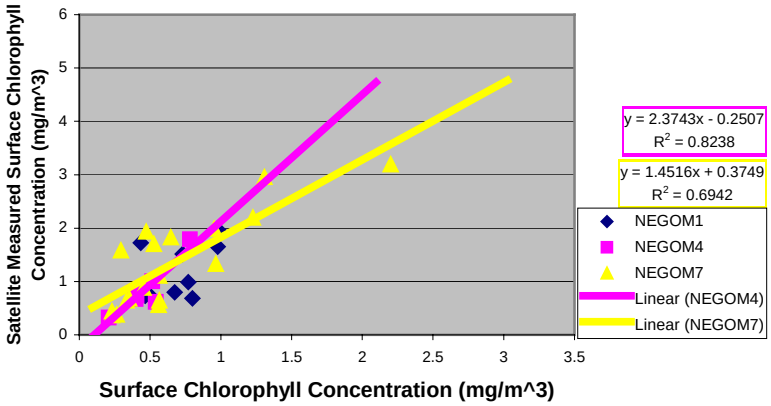

Figure B46. Comparison of in situ measured surface chl-α concentration and satellite measured surface chl-α concentration for coastal stations of winter cruises.

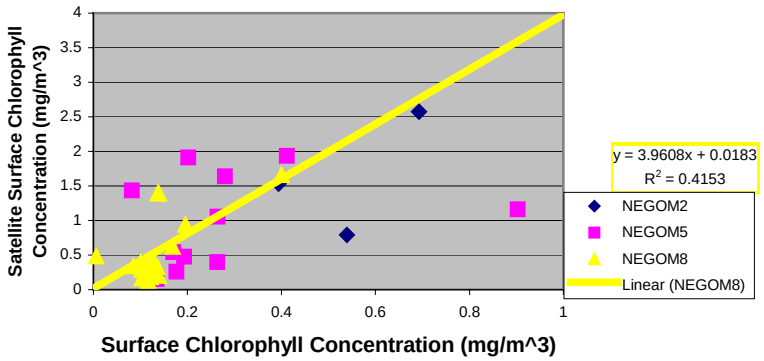

Figure B47. Comparison of in situ measured surface chl-α concentration and satellite measured surface chl-α concentration for coastal stations of spring cruises.

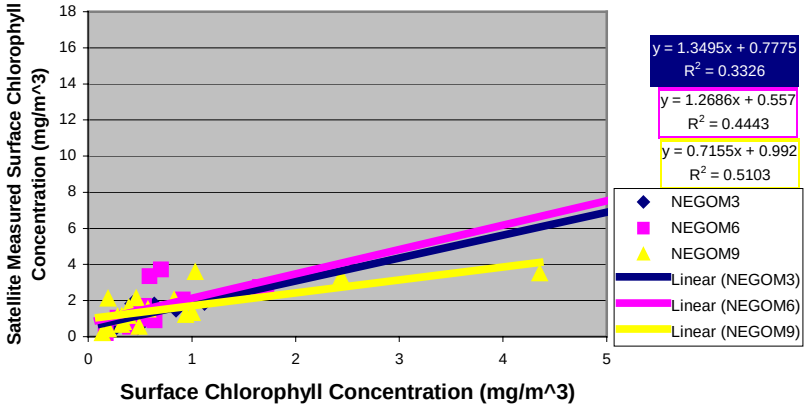

Figure B48. Comparison of in situ measured surface chl-α concentration and satellite measured surface chl-α concentration for coastal stations of summer cruises.

VITA

William W. Fletcher was born on March 8, 1977 in Gainesville, Florida and raised as a Hoosier in Indianapolis, Indiana. He graduated from Kenyon College with honors with a B.A. in biology, with an emphasis of his studies dealing with aquatic ecology. In August of 2000 he was fortunate enough to participate in the final NEGOM cruise before beginning his studies at Texas A&M that same fall semester. Will Fletcher can be contacted at 460 Crestwood Drive, Athens, GA 30605.